2018

Evaluating sediments as an ecosystem service in western Lake Erie through quantification of nitrogen cycling pathways

Ashlynn Rose Boedecker
Wright State University

EVALUATING SEDIMENTS AS AN ECOSYSTEM SERVICE IN WESTERN LAKE ERIE THROUGH QUANTIFICATION OF NITROGEN CYCLING PATHWAYS

A thesis submitted in partial fulfillment of the
requirements for the degree of
Master of Science

By

ASHLYNN ROSE BOEDECKER
B.S., Wright State University, 2014

2018
Wright State University

WRIGHT STATE UNIVERSITY

GRADUATE SCHOOL

April 27, 2018

I HEREBY RECOMMEND THAT THE THESIS PREPARED UNDER MY SUPERVISION BY Ashlynn Rose Boedecker ENTITLED Evaluating sediments as an ecosystem service in western Lake Erie through quantification of nitrogen cycling pathways BE ACCEPTED IN PARTIAL FULFILLMENT OF THE REQUIREMENTS FOR THE DEGREE OF Master of Science.

Silvia E. Newell, Ph.D.
Thesis Director

David F. Dominic, Ph.D.
Chair, Department of Earth & Environmental Sciences

Committee on
Final Examination

Mark J. McCarthy, Ph.D.

Chad R. Hammerschmidt, Ph.D.

Justin D. Chaffin, Ph.D.

Barry Milligan, Ph.D.
Interim Dean of the Graduate School

ABSTRACT

Boedecker, Ashlynn Rose. M.S. Department of Earth and Environmental Sciences, Wright State University, 2018. Evaluating sediments as an ecosystem service in western Lake Erie through quantification of nitrogen cycling pathways.

Lake Erie experiences annual cyanobacterial harmful algal blooms (HABs), comprised mostly of non-nitrogen-fixing *Microcystis*, due to excess nitrogen (N) and phosphorus (P) inputs (eutrophication). Lake Erie's watershed is mostly agricultural, and fertilizers, manure, and drainage practices contribute to high nutrient loads. This study aimed to clarify the role of Lake Erie sediments in either exacerbating or mitigating conditions that fuel HABs via recycling and/or removal, respectively, of excess N and P. Sediment-water interface N dynamics were evaluated in low HAB (2016, dry) and high HAB (2017, wet spring and early summer) years. Intact sediment cores and overlying water were collected in the western basin of Lake Erie during the ice-free seasons in 2016 and 2017. Cores were incubated in a continuous-flow system with either no isotope addition (unamended control), a $^{15}NO_3^-$ tracer, or a $^{15}NH_4^+$ tracer to help distinguish between N sinks (denitrification and anammox), N links (e.g., DNRA), and N sources (N_2 fixation). Sediments were a net source of NH_4^+ (29.4 ± 7.41 μmol N m^{-2} h^{-1}) and ortho-phosphate (2.19 ± 0.52 μmol P m^{-2} h^{-1}) to the water column across all sampling sites and times. Net N_2 fluxes reflected net N_2 fixation (i.e., N_2 influx) in spring 2016 and 2017, then switched to net denitrification (i.e., N_2 efflux), the primary N removal mechanism,

later in the season. On average, western basin sediments were a net N sink (-77.6 μmol N m^{-2} h^{-1}), suggesting that the sediments perform a valuable ecosystem service. Extrapolated to the entire western basin surface area, and considering Maumee and Detroit River discharges, western basin sediments can remove approximately 28.9 percent of the average annual total N load. However, denitrification rates were lower during the more severe bloom year (2017) than in 2016, suggesting that large blooms, similarly to high N loading, can inhibit the capacity of sediments to perform that ecosystem service. To mitigate HABs in eutrophic systems, such as Lake Erie, management efforts emphasizing reduction of non-point, agricultural sources of both N and P are necessary because high nutrient loads support larger, more toxic HABs, which limit the capacity of sediments to remove N via denitrification.

TABLE OF CONTENTS

Page

LIST OF FIGURES

Figure Page

LIST OF TABLES

ACKNOWLEDGEMENTS

I would first like to thank my advisors, Drs. Silvia Newell and Mark McCarthy, for putting up with me for the last three years and handling both my extreme excitement and (slightly) sullen days. They took me in with just an opinion from a previous grad student, and without that, I would not be where I am now. Even though I may not have realized it then, I am thankful for how much they pushed me, even when I was being stubborn (which was often). But they also not only pushed me academically but were around to help me experience many things I never had before, like traveling, food, and all those other nice things.

I also need to give a shout out to my lab mates: Daniel Hoffman, Justyna Hampel, Desi Niewinski, Megan Reed, Justin Myers, Erica Strope, and Ally Savoie because they are all just awesome. They made my first grad school journey one for the books, and I am so excited to see what the future holds in store for them. An extra shout out goes to Justin because he won the thesis poll with a guess of 100 pages. Along with them are my amazing friends, Amanda Tate and Danie Dalhart, who have dealt with my crap for many years and deserve way more than I can give them. I also need to thank my brother, Austyn, because even though he had no choice in who his sister was, he took it in stride, and I am so proud of who he is and extremely happy I got to spend his first two years of college with him at the same university.

Finally, I need to acknowledge my other two committee members for all their help the last three years. Dr. Justin Chaffin was extremely helpful with sampling (especially that time I forgot the core caps), and I appreciate all the help! Along with teaching awesome classes that have proven very beneficial, Dr. Chad Hammerschmidt also helped me realize that humans contribute $0.02 as an ecosystem service every five times they flatulate, and I will never forget that fact.

I. INTRODUCTION

Since the mid-1990s, Lake Erie has experienced toxic cyanobacterial blooms due to high nutrient (nitrogen and phosphorus) inputs from its tributaries (Murphy et al. 2003). These blooms negatively affect aquatic life, pets, livestock, and humans, as evidenced by the shutdown of the City of Toledo, Ohio, water treatment plant in August 2014 due to high toxin levels (Carmichael and Boyer 2016). Contemporary blooms in Lake Erie differ from those present in the 1960s and 1970s in that they are caused by cyanobacteria taxa that cannot fix atmospheric nitrogen (N; Steffen et al. 2014). The Maumee River delivers high N and phosphorus (P) loads to Maumee Bay and the western basin (Moog and Whiting 2002). The Lake Erie watershed is mostly agricultural, and the associated fertilizer, manure, and drainage practices contribute to high nutrient loads (Stumpf et al. 2012).

Lake Erie is an important resource for Ohio, Michigan, Pennsylvania, New York, and Ontario (Canada). The Maumee River, which travels through northwestern Ohio and northeastern Indiana, delivers about 50 percent (%) of the nutrient load (Maccoux et al. 2016; Verhamme et al. 2016) but only about 3 percent of the water discharge to the western basin (Joosse and Baker 2011). The Maumee River watershed has the largest drainage area in the Great Lakes region (17,115 km^2; Herdendorf 1990), and it also discharges large amounts of suspended sediment to Lake Erie (Moog and Whiting 2002). The ambient concentrations of N and P in surface waters and the loads coming in from rivers depend on watershed activities, including land use, fertilizer application rates, soil

type, and hydrological flow pathways linking the land to its tributaries (Heathwaite and Johnes 1996). The Maumee River watershed is 86.8% agricultural, and only 7.8% forested, 3.1% urban, and 1.3% wetland (Han et al. 2012), which contributes significantly to the eutrophication of Lake Erie.

Nitrogen export from the Maumee River watershed is estimated at more than 1000 kg km^{-2} yr^{-1}, which is the highest in the Great Lakes (Smith et al. 1997). Richards and Baker (2002) reported that there was a 70-90 percent decrease in P concentrations within the Maumee River from 1975 to 1995, but NO_3^- levels remained constant. More recent data shows that both NO_3^- and total N loads from the Maumee River have been decreasing since about 1995 (Stow et al. 2015), but the proportion of total N comprised of total Kjeldahl N (TKN; non-NO_3^- N, including chemically reduced forms, such as urea and NH_4^+) is increasing (Newell et al., in press). Failure to reduce N over-enrichment may have contributed to the formation of toxic, non-N-fixing harmful algal blooms (HABs), both in the river and the western basin of Lake Erie. These annual cyanobacterial blooms are primarily comprised of the genus *Microcystis* (Figure 1; Chaffin et al. 2013).

The management focus to reduce HABs in Lake Erie was and still is focused on P loading reductions (Holdren and Armstrong 1980; Fraser 1987; Muenich et al. 2016; Maccoux et al. 2016). In 1978, an amendment to the Great Lakes Water Quality Agreement (GLWQA) established a maximum P load target of 11,000 metric tons yr^{-1} for the whole lake (Stow et al. 2015). The GLWQA was altered in 2012 to revise target P levels to 186 metric tons of dissolved reactive P and 860 metric tons of total P during the months of March to July in the Maumee River watershed (Muenich et al. 2016). The

Figure 1: *Microcystis* bloom (left) on August 9, 2017 and microscope image of *Microcystis* (right). Photo: Ashlynn Boedecker

focus on P management in Lake Erie has been based on the strong relationship between reactive P loads from the Maumee River and annual bloom biomass (Kane et al. 2014; Stow et al. 2015). One study modeled bloom severity based on the total P and reactive P loading from the Maumee River and found that the spring nutrient load and the lag time between the input of P and the *Microcystis* bloom allows for the total P to be recycled into bioavailable P (Stumpf et al. 2012). However, P is not always the limiting nutrient in Lake Erie (Chaffin et al. 2013, 2014) or other aquatic systems (e.g., Elser et al. 2007). Significant anthropogenic biases can cause shifts in the nutrient status of lakes (Lewis and Wurtsbaugh 2008); for example, overusing N based fertilizers can cause P limitation in downstream systems. In the western basin, phytoplankton growth is seasonally limited by N (Chaffin et al. 2013). Seasonal variation between N, P, and N+P co-limitation has also been reported in Lake Taihu, China, a hypereutrophic lake that is slightly smaller (2336 km^2) than the western basin (2980 km^2) of Lake Erie (Xu et al. 2010). Many other lakes also exhibited dual nutrient limitation in whole-lake nutrient addition experiments (Paerl et al. 2016).

In addition to nutrient concentrations, nutrient forms may also influence HABs. Phytoplankton community structure can shift from diatoms in nitrate (NO_3^-) dominated waters to cyanobacteria in ammonium (NH_4^+) dominated waters (McCarthy et al. 2009; Glibert et al. 2016), corresponding to a shift from a clear, oligotrophic status to a eutrophic or hypereutrophic status. Different forms of N (e.g., urea) can also contribute to the toxicity of HABs (Donald et al. 2011), further supporting calls for both nutrients to be regulated. In the 1990s, the predominant N form in fertilizers switched from NH_4^+ and NO_3^- to urea (Glibert et al. 2006, 2014b), which is an organic form of N that is

bioavailable for cyanobacteria (Belisle et al. 2016). Nutrient reductions can be complicated and expensive when shifts in technology are required, and there are additional challenges in agricultural watersheds, where nonpoint nutrient sources dominate (Mitsch 1992). Point sources of nutrient pollution have been regulated through the Clean Water Act since the 1970s (33 U.S.C. §1251 et seq. 1972), but nonpoint sources and N have largely been ignored, and these high loads continuously contribute to the ongoing HABs problem. Many studies (Han et al. 2012; Bridgeman et al. 2013; Baker et al. 2014; Kane et al. 2014; Stow et al. 2015) have compared nutrient loads from the Maumee River relative to HABs in Lake Erie; however, few studies have evaluated the transformations and fate of N within the lake or the sediments.

Understanding sediment nutrient dynamics is critical to mitigating HABs. Sediments can exacerbate oxygen drawdown and contribute to hypoxia. Dissolved oxygen (DO) can be consumed by the decomposition of organic matter through aerobic respiration (Wilson and DePaul 2017) in the water column and in the sediments. Oxygen uptake into sediments is referred to as sediment oxygen demand (SOD). As organic matter is respired, phosphate (PO_4^{3-}) and NH_4^+ can also be released. Sediments can also store P for long periods of time bound to iron or aluminum, which makes them a potential legacy nutrient source (Heisler et al. 2008). Over the years, studies (i.e., Holdren and Armstrong 1980; Paytan et al. 2017) have quantified P fluxes from Lake Erie sediments and found that sediments are a consistent source of bioavailable P to the water column. Gross sediment N fluxes have been reported in Sandusky Bay (Salk et al. 2018) and Old Woman Creek (McCarthy et al. 2007), two coastal Lake Erie subsystems, and Small et al. (2014) reported N fluxes from single sampling events at one site within the western

basin, three in the central basin, and one in the eastern basin of Lake Erie. Taken together, these studies established that sediment N cycling plays an essential role in nutrient cycling in Lake Erie. While these studies represent a baseline, little work on N transformations in sediments has been conducted in the main basins of Lake Erie.

Quantifying sediment N loss and recycling pathways is needed to understand the fate and transport of N within lake systems. Unlike P, which is assimilated by cells primarily as orthophosphate ($o\text{-}PO_4^{3-}$; Vymazal 2007), N has many forms – spanning eight oxidation states – that can be bioavailable. Anoxic sediments play a major role in N cycling. Anaerobic N removal (sinks) and recycling pathways include: denitrification, the reduction of NO_3^- to nitrous oxide (N_2O) and dinitrogen gas (N_2); anaerobic ammonium oxidation (anammox), the reduction of NH_4^+ and nitrite (NO_2^-) to N_2; dissimilatory NO_3^- reduction to NH_4^+ (DNRA); and organic matter remineralization to NH_4^+ (Canfield et al. 2010). Atmospheric N_2 can be fixed back into organic matter via N fixation, which reflects a N source and counteracts the N sinks (McCarthy et al. 2007).

Denitrification is the primary N removal pathway in most aquatic systems (Mulholland et al. 2008). In respiratory denitrification, NO_3^- acts as the terminal electron acceptor for the oxidation of organic matter under anaerobic conditions, and in aquatic sediments, most NO_3^- is fully reduced to N_2, with a small fraction escaping as N_2O (Burgin and Hamilton 2007). These gases escape to the atmosphere as either relatively inert N_2 or a potent greenhouse gas (N_2O). Denitrification is measured directly as an increase in dissolved N_2, and it can improve water quality, partially mitigating the effects of N pollution (Laursen and Seitzinger 2002). It is mediated by facultative anaerobic bacteria under low oxygen concentrations, and rates increase with warming temperatures

(Herrman and White 2008). The highest denitrification rates occur at the oxic-anoxic boundary within the sediments and can be coupled with nitrification (the oxidation of NH_4^+ to NO_3^-), which occurs in the oxidized layer of the sediment (de Klein et al. 2017). Denitrification has been enhanced by human activity (Vitousek et al. 1997) and is favored over DNRA when NO_3^- concentrations are high and carbon is in limited supply (Kelso et al. 1997). NO_3^- is the next most energetically favorable terminal electron acceptor to O_2, and denitrification is stimulated when NO_3^- is abundant (An and Gardner 2002).

Anammox is another N removal pathway and occurs when chemolithoautotrophic bacteria (which use CO_2 as a carbon source) convert NH_4^+ and NO_2^- directly to N_2 under anaerobic conditions (Beaulieu et al. 2011). While NO_2^- is not typically abundant, these bacteria can obtain NO_2^- from the reduction of NO_3^-, possibly by denitrifiers (Burgin and Hamilton 2007). The percentage of total N removal represented by anammox varies widely among aquatic systems. Anammox accounted for 0-30 % of total N removal in various freshwater systems where it was evaluated (Schubert et al. 2006; Wenk et al. 2013; McCarthy et al. 2016), 0-26 % in estuarine sediments (Rich et al. 2008), and ~27 % overall in marine systems (but possibly as high as 50 percent spatially and temporally; Dalsgaard et al. 2005; Babbin et al. 2014).

N recycling pathways include remineralization from organic matter and DNRA, the reduction of NO_3^- to NO_2^- and, subsequently, NH_4^+, which is the most reduced and bioavailable form of N. NH_4^+ has a lower energy requirement for cellular uptake than NO_3^- and will be assimilated first (Glibert et al. 2016). It is the main N "currency" of primary productivity, particularly in promoting cyanobacterial blooms (Blomqvist et al. 1994). NH_4^+ is also very difficult to measure accurately in situ because it is recycled and

assimilated so quickly (Holmes et al. 1999). Thus, the partitioning between NO_3^- reduction pathways (e.g., denitrification and DNRA) has important implications for aquatic systems (An and Gardner 2002). Denitrification converts bioavailable N to inert N_2 gas, providing a valuable ecosystem service via N removal (Laursen and Seitzinger 2002), while DNRA recycles N to the system as the most bioavailable N form (An and Gardner 2002). DNRA can thus perpetuate eutrophication and cyanobacterial blooms (Glibert et al. 2014a). DNRA is most common when NO_3^- is limiting and labile carbon is abundant in sediments (Kelso et al. 1997; Burgin and Hamilton 2007). DNRA occurs in anoxic environments, carried out by primarily anaerobic fermentative microorganisms, usually mediated by sulfur-cycling microbes (Bernard et al. 2015). When hydrogen sulfide (H_2S) is produced, it can inhibit nitrification and the final step in denitrification (An and Joye 2001), which then limits total denitrification and promotes DNRA (Bernard et al. 2015). DNRA is controlled by the ratio of carbon to electron acceptors, as well as oxygen availability (Mørkved et al. 2005).

The pathway to produce new N within the system is N fixation of N_2 gas into biomass, which can then be remineralized to a more bioavailable N form (McCarthy et al. 2007). N fixation is an energy intensive reaction (requires 16 ATP per 1 mol of N fixed; Welsh 2000) and typically occurs when both N concentrations and N:P ratios are low (Vitousek et al. 2002). Sediment N fixation was historically considered insignificant (Howarth et al. 1988), but new research has shown that rates can be equal to or even higher than sediment denitrification in some seasons (Fulweiler et al. 2007; Fulweiler and Heiss 2014; Newell et al. 2016), even at high porewater N concentrations (Knapp 2012). Net N_2 fluxes across the sediment-water interface can be negative (net N fixation, influx)

or positive (net denitrification, efflux) depending on temperature, NO_3^- availability, organic matter quantity and lability, oxygen, and other factors. Of the N cycling pathways, N fixation is one of the most anthropogenically altered, with industrial N fixation for use in fertilizers adding ~187 Tg of bioavailable N to the global N pool every year (Vitousek et al. 2013).

The fate of N and cycling rates in aquatic systems depends on concentration, biotic and abiotic uptake activity, secondary consumer population dynamics, and physical characteristics (Peterson et al. 1997). To determine the extent to which Lake Erie sediments act as a N source or sink, rates and pathways of N transformations at the sediment water interface were identified and quantified using intact sediment cores collected from the western basin of Lake Erie. Four sampling events for each of the four sites (two sites sampled per trip) occurred from April to October 2016 and 2017 for a total of 16 sampling trips. N removal rates via denitrification and/or anammox in the western basin were measured, as well as the extent to which DNRA contributed to internal N recycling. The amount of N fixation that brought new, bioavailable N to the system was calculated from isotopic N_2 measurements, as well as the contribution of sediments to P uptake or removal.

The overall objective of this work was to determine whether sediments in the western basin of Lake Erie act as a source of bioavailable N to the lake or sequester nutrients and release N_2, acting as a net N sink. It was hypothesized that: (1) sediment N_2 fluxes vary seasonally, with denitrification occurring in the spring through mid-summer, then switching to N fixation in the late-summer to early fall; (2) denitrification is the major N loss pathway, with a small fraction lost via anammox. DNRA is also a possible

mechanism of NO_3^- reduction, but it is a minor pathway compared to denitrification; and (3) sediments are an overall source of bioavailable NH_4^+ and P to the system.

II. METHODS

Study Sites and Field Sampling

Water samples and sediment cores were collected from four locations along the Maumee River discharge gradient in the western basin of Lake Erie (Figure 2). The sampling gradient begins in Maumee Bay and extends towards the center of the basin. Site depths increased with distance from the river mouth: MB18 was 2.5 m deep, WE2 was 5 m deep, WE4 was 8 m deep, and WE13 was 8.5 m deep. Intact sediment cores were collected in spring (April/May), early summer (June/July), late summer (August), and fall (September/October) of 2016 and 2017 (Table 1) for a total of eight rounds of incubations conducted over 16 trips (two sites visited per trip).

At each site, Secchi depth was measured, and water temperature, depth, pH, chlorophyll a fluorescence, specific conductance, dissolved oxygen, and phycocyanin (cyanobacterial pigment) were measured using either a Eureka Manta-2 or YSI Exo 2 multiparameter sonde. Surface and bottom water (~1 m above sediment) samples were collected using a 7 L Niskin bottle at each site and filtered immediately on location using 0.2 μm syringe filters for analysis of NH_4^+, NO_2^-, NO_3^-, o-PO_4^{3-}, and urea concentrations. All nutrient samples were transported on ice and in the dark for transport back to the lab, and frozen at -20°C until analysis.

For each of the sediment core incubations, six intact sediment cores were collected from each site using a custom sediment coring lander designed to maintain

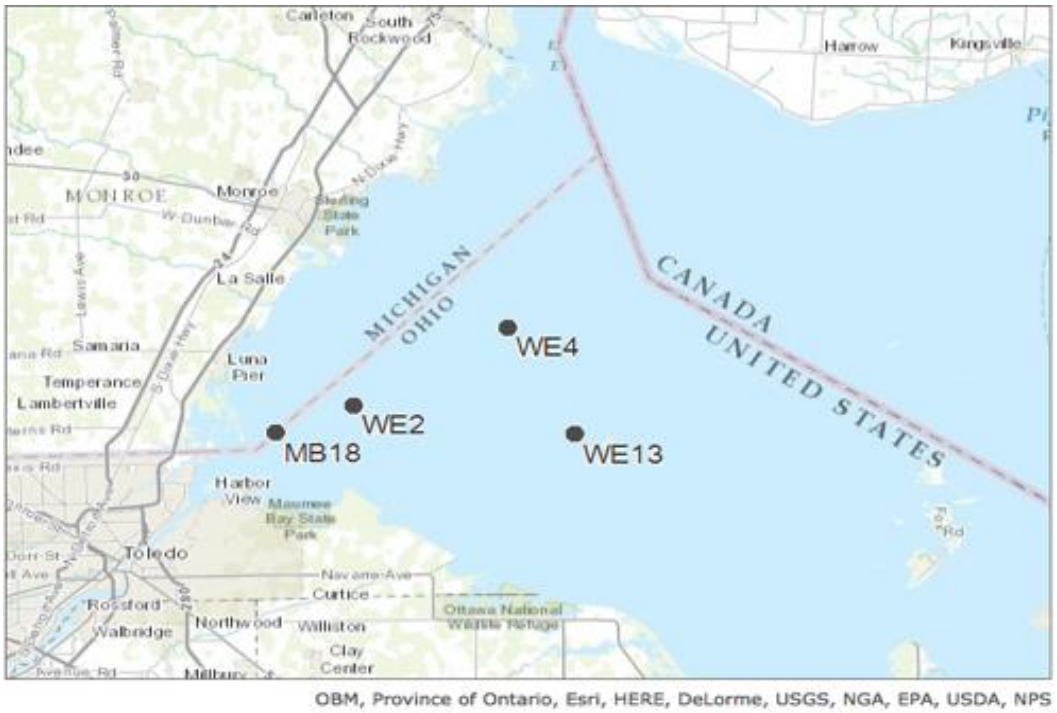

Figure 2: Map showing the sampling sites in the western basin of Lake Erie (map created with ArcGIS Online).

Table 1: Sampling dates and sites for each trip in 2016 and 2017.

2016		2017	
Date	Site	Date	Site
5/18/2016	WE4	4/25/2017	MB18
	WE13		WE2
6/28/2016	WE4	6/9/2017	WE4
	WE13		WE13
7/13/2016	MB18	7/11/2017	MB18
	WE2		WE2
8/3/2016	MB18	7/14/2017	WE4
	WE2		WE13
8/10/2016	WE4	8/2/2017	WE4
	WE13		WE13
9/19/2016	MB18	8/9/2017	MB18
	WE2		WE2
10/3/2016	WE4	10/3/2017	MB18
	WE13		WE2
10/17/2016	MB18	10/20/2017	WE4
	WE2		WE13

sediment core (7.6 cm diameter, ~15 cm depth) and overlying water integrity (Gardner et al. 2009). Along with the sediment cores, ~60 L of bottom water was collected in three pre-rinsed 20 L cubitainers® using a 7 L Niskin bottle. After collection, cores were sealed at both ends with a vinyl cap and stored in a dark cooler until incubation set up.

Sediment Core Incubation and Analysis

All sediment cores were either brought to Wright State University (WSU) for incubation or incubated at The Ohio State University Stone Laboratory in Put-In-Bay, Ohio. All samples were analyzed at WSU. To prepare sediment cores for incubation, overlying water was decanted, being careful not to disturb the sediment-water interface, until about 10 cm of overlying water remained above the sediment surface. An air- and water-tight plunger fitted with gastight inflow and outflow tubing (PEEK) was pushed into the core tube until the inflow line was about 1 cm above the sediment-water interface (Figure 3). Each sediment core was wrapped in aluminum foil to prevent light effects. Two 8-channel peristaltic pumps (Rainin Dynamax®) were used to supply the overlying water with a constant flow of reservoir water at ~1.35 mL min^{-1}. Aquarium bubblers were used to ensure that reservoir water remained oxygenated throughout the incubation, since the western basin of Lake Erie does not usually experience bottom water hypoxia.

Nitrogen removal and recycling rates were measured using an established, continuous-flow protocol (Lavrentyev et al. 2000; McCarthy et al. 2015; McTigue et al. 2016). Treatments for each incubation included duplicate cores for: (1) an unamended control ("C") for net $^{28}N_2$, nutrient (NH_4^+, NO_2^-, NO_3^-, urea, and o-PO_4^{3-}), and oxygen fluxes; (2) a $^{15}NH_4^+$ tracer addition ("A") for possible anammox rates; and (3) a $^{15}NO_3^-$

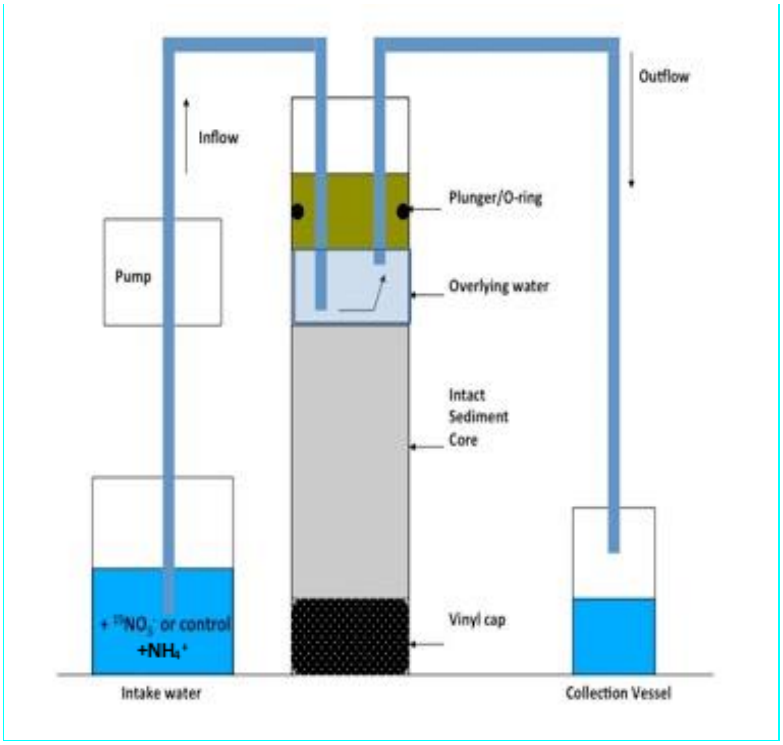

Figure 3: Diagram of the incubation system for the continuous-flow experiments using intact sediment cores (modified from Lavrentyev et al. 2000).

tracer addition ("N") for total denitrification, N fixation occurring simultaneously with denitrification (An et al. 2001), and potential DNRA. $^{15}NH_4Cl$ (98%; Sigma Aldrich) was added to the "A" reservoirs to achieve an added concentration of ~10 μM for sites WE2, WE4, and WE13 and ~20 μM for site MB18. $Na^{15}NO_3$ (98%; Sigma Aldrich) was added to the "N" reservoirs for final concentrations of 100 μM (WE2, WE4, WE13) and 200 μM (MB18). Immediately after isotope additions to the inflow reservoirs, nutrient samples were collected, filtered immediately, and frozen as described previously for field samples to confirm spike concentrations. Bottom water from the inflow reservoirs flowed continuously over intact sediment cores at about 1.35 mL min^{-1} for a residence time of about 5 hours, and, before sampling commenced, cores were allowed to re-establish steady-state for at least 12 hours after flow was started. Nutrient and dissolved gas samples were collected once daily for three days from both inflow reservoirs and outflows.

When feasible, dissolved gas samples were analyzed immediately for $^{28,29,30}N_2$, O_2, and Ar using membrane inlet mass spectrometry (MIMS; Kana et al. 1994; An et al. 2001). When core incubations occurred at the Stone Laboratory (August 3-6, 2016, and July 11-13, 2017), dissolved gas samples were collected to overflowing in 15 mL, tall, ground-glass stoppered test tubes (Chemglass), preserved with 200 μL of 50% (w/w) $ZnCl_2$, stored submerged in 4 L Nalgene bottles, and analyzed within one week using MIMS.

The OXMIMS method (Yin et al. 2014) was used to determine $^{15}NH_4^+$ concentrations and production from unamended and $^{15}NO_3^-$ amended cores to estimate potential DNRA. OXMIMS samples were filtered to 0.2 μm and stored in the dark in

Exetainers® with no head space. Eleven $^{15}NH_4Cl$ calibration standards were made the day of analysis (0, 0.1, 0.25, 0.5, 1, 2.5, 5, 10, 25, 50, and 100 μM). Samples were injected with 200 μL of potassium iodine hypobromite solution (BrO+KI), which converts all of the NH_4^+ to N_2. The samples were then analyzed for $^{29}N_2$ and $^{30}N_2$ using the MIMS (An et al. 2001). $^{15}NH_4^+$ concentrations in the samples were determined using the calibration curve most appropriate for the measured signals (e.g., 0-10 or 0-100 μM). Measured $^{29}N_2$ and $^{30}N_2$ concentrations were corrected for any heavy N_2 already present in the samples before treatment with the hypobromite solution.

Loss on Ignition

Loss on ignition (LOI) was calculated on a subset of the sediments using standard methods (Dean 1974; Heiri et al. 2001). 20 different sediment samples were dried overnight at 105ºC, and then the mass of each crucible was recorded. The crucibles were then placed in a muffle furnace at 550ºC for four hours to allow organic matter to oxidize to CO_2, and the mass was then compared to the initial mass using the equation:

$$LOI = ((DW_{105} - DW_{550})/DW_{105})*100,$$

where DW_{105} is the mass of the sample after drying at 105ºC, and DW_{550} is the mass after being dried at 550ºC. LOI is expressed as a percentage of the loss of mass and is proportional to the amount of organic carbon in the sediments.

Nutrient Analysis

After collection, filtered nutrient samples were frozen at -20°C until analysis using a Lachat QuikChem© 8500 Flow Injection Analysis system. NH_4^+ (QuikChem©

Method 31-107-06-1-G) was analyzed using the Berthelot reaction, where NH_4^+ reacts with sodium phenolate and sodium dichloroisocyanurate (DCIC) to form indophenol blue. The absorbance of this pigment is measured at 630 nm. The determined detection limit of the NH_4^+ method was 0.038 μM, and calibration standards were made using NH_4Cl (0, 0.1, 0.25, 0.75, 1.5, 2.5, 5, 10, and 25 μM). NO_x (QuikChem© Method 31-107-04-1-E) was measured using two channels simultaneously; one measured NO_2^-, and the other measured $NO_3^- + NO_2^-$, which was determined by reducing NO_3^- to NO_2^- using a granulated copper-cadmium column. Both analyses mix NO_2^- with sulfanilamide and N-(1-napthyl)-ethylenediamine dihydrochloride (NED) to form an azo dye, which is measured colorimetrically at 540 nm. The concentration of NO_2^- was subtracted from the concentration of $NO_3^- + NO_2^-$ to determine the final NO_3^- concentration. $NaNO_2$ standards were used for both analyses (0, 0.1, 0.25, 0.5, 1, 5, 10, 20, and 40μM), and the determined detection limits were 0.032 and 0.026 μM for NO_2^- and NO_3^-, respectively. Urea (QuikChem© Method 31-206-00-1-A) concentrations were measured at 530 nm when urea in the sample reacted with diacetyl in the presence of ferric ions. The determined detection limit was 0.072 μM (as urea), and eight urea standards (0, 0.37, 0.75, 1, 2.5, 5, 10, and 20 μM) were used for calibration. Concentrations of o-PO_4^{3-} (QuikChem© Method 31-115-01-1-I) were determined at 880 nm using a reaction with NH_4^+ molybdate and antimony potassium tartrate in acid to form a blue dye, with a determined detection limit of 0.0046 μM. Potassium phosphate standards (0, 0.03, 0.1, 0.5, 1, 2, 5, and 10 μM) were used for calibration. In all cases, standard curves were acceptable at a coefficient of determination (R^2) greater than 0.999.

Data Calculations and Statistics

Dissolved gas and nutrient fluxes into and out of the sediment were calculated for each core and sampling event (n = 6 per incubation and treatment). A positive net $^{28}N_2$ flux (N_2 production) from unamended cores indicated that the combination of denitrification and anammox were higher than N fixation. The sum of the fluxes of all N_2 species ($^{28,29,30}N_2$), plus any calculated N fixation occurring simultaneously from $^{15}NO_3^-$-amended cores (An et al. 2001), represented potential denitrification. A negative net $^{28}N_2$ flux in unamended cores indicated that N fixation exceeded the sum of denitrification and anammox. In $^{15}NH_4^+$-amended cores, a positive $^{29}N_2$ flux indicated possible anammox. It is called "possible anammox" because the production of $^{29}N_2$ cannot be distinguished from nitrification of added $^{15}NH_4^+$ to $^{15}NO_x$ combined via denitrification with in situ $^{14}NO_x$ to form $^{29}N_2$. Potential DNRA was determined as $^{15}NH_4^+$ production from $^{15}NO_3^-$-amended cores that significantly exceeded any $^{15}NH_4^+$ production in unamended control cores.

Dissolved gas concentrations (N_2, Ar, and O_2) were calculated using temperature-controlled water bath standards at 20°C and 30°C. These standards were compared with saturation tables of the dissolved gases at those temperatures, and measured signals were corrected for machine drift (Kana et al. 1994). The drift calculated from the standards was used to adjust N_2/Ar and O_2/Ar measurements, and the resulting ratios were multiplied by the saturation concentration of Ar at 20°C (the temperature of the water bath in which the MIMS inlet is immersed) to determine N_2 and O_2 concentrations. The one exception to this protocol was the $^{28}N_2$ concentrations at sites MB18 and WE2 sampled on August 3, 2016. Those concentrations were determined from the raw mass

$^{28}N_2$ signals (Kana et al. 1994) because the standards for this run were not usable. This procedure is not as precise as using ratio data for mass $^{28}N_2$ concentrations (Kana et al. 1994), but since net $^{28}N_2$ fluxes were the target result, concentration data was not as important as the relative differences in signal between inflowing and outflowing water for the experimental cores.

Fluxes were calculated (Lavrentyev et al. 2000) by subtracting the inflow concentrations of the nutrients and dissolved gases from the outflow concentrations and dividing that value by the water flow rate (measured daily, L hr^{-1}) multiplied by the sediment core surface area (0.0045 m^2). A negative flux indicated movement of solute into the sediments, and a positive flux represented efflux out of the sediments into overlying water. The exceptions were SOD and calculated N fixation (explained below), which were reported as positive values, even though they were measured as net O_2 and N_2 uptake, respectively. Fluxes of $^{28,29,30}N_2$ were then used, along with the abundances of $^{29,30}N_2$ relative to the total N_2 pool, to calculate N fixation and denitrification simultaneously (An et al. 2001). N fixation was calculated from a quadratic equation, and potential denitrification was calculated as the sum of $^{28,29,30}N_2$ plus calculated N fixation, if any. N fixation was reported as zero if the calculation returned a negative value (An et al. 2001).

Daily precipitation data for Toledo, Ohio, was downloaded from NOAA's National Centers for Environmental Information (www.ncei.noaa.gov), and Maumee River discharge rates, along with daily nutrient loads, were downloaded from the Lake Erie Tributary Monitoring Program maintained by the National Center for Water Quality Research at Heidelberg University in Tiffin, Ohio. Fluxes and error bars were graphed

using the ggplot2 (Wickham 2009) and gridExtra (Auguie 2017) packages in R (version 3.4.4, R Core Team), and statistics were performed in JMP (version 13.0.0, SAS Institute, Inc.) using a Spearman's ρ distribution because the data were not normally distributed. Comparisons between two different years of the same variable were performed using a paired two-way ANOVA. P values of 0.05 or less were considered significant. Correlation plots, as well as river discharge and precipitation graphs, were constructed using Kaleidagraph (Version 4.5.2, Synergy Software).

III. RESULTS

Ambient Conditions

Average precipitation amounts (Figure 4), river discharge rates (Figure 5; ANOVA, $p < 0.0001$), and wind speed (April 1 – July 31; ANOVA, $p = 0.04$) were all higher in 2017 than in 2016. There was no significant difference between surface water (Table 2) and bottom water (Table 3) temperatures throughout the year at any of the sites or between 2016 and 2017. The water temperature varied as expected, colder in the spring (average: 12.5ºC), peaking in mid-summer (average: 25.6ºC), and cooling off in the fall (average: 17.7ºC). 2016 had a slightly warmer average water temperature by 0.4ºC, but the difference was not significant. Overall, pH remained between 7.8 and 8.5 at all sites, depths, and sampling times. The specific conductance at MB18 was significantly higher than all other sites in both the surface and bottom water (ANOVA; $p < 0.01$), with the highest 2016 value recorded in September (566 µS cm^{-1}) and the highest 2017 value recorded in April (440 µS cm^{-1}). Chlorophyll-α (chl-a) fluorescence was generally higher in the surface water than in the bottom water, but this difference was not significant (ANOVA; $p = 0.6$). In 2016, the highest chl-a concentration was recorded in July, and while 2017 also had high chl-a concentrations in July, the highest concentrations occurred in April in both the surface and bottom waters. Note that fluorescence measured with the sonde would not capture surface scums during HABs. Dissolved oxygen (DO) concentrations in the water column did not reach hypoxic levels

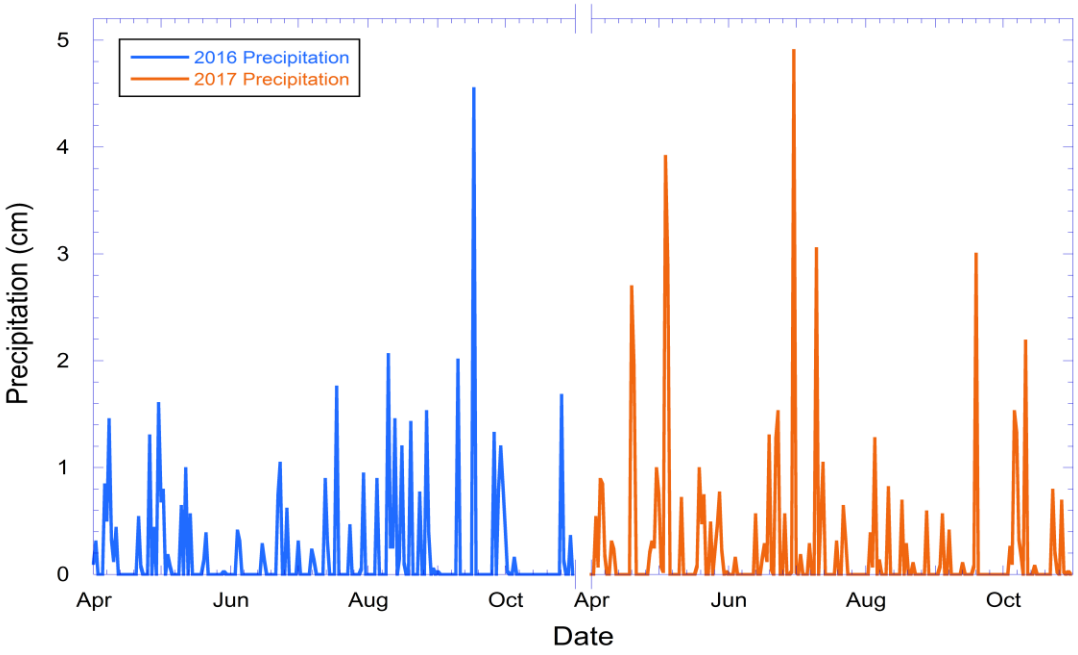

Figure 4: Daily mean precipitation data from April 1 – October 31, 2016 and 2017. Data downloaded from NOAA's National Centers for Environmental Information (www.ncei.noaa.gov) from station USW00004848 located at Toledo Metcalf Field, Ohio.

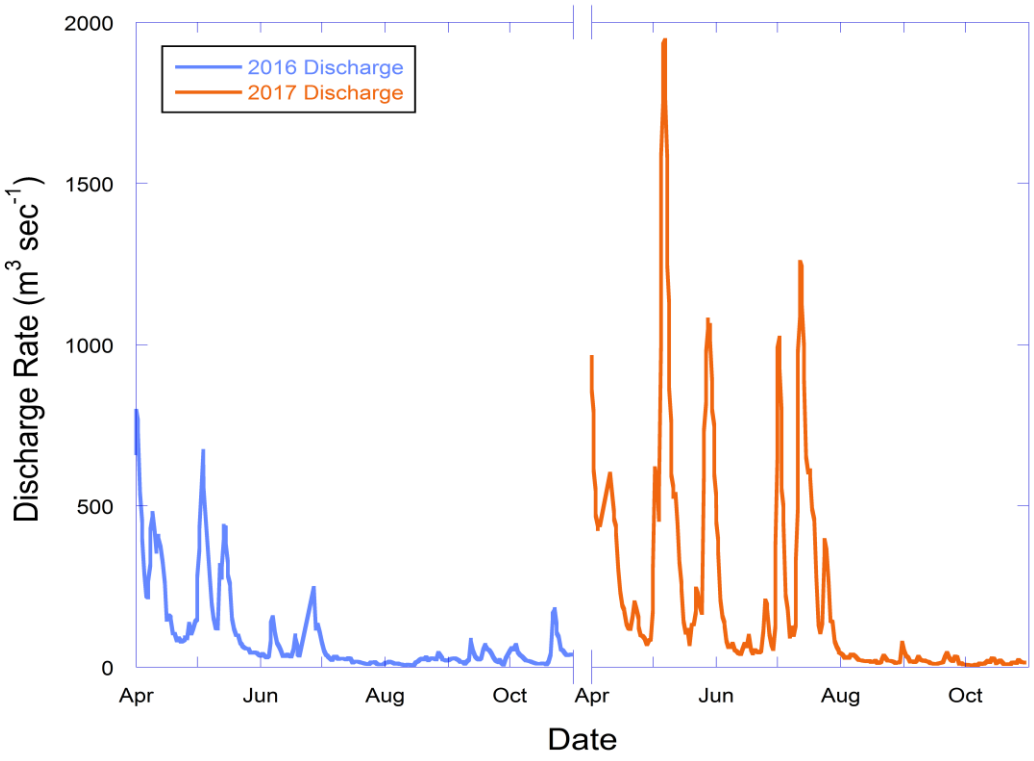

Figure 5: Daily Maumee River discharge data from April 1 – October 31, 2016 and 2017. Data downloaded from the Lake Erie Tributary Monitoring Program maintained by the National Center for Water Quality Research at Heidelberg University in Tiffin, Ohio. Data from USGS stream gauge 04193500 located in the Maumee River near Waterville, Ohio.

Table 2: Surface water sonde data from every sampling date and site. Missing data is indicated with ND. Data retrieved using NOAA GLERL's real time buoys (https://www.glerl.noaa.gov/res/HABs_and_Hypoxia/rtMonSQL.php) is shown with an asterisk (*), and data from the NOAA GLERL Weekly Data Share (2016, 2017) is shown with a carrot (^). DO saturation (DO SAT %) calculated from temperature and DO concentration is shown with two asterisks (**). MB18 is essentially the same as GLERL site WE6. Temp = Temperature, Sp. Cond. = Specific Conductance, and DO = Dissolved Oxygen.

Site	Date	Temp °C	pH	Sp Cond µS cm^{-1}	Chl-a µg L^{-1}	DO mg L^{-1}	DO SAT %
Spring							
WE4	5/18/2016	12.1	8.25	235	0.850	10.9	101
WE13		12.0	8.34	234	1.65	11.1	103
Early Summer							
WE4	6/28/2016	^24.2	*8.56	^256	^1.25	^8.83	**105
WE13		^23.8	ND	^234	^0.77	^6.67	**78.9
MB18	7/13/2016	^25.1	ND	^439	^13.4	^8.65	**105
WE2		25.1	8.53	342	3.58	8.32	101
Late Summer							
MB18	8/3/2016	27.2	8.91	323	2.91	10.7	135
WE2		26.6	8.58	253	3.34	9.68	121
WE4	8/10/2016	26.6	8.47	239	3.01	8.02	100
WE13		26.2	8.84	242	8.44	8.13	101
MB18	9/19/2016	21.8	8.66	566	^8.84	8.33	95.0
WE2		22.1	8.34	463	^1.92	7.88	90.4
Fall							
WE4	10/3/2016	18.2	8.33	359	^1.58	8.94	94.6
WE13		18.8	8.30	418	^1.83	8.72	93.7
MB18	10/17/2016	16.5	8.05	427	ND	9.12	93.4
WE2		16.9	7.85	250	*0.554	9.24	95.5
Spring							
MB18	4/25/2017	14.0	8.22	440	6.68	10.5	101
WE2		11.8	8.43	312	13.6	11.3	103
WE4	6/9/2017	17.9	8.67	231	0.84	9.71	101
WE13		18.9	8.30	252	1.03	9.64	103
Early Summer							
MB18	7/11/2017	26.3	8.31	402	12.6	8.65	106
WE2		26.1	8.33	267	1.05	8.29	101
WE4	7/14/2017	23.7	8.45	250	2.43	8.57	100
WE13		23.2	8.50	243	2.03	8.64	100
Late Summer							
WE4	8/2/2017	25.0	8.29	271	*0.172	8.38	102
WE13		25.4	8.73	245	*0.823	8.90	109
MB18	8/9/2017	24.0	8.83	280	4.19	9.18	108
WE2		^23.9	ND	^263	^0.160	^5.74	**68.1
Fall							
MB18	10/3/2017	18.48	8.59	278.7	7.36	9.58	
WE2		19.7	8.43	236.6	3.27	9.62	103.9
WE4	10/20/2017	16.11	7.43	226.3	0.88	10.14	101.9
WE13		16.74	8.18	235.9	2.88	9.97	101.4

Table 3: Bottom water sonde data (within 1 m above sediment surface) from every sampling trip. Missing data is indicated with ND. Data retrieved using NOAA GLERL's real time buoys (https://www.glerl.noaa.gov/res/HABs_and_Hypoxia/rtMonSQL.php) is shown with an asterisk (*), and data from the NOAA GLERL Weekly Data Share (2016, 2017) is shown with a carrot (^). DO saturation (DO SAT %) calculated from temperature and DO concentration is shown with two asterisks (**). MB18 is essentially the same as GLERL site WE6. Temp = Temperature, Sp. Cond. = Specific Conductance, and DO = Dissolved Oxygen.

Site	Date	Temp °C	pH	Sp Cond µS cm^{-1}	Chl-a µg L^{-1}	DO mg L^{-1}	DO SAT %
Spring							
WE4	5/18/2016	12.1	8.23	235	2.62	10.8	101
WE13		11.9	8.30	233	4.78	11.1	103
Early Summer							
WE4	6/28/2016	*23.3	*8.56	*248	*0.350	*9.33	**96.2
WE13		^22.8	ND	^235	^3.61	^6.77	**78.6
MB18	7/13/2016	^25.1	ND	^439	^13.4	^8.65	**105
WE2		24.9	8.45	342	1.86	8.21	99.3
Late Summer							
MB18	8/3/2016	26.8	8.84	350	3.52	9.27	116
WE2		25.7	7.83	226	1.23	6.32	77.5
WE4	8/10/2016	25.7	8.39	236	2.92	8.53	105
WE13		25.9	8.54	235	7.19	8.36	103
MB18	9/19/2016	21.7	8.68	520	^8.84	8.23	93.8
WE2		21.9	8.34	436	*0.530	7.35	84.1
Fall							
WE4	10/3/2016	18.1	8.33	338	*0.160	8.78	93.1
WE13		18.8	8.30	418	*0.280	8.72	93.7
MB18	10/17/2016	16.5	8.07	427	0.430	9.09	93.2
WE2		16.9	7.82	250	*0.560	9.23	95.4
Spring							
MB18	4/25/2017	14.0	8.18	440	7.52	10.0	96.1
WE2		11.8	8.37	310	10.1	11.4	104
WE4	6/9/2017	17.6	8.33	231	1.15	9.94	103
WE13		18.2	8.28	251	1.70	9.53	100
Early Summer							
MB18	7/11/2017	23.6	7.88	375	3.40	7.04	82.1
WE2		22.8	8.15	259	1.18	7.81	89.7
WE4	7/14/2017	23.6	8.41	250	1.85	8.28	96.5
WE13		23.2	8.38	243	2.14	8.40	97.2
Late Summer							
WE4	8/2/2017	24.2	8.33	264	*0.198	5.89	70.3
WE13		23.8	8.28	246	0.12	6.01	71.2
MB18	8/9/2017	23.0	8.72	280	3.59	8.55	98.6
WE2		*23.0	*8.24	*221	*0.221	*8.23	**96.0
Fall							
MB18	10/3/2017	18.5	8.81	277	9.43	9.51	100
WE2		19.8	8.35	238	3.52	8.81	95.3
WE4	10/20/2017	16.1	8.28	226	1.44	9.91	99.5
WE13		16.7	8.25	236	5.41	9.6	97.6

(less than 2 mg L^{-1}; Zhou et al. 2013), but DO concentrations were significantly higher in surface water (ANOVA; $p = 0.04$). There were no seasonal DO trends, and none of the sites in the western basin exhibited strong stratification (temperature and DO) during the sampling seasons.

Ambient Nutrients

Overall, ambient nutrient concentrations (Tables 4 and 5) were higher in 2017 than in 2016, and they were primarily higher earlier in the season. NH_4^+ concentrations in the surface and bottom water were not significantly different (ANOVA; $p = 0.1$). In 2016, surface NH_4^+ concentrations ranged from 0.086 µM at WE2 on July 13 to 5.95 µM at MB18 on August 3. Bottom water NH_4^+ concentrations ranged from 0.226 µM at WE2 on October 17 to 7.87 at WE2 on September 19. In 2017, both surface and bottom water NH_4^+ concentrations ranged from below the detection limit (0.04 µM) at MB18 on October 3 to 7.24 µM at the surface and 7.27 µM at the bottom on July 11, also at MB18. NO_2^- was always detectable in both surface and bottom water samples but was usually less than 3 µM. Exceptions occurred on May 18, 2016, when surface and bottom water samples at WE4 and WE13 were 7.29 µM, and on July 11, 2017, at MB18, when the surface water had a NO_2^- concentration of 11.2 µM, and the bottom water had a concentration of 10.8 µM. NO_3^- concentrations were the most variable and not significantly different between depths or years. In 2016, surface water NO_3^- concentrations ranged from 1.62 µM at WE13 on August 10 to 53.4 µM at MB18 on July 13, and bottom water concentrations ranged from 2.75 at WE13 on August 10 to 66.1 at MB18 on August 3. In 2017, surface and bottom water NO_3^- concentrations ranged from

Table 4: Surface water geochemical data collected at each site and time. Units are in μM N (or P). Measurements below the detection limit are reported as less than that method's detection limit.

Site	Date	Surface				
		NH4+	NO2-	NO3-	Urea	OP
Spring						
WE4	5/18/2016	0.828	7.29	6.75	0.435	0.0575
WE13		0.291	7.29	19.7	0.279	0.0457
Early Summer						
WE4	6/28/2016	1.58	1.02	23.3	2.42	0.025
WE13		0.276	0.421	21.9	1.01	0.0304
MB18	7/13/2016	0.203	1.38	53.4	6.20	0.203
WE2		0.0863	1.44	17.7	4.03	0.0863
Late Summer						
MB18	8/3/2016	5.95	2.92	50.3	0.279	0.0448
WE2		0.275	1.61	4.01	1.47	0.0458
WE4	8/10/2016	3.20	1.94	8.85	1.15	0.0516
WE13		0.203	0.842	1.62	3.23	0.0661
Fall						
MB18	9/19/2016	0.489	0.799	9.84	1.30	0.631
WE2		2.41	7.87	5.78	1.57	0.892
WE4	10/3/2016	1.86	0.429	18.9	0.941	0.566
WE13		0.950	2.56	7.83	1.12	1.13
MB18	10/17/2016	2.06	0.652	27.4	1.05	0.742
WE2		0.426	0.741	20.0	0.727	0.375
Spring						
MB18	4/25/2017	4.60	3.08	228	3.51	1.35
WE2		3.81	0.750	60.0	2.07	0.0976
Early Summer						
WE4	6/9/2017	0.302	0.308	31.0	0.698	0.0103
WE13		1.91	0.453	33.1	0.879	0.0122
MB18	7/11/2017	7.24	11.2	487	4.95	1.76
WE2		1.17	0.680	51.9	1.93	0.0969
WE4	7/14/2017	1.21	1.19	37.9	1.17	0.0314
WE13		1.19	0.983	34.7	0.531	0.0446
Late Summer						
WE4	8/2/2017	0.987	2.25	93.8	0.931	0.0310
WE13		< 0.04	0.610	41.0	0.304	0.0354
MB18	8/9/2017	1.12	1.35	98.7	1.39	0.215
WE2		1.03	0.738	34.8	3.58	0.0441
Fall						
MB18	10/3/2017	< 0.04	0.0747	0.0135	0.666	0.0874
WE2		0.833	0.647	14.5	0.953	0.126
WE4	10/20/2017	0.414	0.171	14.8	0.333	0.0872
WE13		0.533	0.341	14.6	0.431	0.361

Table 5: Bottom water geochemical data collected at each site and time. Units are in μM N (or P). Measurements below the detection limit are reported as less than that method's detection limit.

Site	Date	Bottom				
		NH4+	NO2-	NO3-	Urea	OP
Spring						
WE4	5/18/2016	1.72	7.29	9.46	0.589	0.0494
WE13		6.04	7.28	15.5	0.414	0.0606
Early Summer						
WE4	6/28/2016	1.02	0.635	23.1	0.606	0.0253
WE13		0.421	1.22	27.1	1.27	0.0280
MB18	7/13/2016	2.53	1.42	58.0	1.43	0.135
WE2		1.84	0.801	38.4	1.71	0.0862
Late Summer						
MB18	8/3/2016	2.92	1.52	66.1	1.24	0.0730
WE2		1.61	0.489	12.2	1.37	0.0474
WE4	8/10/2016	1.94	0.792	10.2	2.13	0.0760
WE13		0.842	0.227	2.75	1.27	0.0732
Fall						
MB18	9/19/2016	0.799	0.567	9.99	2.15	0.789
WE2		7.87	0.750	5.68	1.13	0.936
WE4	10/3/2016	1.90	0.430	18.8	0.783	0.560
WE13		0.906	2.53	7.81	1.21	1.13
MB18	10/17/2016	1.87	0.737	30.0	1.21	0.795
WE2		0.226	0.751	20.4	0.447	0.383
Spring						
MB18	4/25/2017	4.60	3.22	241	4.28	1.17
WE2		3.59	0.665	58.5	1.53	0.0505
Early Summer						
WE4	6/9/2017	0.835	0.289	31.3	1.04	0.0280
WE13		2.88	0.446	33.3	4.40	0.0572
MB18	7/11/2017	7.27	10.8	481	3.71	1.94
WE2		2.80	0.745	46.5	1.78	0.158
WE4	7/14/2017	1.40	0.820	37.5	0.932	0.0324
WE13		0.564	0.358	34.8	0.708	0.0275
Late Summer						
WE4	8/2/2017	0.258	2.37	90.2	1.33	0.0401
WE13		0.283	0.534	35.3	0.706	0.0419
MB18	8/9/2017	1.41	1.26	97.0	6.18	0.201
WE2		1.11	0.706	34.6	2.00	0.0603
Fall						
MB18	10/3/2017	< 0.04	0.0281	0.0781	0.530	0.178
WE2		0.686	0.612	14.6	0.858	0.124
WE4	10/20/2017	0.321	0.172	14.8	0.289	0.0868
WE13		0.465	0.336	14.2	0.422	0.365

0.014 to 0.078 µM, respectively, at MB18 on October 3 to 487 and 481 µM, respectively, at MB18 on July 11. Ambient NO_2^- and NO_3^- concentrations were positively correlated in both surface water ($p < 0.0007$) and bottom water ($p < 0.0001$). Urea was the only nutrient that had the highest concentration in 2016 rather than 2017. In 2016, surface water urea concentrations ranged from 0.279 µM at WE13 on May 18 and MB18 on August 3 to 6.20 µM at MB18 on July 13. Bottom water concentrations ranged from 0.414 µM at WE13 on May 18 to 2.15 µM at MB18 on September 19. In 2017, surface water urea concentrations ranged from 0.304 µM at WE13 on August 2 to 4.95 at MB18 on July 11, and bottom water concentrations ranged from 0.289 µM at WE4 on October 20 to 6.18 µM at MB18 on August 9. Surface and bottom water concentrations were not significantly different, and there were no spatial or seasonal differences in ambient urea concentrations. Surface and bottom water concentrations of o-PO_4^{3-} were also low and did not show any significant differences between depths or years. In 2016, surface and bottom water concentrations of o-PO_4^{3-} ranged from 0.025 at WE4 on June 28 to 1.13 µM at WE13 on October 3. In 2017, surface water o-PO_4^{3-} concentrations ranged from 0.010 µM at WE4 on June 9 to 1.76 µM at MB18 on July 11, and bottom water concentrations ranged from 0.028 µM at WE13 on July 14 to 1.94 µM at MB18 on July 11.

Sediment Nutrient Fluxes

Ambient nutrient fluxes were calculated from the unamended "control" cores, where positive values indicated nutrient release from sediments, and negative values show an influx from the overlying water into the sediments. NH_4^+ fluxes (Figure 6) were significantly greater in 2016 than in 2017 across all sites (ANOVA; $p = 0.01$). In 2016,

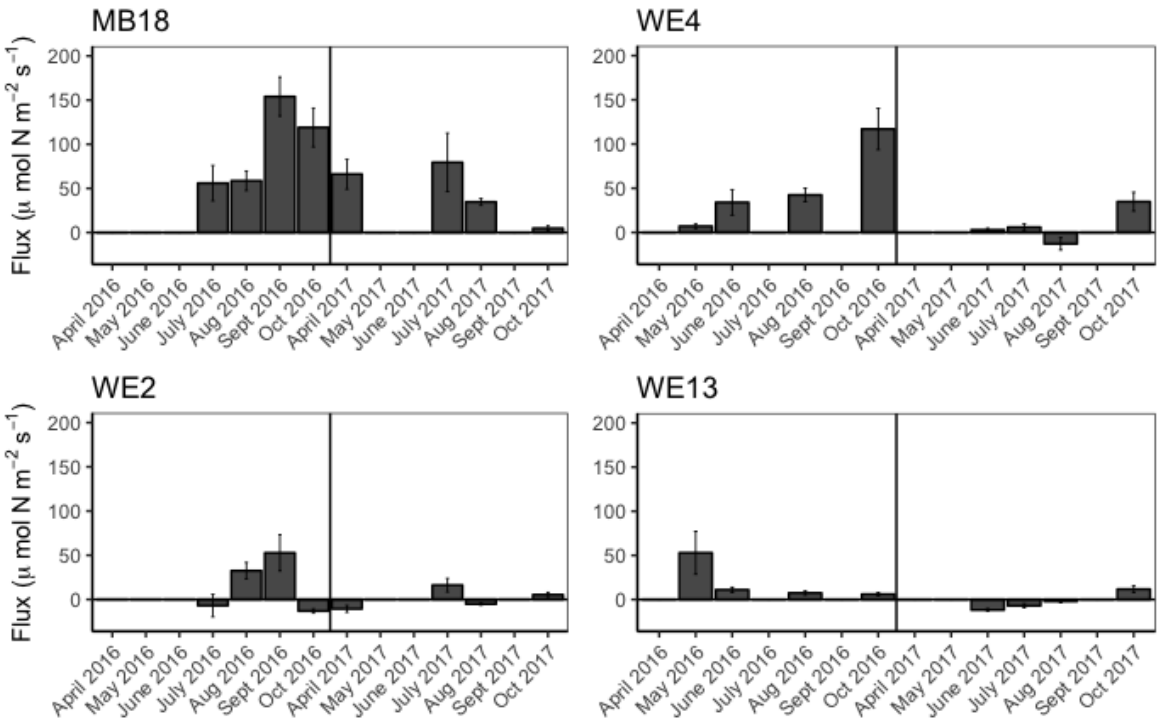

Figure 6: Sediment NH_4^+ fluxes from each site from all sampling events from April to October in 2016 (left of center line) and 2017 (right of center line). Sites MB18/WE2 and WE4/WE13 were sampled together and are stacked for scale. A positive value indicates an efflux of NH_4^+ from the sediments, and a negative value indicates NH_4^+ influx into the sediments.

sediments were, on average, a net NH_4^+ source at all sites (MB18 = 96.9 ± 24.0 µmol N m^{-2} hr^{-1}; WE2 = 16.3 ± 15.8 µmol N m^{-2} hr^{-1}; WE4 = 50.0 ± 23.5 µmol N m^{-2} hr^{-1}; WE13 = 19.3 ± 11.2 µmol N m^{-2} hr^{-1}), whereas 2017 had lower average NH_4^+ fluxes, and WE13 was a net NH_4^+ sink (MB18 = 46.2 ± 16.7 µmol N m^{-2} hr^{-1}; WE2 = 1.43 ± 5.95 µmol N m^{-2} hr^{-1}; WE4 = 7.71 ± 9.94 µmol N m^{-2} hr^{-1}; WE13 = -2.38 ± 5.10 µmol N m^{-2} hr^{-1}). The largest efflux occurred in September 2016 at MB18 (154 ± 22.1 µmol N m^{-2} hr^{-1}), and the largest NH_4^+ uptake was observed in August 2017 at site WE4 (-12.9 ± 6.90 µmol N m^{-2} hr^{-1}). NH_4^+ fluxes were significantly greater at MB18 than at WE2 (ANOVA; $p = 0.004$), WE4 ($p = 0.03$), and WE13 ($p = 0.01$), and the fluxes were correlated to the ambient bottom water concentrations of NH_4^+ in the water column ($\rho = 0.474$; $p = 0.006$).

NO_2^- flux direction was variable (Figure 7), but both NO_2^- uptake and efflux generally occurred at low rates. On average, NO_2^- uptake occurred at all sites in 2016 (MB18 = -0.171 ± 3.23 µmol N m^{-2} hr^{-1}; WE2 = -0.941 ± 0.713 µmol N m^{-2} hr^{-1}; WE4 = -0.526 ± 1.17 µmol N m^{-2} hr^{-1}; WE13 = -2.01 ± 3.04 µmol N m^{-2} hr^{-1}), and in 2017, there was average NO_2^- uptake at MB18 (-10.5 ± 7.64 µmol N m^{-2} hr^{-1}) and WE4 (-0.091 ± 2.20 µmol N m^{-2} hr^{-1}) and average NO_2^- efflux at WE2 (0.715 ± 1.91 µmol N m^{-2} hr^{-1}) and WE13 (0.161 ± 1.06 µmol N m^{-2} hr^{-1}). The largest NO_2^- uptake occurred in July 2017 at MB18 (-31.5 ± 11.5 µmol N m^{-2} hr^{-1}), and the largest efflux occurred in October 2016 at MB18 (8.12 ± 2.96 µmol N m^{-2} hr^{-1}). NO_2^- fluxes were positively correlated to bottom water NO_2^- concentrations in the water column ($\rho = 0.438$; $p = 0.01$).

Sediments usually exhibited net NO_3^- uptake (Figure 8), but low rates of efflux also occurred on some occasions. Lower fluxes (e.g., < 50 µmol N m^{-2} hr^{-1}) were often

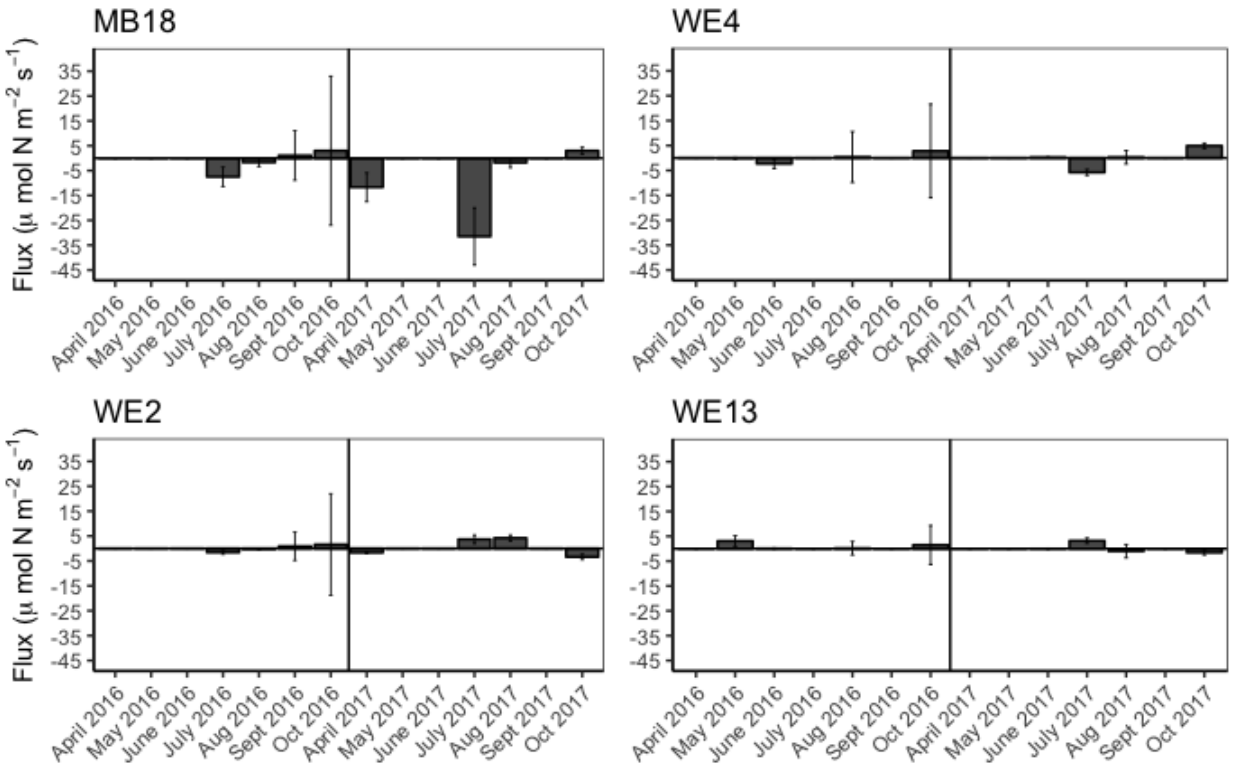

Figure 7: Sediment NO_2^- fluxes from each site from all sampling events from April to October in 2016 (left of center line) and 2017 (right of center line). Sites MB18/WE2 and WE4/WE13 were sampled together and are stacked for scale. A positive value indicates an efflux of NO_2^- from the sediments, and a negative value indicates NO_2^- influx into the sediments.

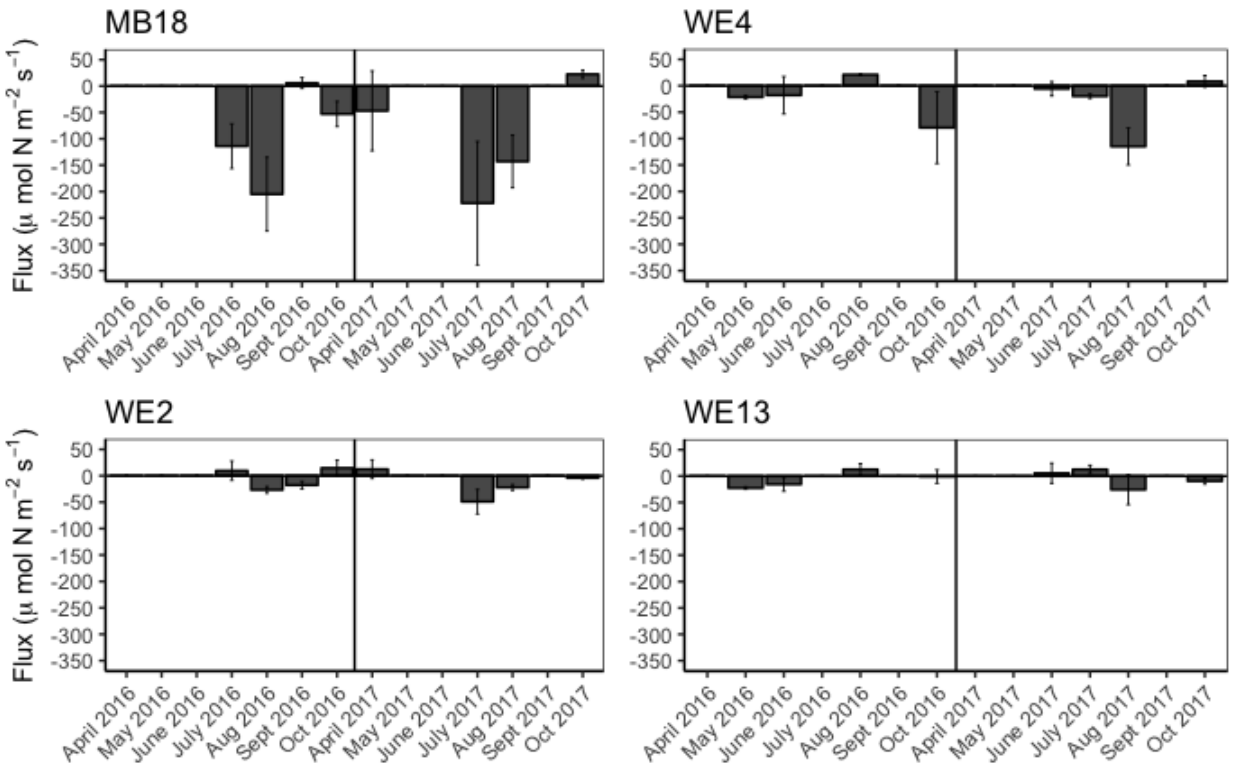

Figure 8: Sediment NO_3^- fluxes from each site from all sampling events from April to October in 2016 (left of center line) and 2017 (right of center line). Sites MB18/WE2 and WE4/WE13 were sampled together and are stacked for scale. A positive value indicates an efflux of NO_3^- from the sediments, and a negative value indicates NO_3^- influx into the sediments.

characterized by large error bars overlapping zero, indicating that the duplicate cores exhibited opposite NO_3^- flux directions. NO_3^- fluxes ranged from -222 ± 117 µmol N m^{-2} hr^{-1} at MB18 in July 2017 to 22.4 ± 7.42 µmol N m^{-2} hr^{-1} at MB18 in October 2017. In 2016, all sites, on average, exhibited NO_3^- uptake (MB18 = -91.5 ± 44.9 µmol N m^{-2} hr^{-1}; WE2 = -5.13 ± 10.1 µmol N m^{-2} hr^{-1}; WE4 = -24.5 ± 20.7 µmol N m^{-2} hr^{-1}; WE13 = -6.6 ± 7.86 µmol N m^{-2} hr^{-1}). The same trend was observed in 2017 (MB18 = -97.5 ± 53.8 µmol N m^{-2} hr^{-1}; WE2 = -15.7 ± 13.2 µmol N m^{-2} hr^{-1}; WE4 = -33.1 ± 27.9 µmol N m^{-2} hr^{-1}; WE13 = -4.37 ± 8.52 µmol N m^{-2} hr^{-1}). NO_3^- fluxes at MB18 were significantly greater than those at WE2 (ANOVA; $p = 0.02$) and WE13 ($p = 0.03$), but not at WE4 ($p = 0.07$). NO_3^- fluxes were not only negatively correlated with ambient bottom water NO_3^- concentrations in the water column ($\rho = -0.590$; $p = 0.0004$), but also with ambient NO_2^- ($\rho = -0.507$; $p = 0.003$) and ambient NH_4^+ concentrations ($\rho = -0.403$; $p = 0.02$), as well as NH_4^+ fluxes ($\rho = -0.464$; $p = 0.008$).

The direction of urea fluxes (Figure 9) varied at every site except MB18, where they were always positive. However, in both 2016 and 2017, sediments were, on average, a net source of urea at all sites (MB18 = 6.57 ± 3.04 and 10.7 ± 5.47 µmol N m^{-2} hr^{-1}; WE2 = 4.13 ± 4.47 and 6.28 ± 4.29 µmol N m^{-2} hr^{-1}; WE4 = 2.71 ± 2.17 and 5.09 ± 2.78; WE13 = 2.42 ± 1.20 and 1.65 ± 2.84 µmol N m^{-2} hr^{-1}, all respectively). The highest urea uptake occurred at WE2 in July 2016 (-4.44 ± 5.36 µmol N m^{-2} hr^{-1}), and the highest urea efflux occurred at MB18 in July 2017 (26.5 ± 7.13 µmol N m^{-2} hr^{-1}). Urea fluxes were negatively correlated with NO_3^- fluxes ($\rho = -0.454$; $p = 0.009$; Figure 10) and positively correlated with NH_4^+ fluxes ($\rho = 0.477$; $p = 0.006$; Figure 11).

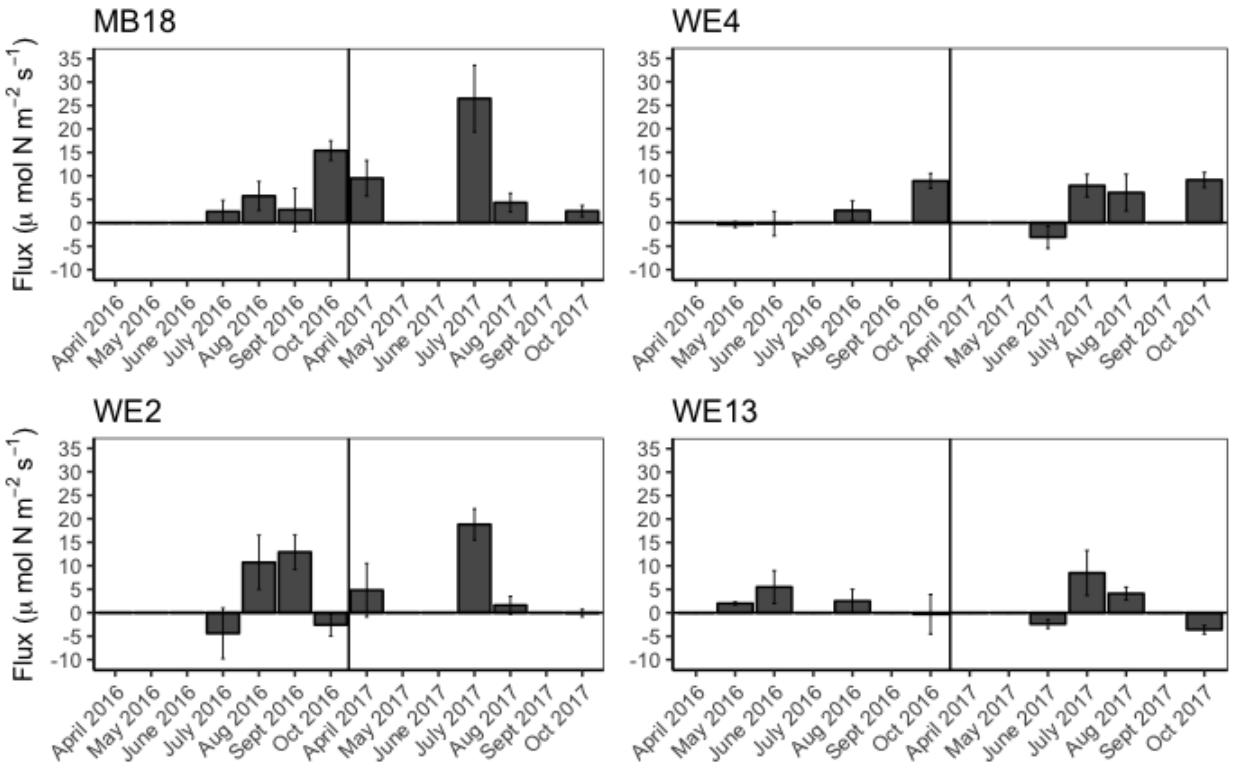

Figure 9: Sediment urea fluxes from each site from all sampling events from April to October in 2016 (left of center line) and 2017 (right of center line). Sites MB18/WE2 and WE4/WE13 were sampled together and are stacked for scale. A positive value indicates an efflux of urea from the sediments, and a negative value indicates urea influx into the sediments.

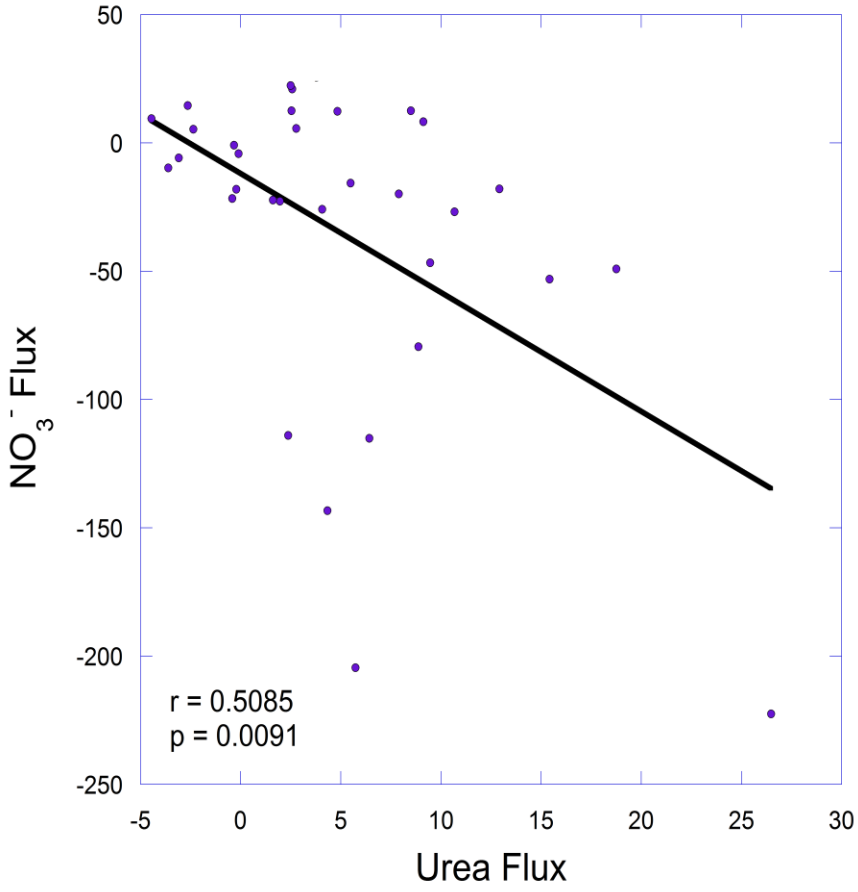

Figure 10: Relationship between urea fluxes and NO_3^- fluxes from all 32 sampling points (4 sites at 8 different sampling events; $\rho = -0.45$).

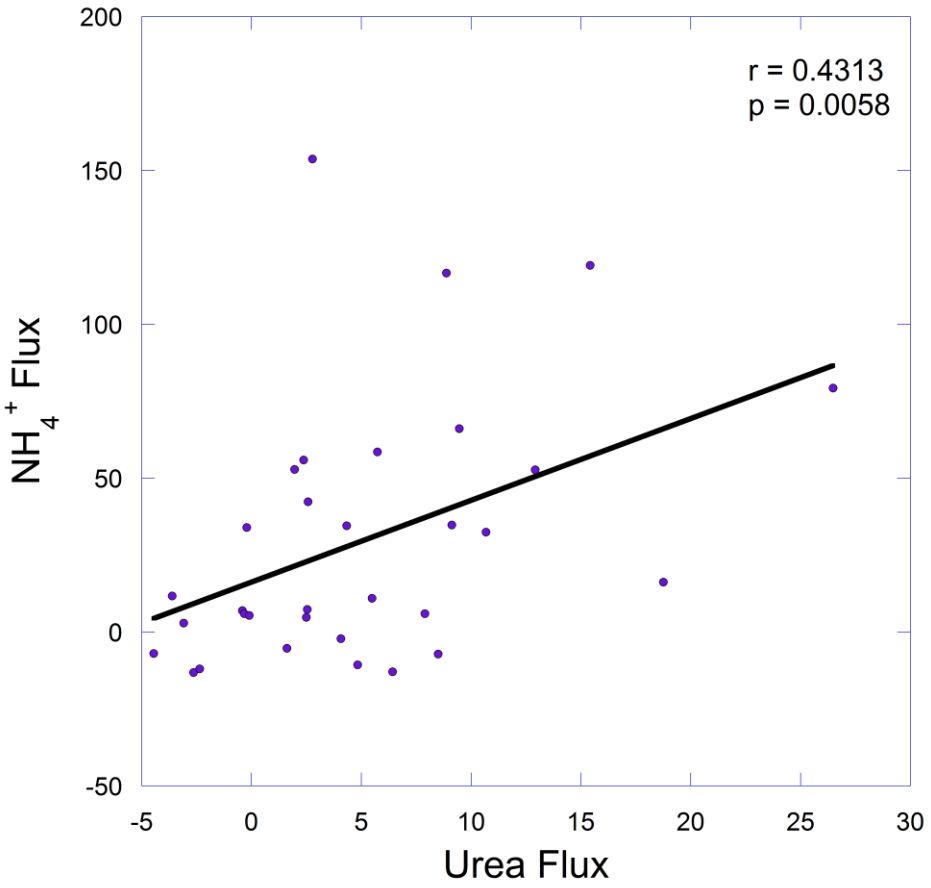

Figure 11: Relationship between urea fluxes and NH_4^+ fluxes from all 32 sampling points (4 sites at 8 different sampling events; $\rho = 0.48$).

In 2016, sediments were a net source of o-PO_4^{3-} (Figure 12) at all sites except for WE13, where the sediments were a net o-PO_4^{3-} sink (MB18 = 4.42 ± 1.12 µmol N m^{-2} hr^{-1}; WE2 = 2.03 ± 0.284 µmol N m^{-2} hr^{-1}; WE4 = 2.43 ± 0.828 µmol N m^{-2} hr^{-1}; WE13 = -0.029 ± 0.385 µmol N m^{-2} hr^{-1}), while in 2017, sediments were a net source of o-PO_4^{3-} at all sites (MB18 = 6.77 ± 2.66 µmol N m^{-2} hr^{-1}; WE2 = 0.466 ± 0.055 µmol N m^{-2} hr^{-1}; WE4 = 0.807 ± 0.533 µmol N m^{-2} hr^{-1}; WE13 = 0.644 ± 0.313 µmol N m^{-2} hr^{-1}). o-PO_4^{3-} fluxes generally decreased from Maumee Bay into the main part of the western basin. The largest o-PO_4^{3-} efflux occurred at MB18 in July 2011 (13.0 ± 2.06 µmol N m^{-2} hr^{-1}). WE13 was the only site to exhibit o-PO_4^{3-} uptake, and the largest uptake occurred in October 2016 (-1.01 ± 0.922 µmol N m^{-2} hr^{-1}). o-PO_4^{3-} fluxes were significantly higher at MB18 than at WE2 (ANOVA; $p = 0.02$) and at WE13 ($p = 0.009$), but only marginally at WE4 ($p = 0.06$). o-PO_4^{3-} fluxes were also positively correlated with ambient bottom water o-PO_4^{3-} concentrations ($\rho = 0.589$; $p = 0.0004$) and NH_4^+ fluxes ($\rho = 0.620$; $p = 0.0002$; Figure 13).

Sediment Oxygen Demand

SOD ranged from 312 ± 12.8 µmol O_2 m^{-2} hr^{-1} at WE13 in July 2017 to 2160 ± 291 µmol O_2 m^{-2} hr^{-1} at MB18 in July 2017 (Figure 14). SOD fluxes at MB18 were significantly higher than fluxes at WE2 ($p = 0.004$), WE4 ($p = 0.04$), and WE13 ($p = 0.007$). SOD generally decreased with distance from the river mouth; however, in October 2017, WE13 had the highest SOD, and MB18 and WE2 had the lowest. SOD was significantly higher in 2016 (MB18 = 1760 ± 135 µmol O_2 m^{-2} hr^{-1}; WE2 = 1040 ±

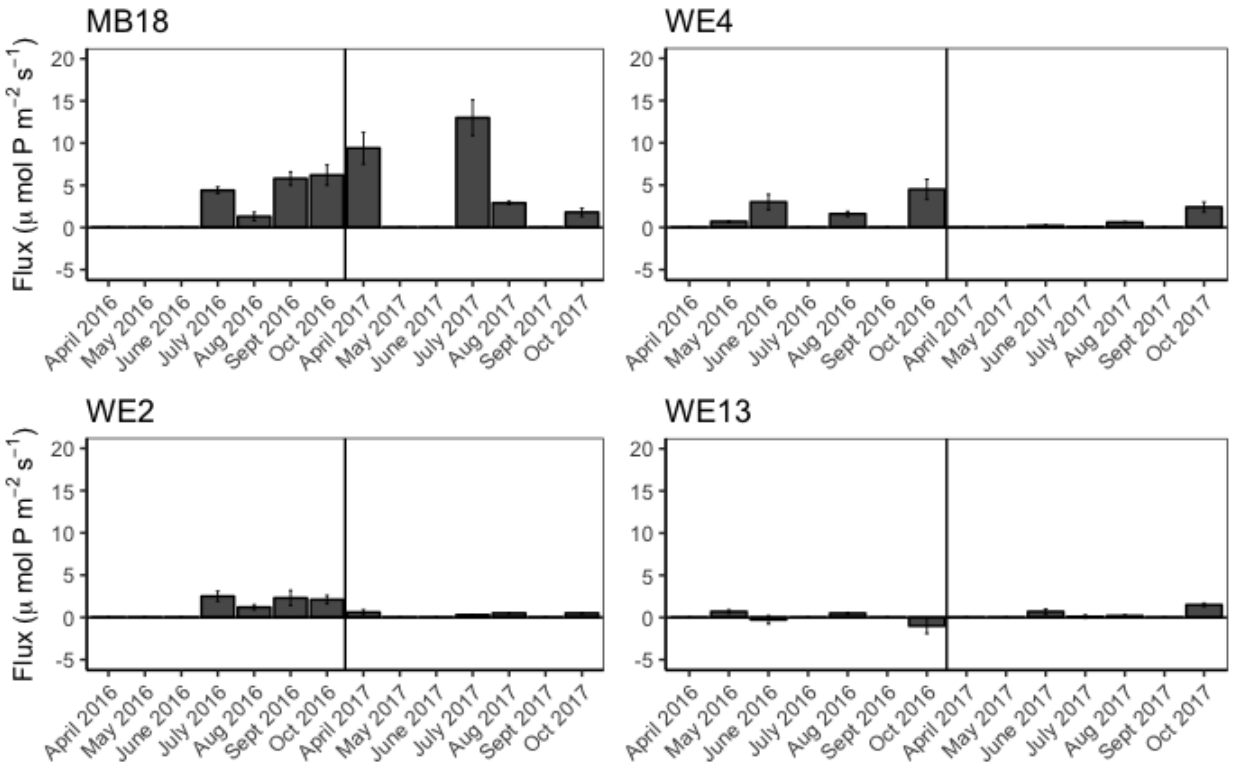

Figure 12: Sediment o-PO_4^{3-} fluxes from each site from all sampling events from April to October in 2016 (left of center line) and 2017 (right of center line). Sites MB18/WE2 and WE4/WE13 were sampled together and are stacked for scale. A positive value indicates an efflux of o-PO_4^{3-} from the sediments, and a negative value indicates o-PO_4^{3-} influx into the sediments.

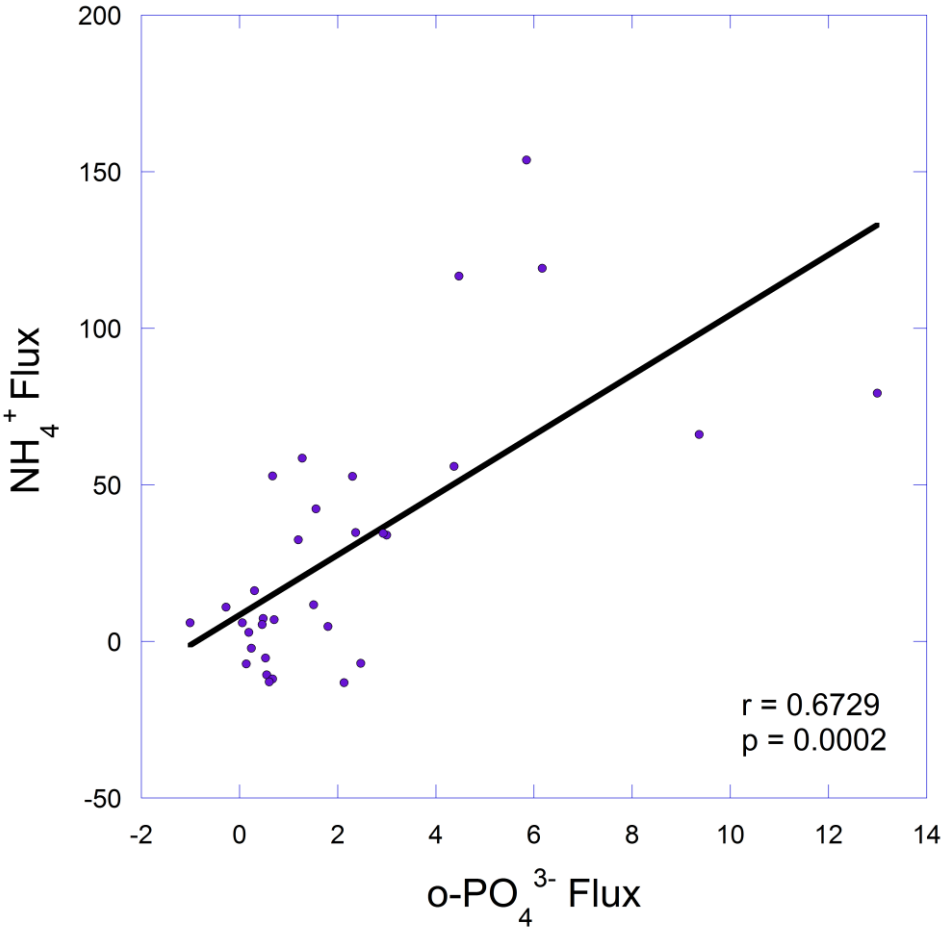

Figure 13: Relationship between o-PO_4^{3-} fluxes and NH_4^+ fluxes from all 32 sampling points (4 sites at 8 different sampling events; $\rho = 0.62$)

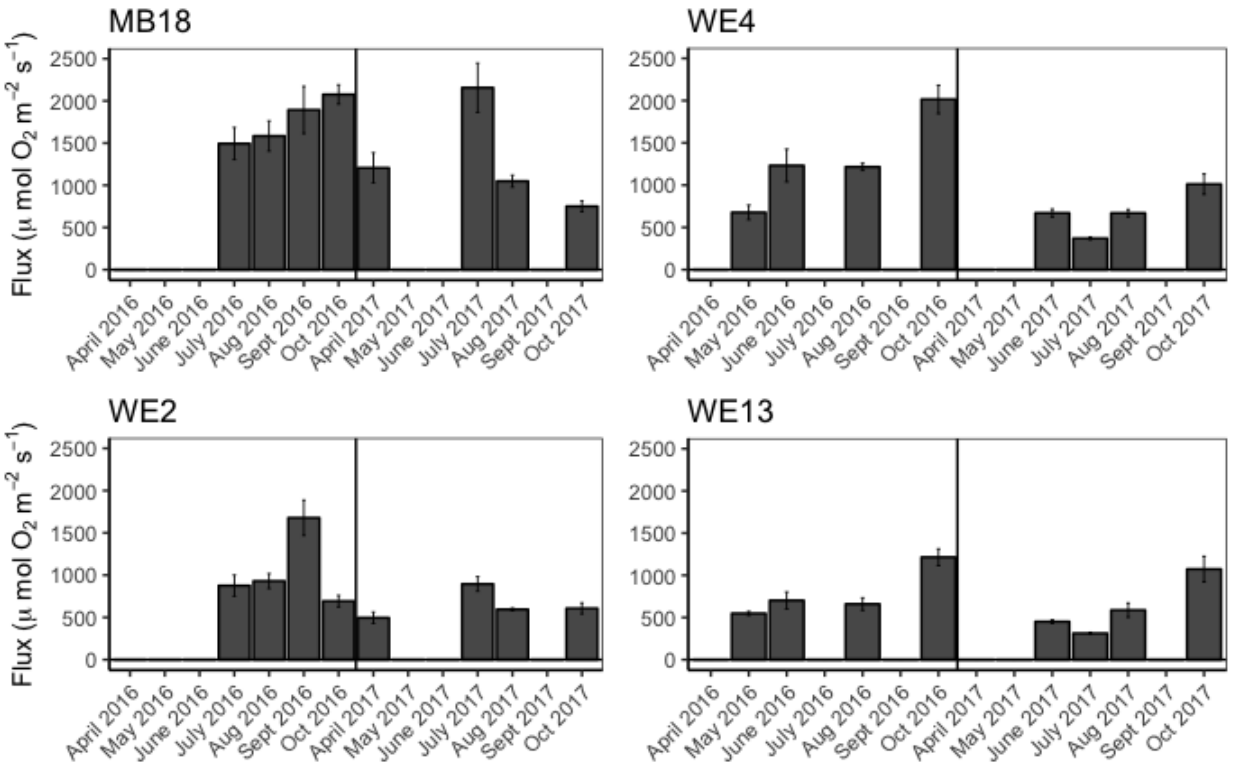

Figure 14: Sediment oxygen demand (SOD) from each site from all sampling events from April to October in 2016 (left of center line) and 2017 (right of center line). Sites MB18/WE2 and WE4/WE13 were sampled together and are stacked for scale. A positive value indicates a positive demand of oxygen (i.e., oxygen influx into sediments).

217 µmol O_2 m^{-2} hr^{-1}; WE4 = 1280 ± 275 µmol O_2 m^{-2} hr^{-1}; WE13 = 781 ± 148 µmol O_2 m^{-2} hr^{-1}) than in 2017 (MB18 = 1290 ± 303 µmol O_2 m^{-2} hr^{-1}; WE2 = 648 ± 85.9 µmol O_2 m^{-2} hr^{-1}; WE4 = 680 ± 131 µmol O_2 m^{-2} hr^{-1}; WE13 = 606 ± 165 µmol O_2 m^{-2} hr^{-1}; ANOVA; p = 0.02). SOD was positively correlated with NH_4^+ flux (ρ = 0.792), o-PO_4^{3-} bottom water concentrations (ρ = 0.655), and o-PO_4^{3-} fluxes (ρ = 0.728; p <0.001 for all relationships, Figure 15) and negatively correlated with NO_3^- fluxes (ρ = -0.360; p = 0.04, Figure 15). SOD was also positively correlated with specific conductance (ρ = 0.595; p < 0.001, Figure 16).

LOI ranged from 1.44% at WE4 in June 2016 to 7.01% at WE13 in July 2017 (Figure 17). LOI was not significantly different between 2016 (4.21%) and 2017 (4.88%). In contrast to SOD, however, WE13 had the highest LOI on average (6.88%), followed by WE2 (5.03%) and WE4 (4.24%). MB18 had the lowest average LOI (2.29%). LOI was negatively correlated with NH_4^+ fluxes (ρ = -0.337; p = 0.04), o-PO_4^{3-} fluxes (ρ = -0.695; p < 0.0001), and SOD (ρ = -0.495; p = 0.002).

Net $^{28}N_2$ Fluxes in Unamended Cores

Net $^{28}N_2$ fluxes are reported as either negative (net N fixation) or positive (net denitrification; Figure 18) fluxes; both processes occur simultaneously, and the net value represents the balance between the processes and identifies the process occurring at higher rates. In 2016, net N fixation occurred in May at WE4 (-30.6 ± 148 µmol N m^{-2} hr^{-1}) and in July at MB18 (-263 ± 93.0 µmol N m^{-2} hr^{-1}). In 2017, net N fixation was observed in April at MB18 (-135 ± 66.7 µmol N m^{-2} hr^{-1}) and WE2 (-103 ± 11.5 µmol

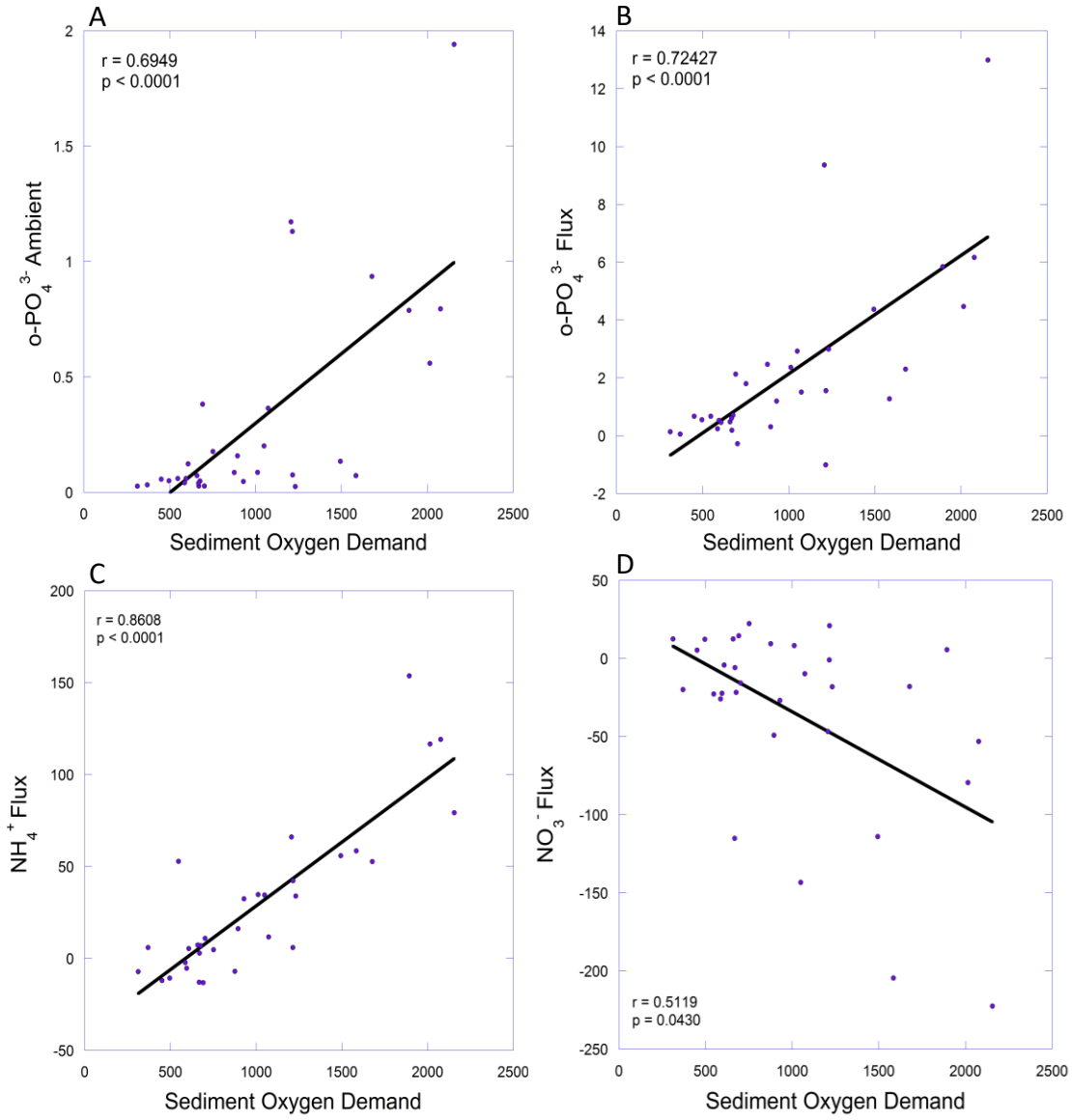

Figure 15: Relationships between SOD and (A) ambient bottom water o-PO_4^{3-} concentrations ($\rho = 0.65$), (B) o-PO_4^{3-} fluxes ($\rho = 0.73$), (C) NH_4^+ fluxes ($\rho = 0.79$), and (D) NO_3^- fluxes ($\rho = -0.36$).

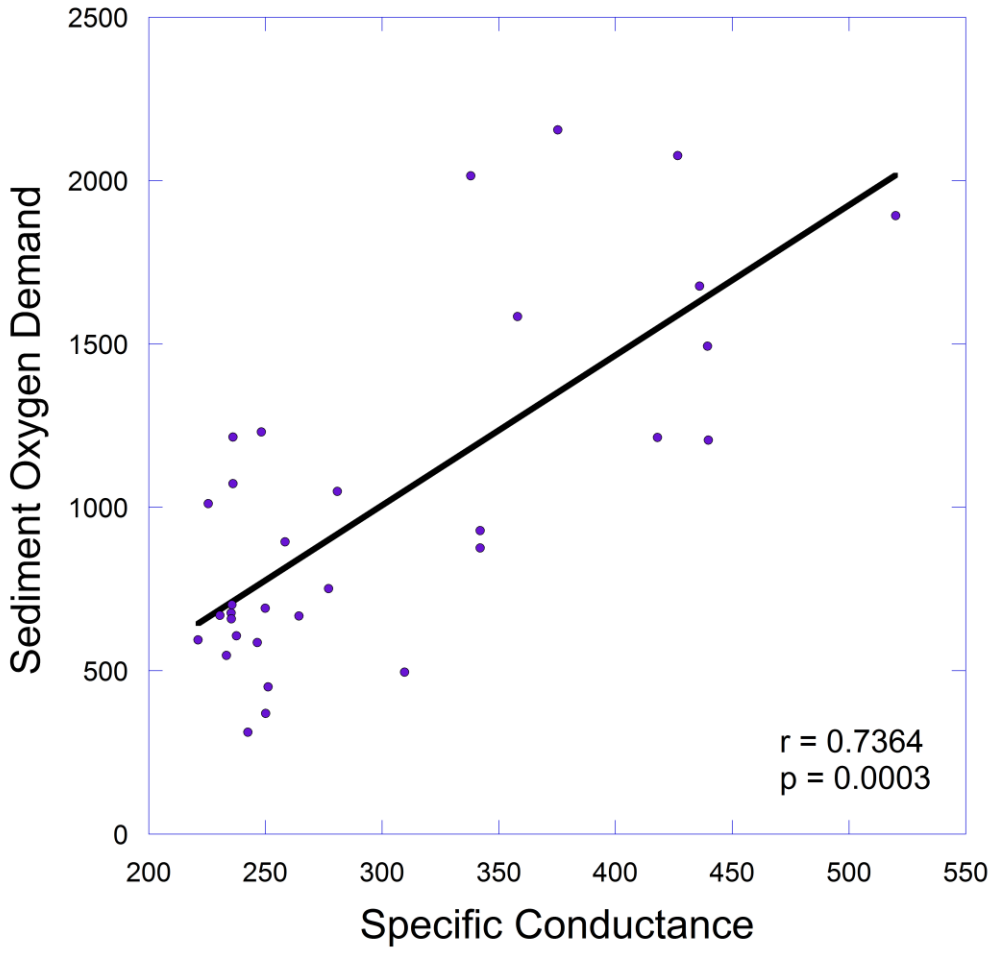

Figure 16: Relationship between specific conductance fluxes and SOD from all 32 sampling points (4 sites at 8 different sampling events; $\rho = 0.595$).

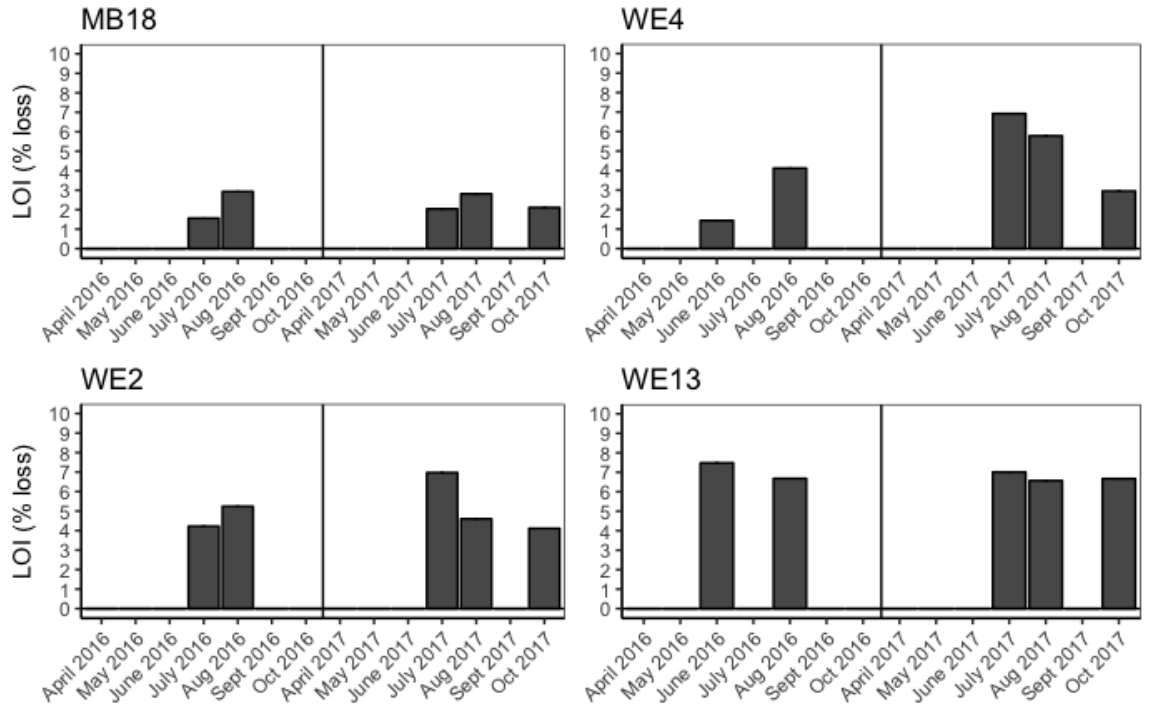

Figure 17: Loss on Ignition (LOI) from 20 subcores sampled in 2016 and 2017. Sites MB18/WE2 and WE4/WE13 were sampled together and are stacked for scale. Data is expressed as percent of mass lost.

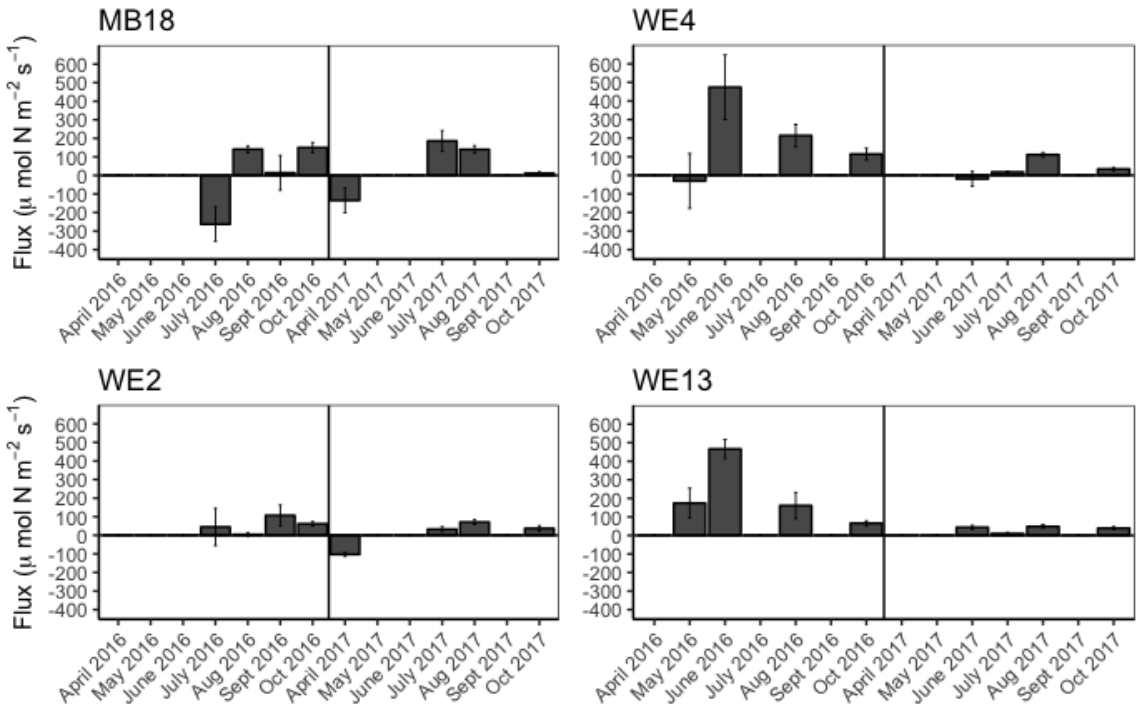

Figure 18: Net $^{28}N_2$ fluxes from each site from all sampling events from April to October in 2016 (left of center line) and 2017 (right of center line). Sites MB18/WE2 and WE4/WE13 were sampled together and are stacked for scale. A positive value indicates an efflux of $^{28}N_2$ from the sediments (net denitrification), and a negative value indicates an influx of $^{28}N_2$ into the sediments (net N fixation).

m^{-2} hr^{-1}) and in June at WE4 (-19.3 ± 39.7 µmol N m^{-2} hr^{-1}). Net $^{28}N_2$ fluxes showed net denitrification at all other sampling times and sites. In 2016, sediments were, on average, net denitrifying (MB18 = 10.4 ± 96.3 µmol N m^{-2} hr^{-1}; WE2 = 54.6 ± 21.3 µmol N m^{-2} hr^{-1}; WE4 = 193 ± 106 µmol N m^{-2} hr^{-1}; WE13 = 217 ± 86.6 µmol N m^{-2} hr^{-1}). Sediments also represented a net N sink in 2017 (MB18 = 50.5 ± 71.9 µmol N m^{-2} hr^{-1}; WE2 = 9.35 ± 38.5 µmol N m^{-2} hr^{-1}; WE4 = 35.8 ± 27.4 µmol N m^{-2} hr^{-1}; WE13 = 35.2 ± 8.61 µmol N m^{-2} hr^{-1}). Net $^{28}N_2$ fluxes were marginally greater in 2016 than in 2017 (ANOVA; $p = 0.06$) but were more consistent in 2017, with less variability between duplicate cores.

Possible Anammox

Possible anammox was measured as $^{29}N_2$ production from $^{15}NH_4^+$ amended cores. Throughout 2016 and 2017, a positive $^{29}N_2$ efflux was consistently detected (Figure 19), ranging from 0.43 ± 0.058 µmol N m^{-2} hr^{-1} at WE13 in May 2016 to 32.4 ± 4.22 µmol N m^{-2} hr^{-1} at MB18 in July 2017. Except in September 2016 and October 2017, the greatest $^{29}N_2$ fluxes occurred at MB18, which were significantly greater than those at WE4 (ANOVA; $p = 0.006$) and WE13 ($p = 0.01$), but not at WE2 ($p = 0.15$). On average, possible anammox could contribute to substantial N removal at all sites in both 2016 (MB18 = 19.7 ± 1.61 µmol N m^{-2} hr^{-1}; WE2 = 11.3 ± 1.96 µmol N m^{-2} hr^{-1}; WE4 = 9.16 ± 4.35 µmol N m^{-2} hr^{-1}; WE13 = 6.54 ± 2.62 µmol N m^{-2} hr^{-1}) and in 2017 (MB18 = 18.9 ± 4.51 µmol N m^{-2} hr^{-1}; WE2 = 13.5 ± 5.85 µmol N m^{-2} hr^{-1}; WE4 = 9.71 ± 4.43 µmol N m^{-2} hr^{-1}; WE13 = 10.7 ± 3.14 µmol N m^{-2} hr^{-1}). Overall, possible anammox accounted for 0.5% to 20.5% of total N_2 production. Possible anammox was significantly correlated (Figure 20) with NH_4^+ flux ($\rho = 0.417$; $p = 0.02$), ambient bottom water o-PO_4^{3-}

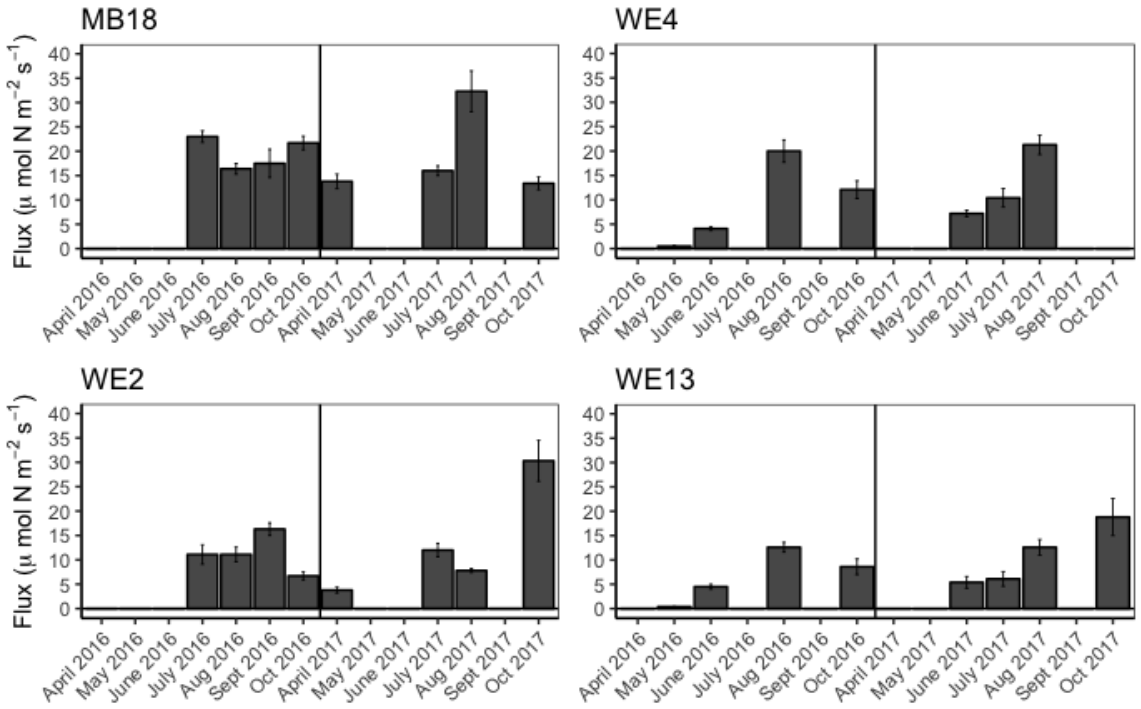

Figure 19: Net $^{29}N_2$ fluxes from each site from all sampling events from April to October in 2016 (left of center line) and 2017 (right of center line) from the $^{15}NH_4^+$ amended cores, indicating possible anammox. Sites MB18/WE2 and WE4/WE13 were sampled together and are stacked for scale.

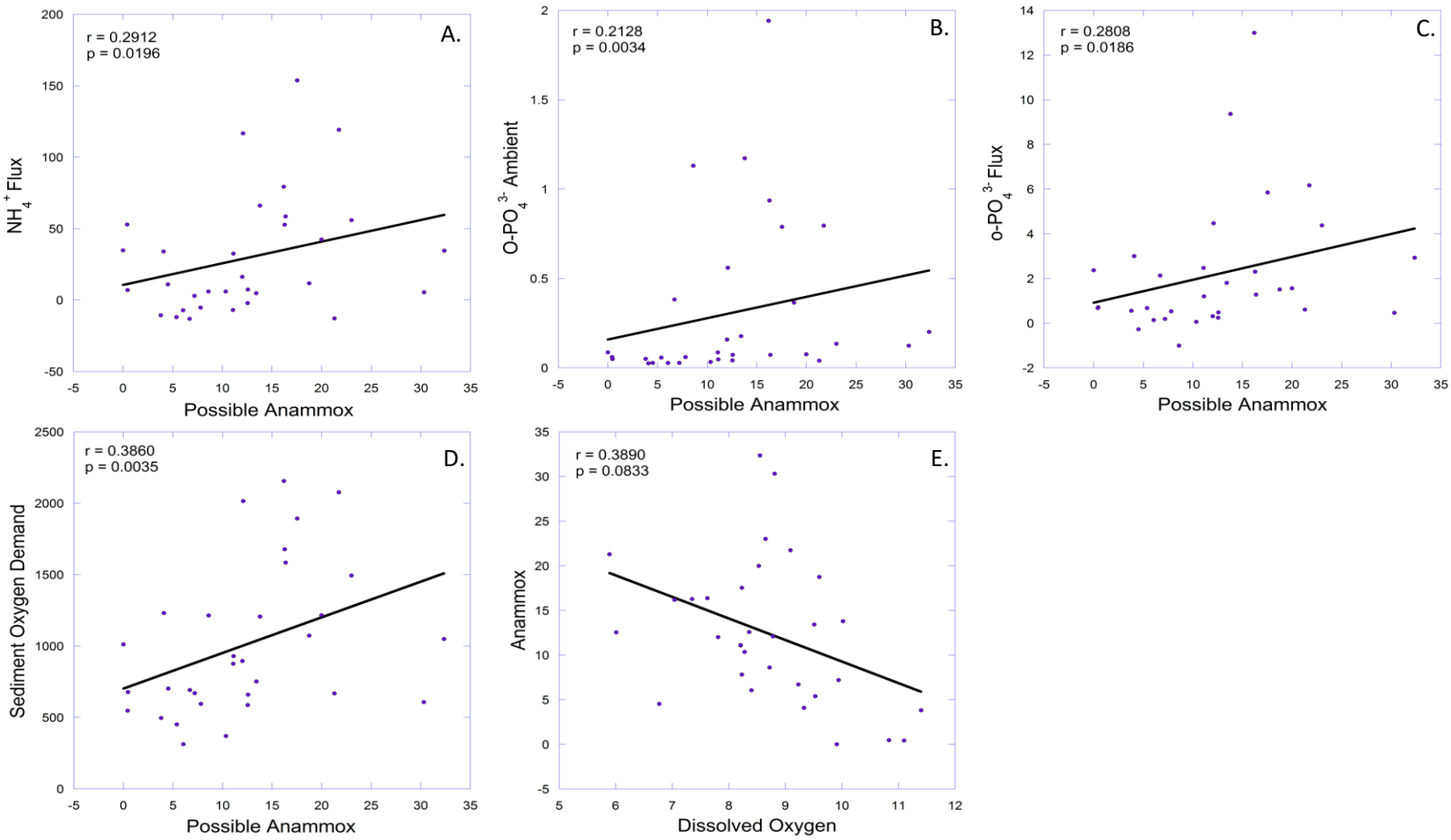

Figure 20: Relationships between possible anammox and (A) NH_4^+ fluxes ($\rho = 0.42$), (B) ambient bottom water o-PO_4^{3-} concentrations ($\rho = 0.51$), (C) o-PO_4^{3-} fluxes ($\rho = 0.42$), (D) SOD ($\rho = 0.51$), and (E) bottom-water DO concentration ($\rho = -0.32$).

concentrations ($\rho = 0.510$; $p < 0.01$), o-PO_4^{3-} fluxes ($\rho = 0.420$; $p = 0.02$), SOD ($\rho = 0.508$; $p < 0.01$), and marginally correlated with bottom water DO concentrations ($\rho = -0.316$; $p = 0.08$).

Effects of $^{15}NO_3^-$ Additions

Potential denitrification (Figure 21) was determined as the sum of $^{28,29,30}N_2$ production in $^{15}NO_3^-$ amended cores. Potential denitrification rates ranged from 20.1 ± 2.74 µmol N m^{-2} hr^{-1} at WE2 in April 2017 to 340 ± 17.6 µmol N m^{-2} hr^{-1} at MB18 in August 2016. On average, potential denitrification was higher at every site in 2016 (MB18 = 187 ± 54.7 µmol N m^{-2} hr^{-1}; WE2 = 126 ± 29.2 µmol N m^{-2} hr^{-1}; WE4 = 230 ± 33.0 µmol N m^{-2} hr^{-1}; WE13 = 165 ± 52.2 µmol N m^{-2} hr^{-1}) than 2017 (MB18 = 149 ± 56.5 µmol N m^{-2} hr^{-1}; WE2 = 53.9 ± 11.3 µmol N m^{-2} hr^{-1}; WE4 = 63.7 ± 24.0 µmol N m^{-2} hr^{-1}; WE13 = 49.8 ± 9.15 µmol N m^{-2} hr^{-1}), and 2016 had significantly higher average potential denitrification rates overall (180 ± 22.4 µmol N m^{-2} hr^{-1}) than 2017 (84.5 ± 17.4 µmol N m^{-2} hr^{-1}; ANOVA, $p = 0.0005$). MB18 (ANOVA, $p = 0.004$) and WE4 ($p = 0.02$) were also significantly different between 2016 and 2017. Potential denitrification was positively correlated with ambient bottom water NO_2^- concentration ($\rho = 0.454$; $p = 0.01$), o-PO_4^{3-} fluxes ($\rho = 0.443$; $p = 0.01$), NH_4^+ fluxes ($\rho = 0.550$; $p = 0.001$), $^{28}N_2$ fluxes ($\rho = 0.595$; $p = 0.0004$), and SOD ($\rho = 0.576$; $p = 0.0007$) from unamended cores. It was negatively correlated (marginally) with bottom water DO concentrations ($\rho = -0.344$; $p = 0.06$, Figure 22).

Calculated N fixation (Figure 23) did not differ significantly between 2016 and

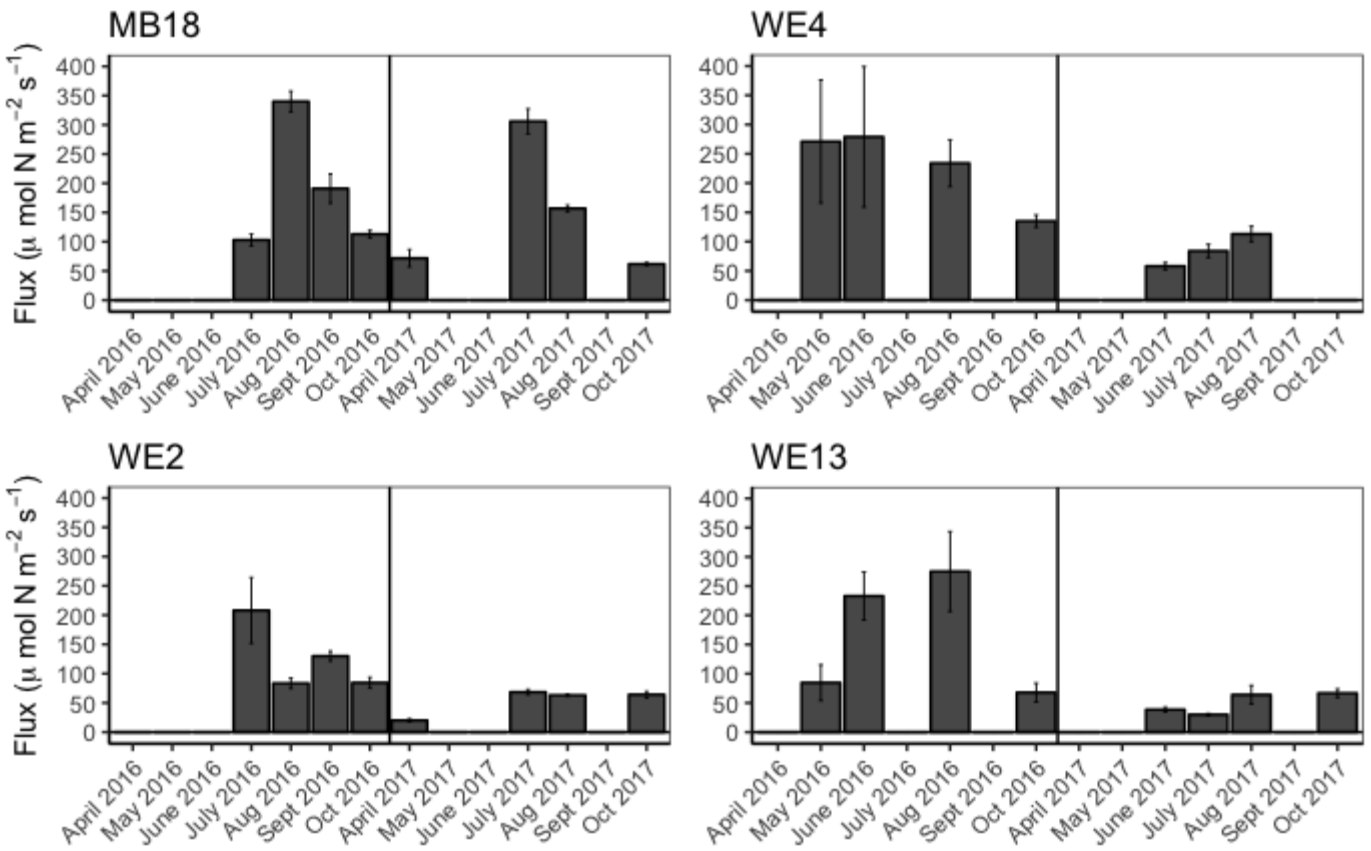

Figure 21: The sum of the $^{28,29,30}N_2$ fluxes from each site from all sampling events from April to October in 2016 (left of center line) and 2017 (right of center line) from the $^{15}NO_3^-$ amended cores, indicating potential denitrification. Sites MB18/WE2 and WE4/WE13 were sampled together and are stacked for scale.

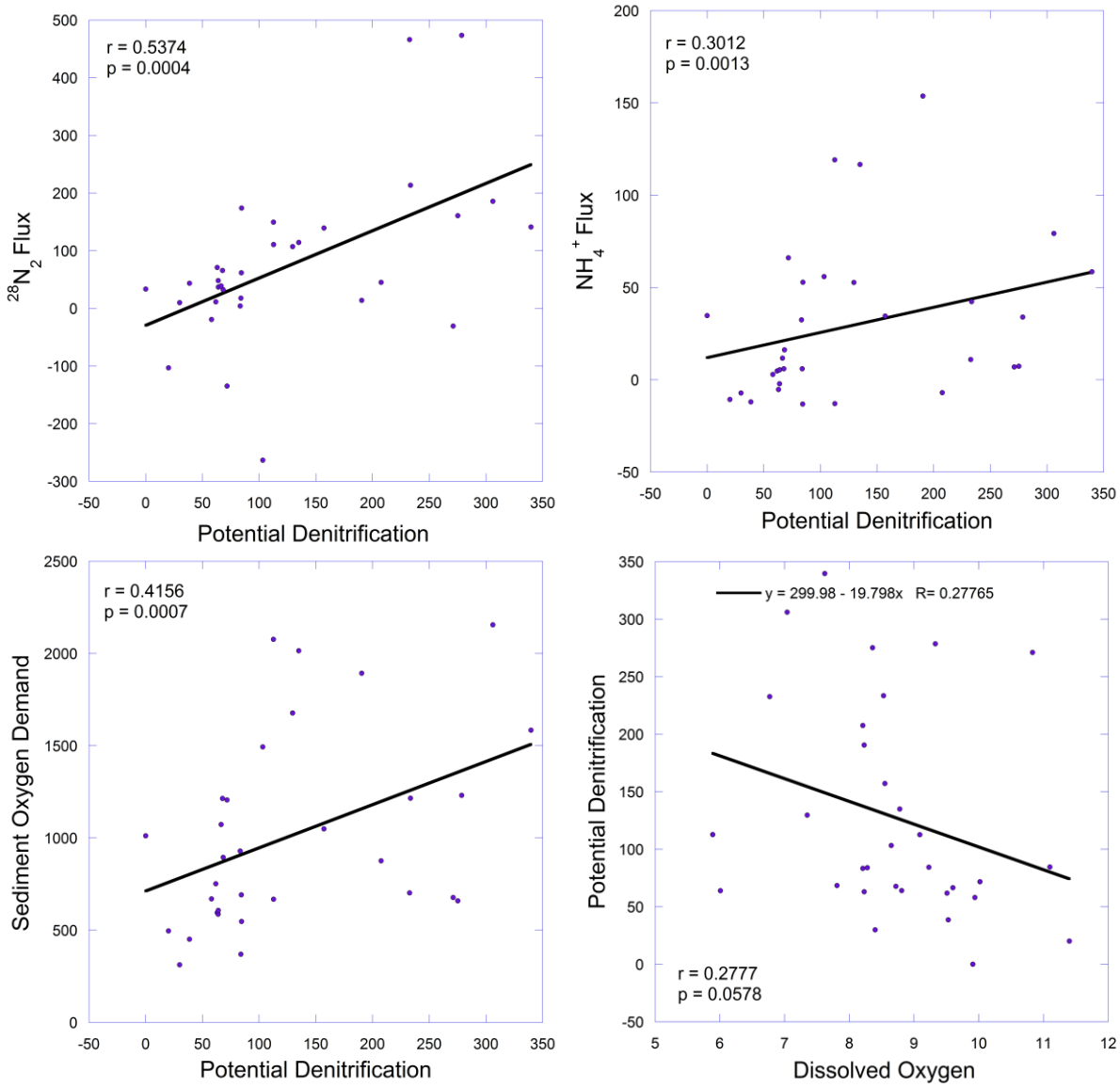

Figure 22: Relationships between potential denitrification and (A) $^{28}N_2$ fluxes ($\rho = 0.60$), (B) NH_4^+ fluxes ($\rho = 0.55$), and (C) SOD ($\rho = 0.58$) from the control cores, as well as (D) bottom-water DO concentrations ($\rho = -0.34$) from all 32 sampling points (4 sites at 8 different sampling events).

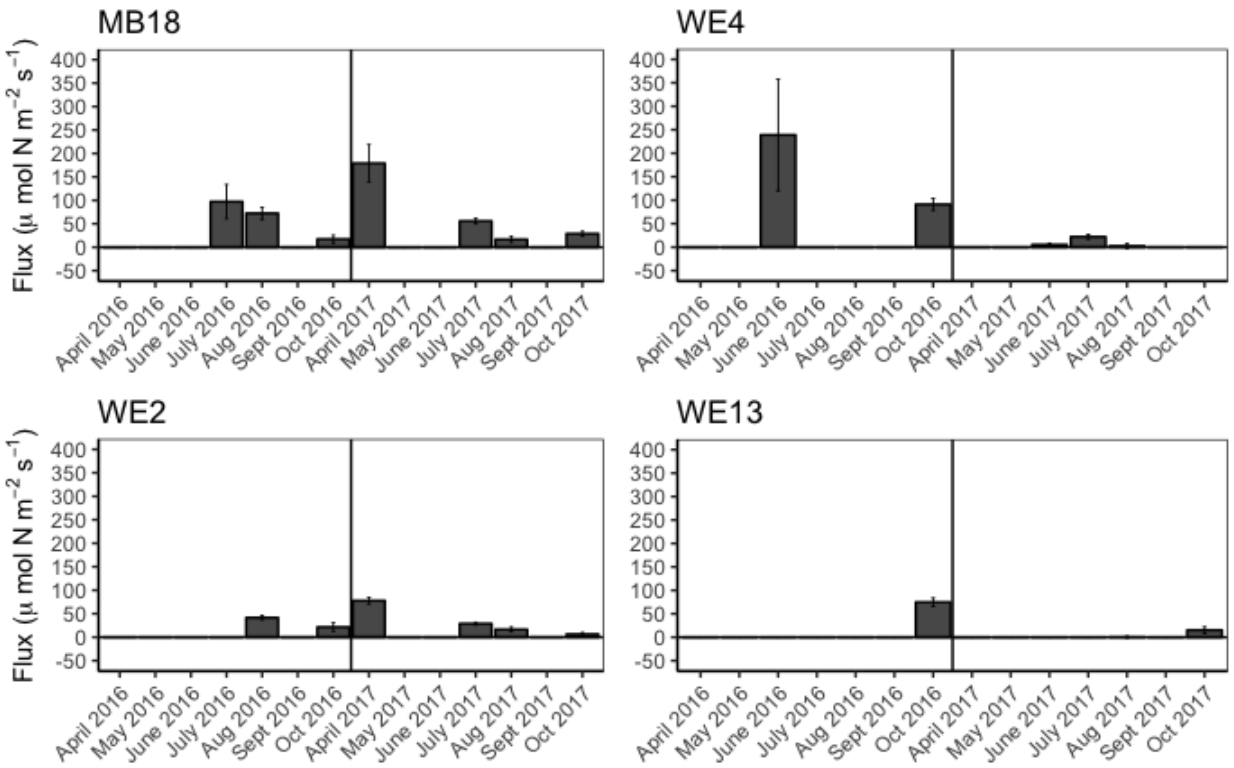

Figure 23: N fixation calculated using isotope patterns in $^{15}NO_3^-$ amended cores (An et al. 2001) over all sites and times. A negative value is reported as zero. Sites MB18/WE2 and WE4/WE13 were sampled together and are stacked for scale.

2017. When it was detected (i.e., N fixation > 0), it ranged from 6.30 ± 3.62 μmol N m^{-2} hr^{-1} at WE2 in October 2017 to 239 ± 119 μmol N m^{-2} hr^{-1} at WE4 in June 2016. The average calculated N fixation rates in 2016 (MB18 = 46.7 ± 22.8 μmol N m^{-2} hr^{-1}; WE2 = 15.8 ± 9.97 μmol N m^{-2} hr^{-1}; WE4 = 82.4 ± 86.3 μmol N m^{-2} hr^{-1}; WE13 = 18.7 ± 18.7 μmol N m^{-2} hr^{-1}) were higher than those in 2017 (MB18 = 70.1 ± 37.3 μmol N m^{-2} hr^{-1}; WE2 = 32.3 ± 15.8 μmol N m^{-2} hr^{-1}; WE4 = 7.48 ± 5.01 μmol N m^{-2} hr^{-1}; WE13 = 3.90 ± 3.76 μmol N m^{-2} hr^{-1}) at MB18 and WE2, but not at WE4 and WE13. There were no significant differences between sites or years. Calculated N fixation rates were positively correlated with SOD ($\rho = 0.374$; $p = 0.04$, Figure 24) and marginally correlated with ambient bottom water NO_3^- concentrations ($\rho = 0.398$; $p = 0.06$) but were negatively correlated with the NO_3^- fluxes ($\rho = -0.404$; $p = 0.02$) from the unamended cores.

Nitrate induced ammonium flux (NIAF, Figure 25) is a possible indicator of DNRA (McCarthy et al. 2016) and was used in this study. High NIAF values were observed for three sampling events in 2016: WE4 in May (140 μmol N m^{-2} hr^{-1}), MB18 in August (183 μmol N m^{-2} hr^{-1}), and WE2 in September (117 μmol N m^{-2} hr^{-1}; Figure 24). NIAF was not detected at MB18 in 2017, but NIAF was observed at the other three sites in 2017 (< 50 μmol N m^{-2} hr^{-1}).

Best Estimate of N_2 Fluxes

Using the $^{28}N_2$ fluxes from the control cores, along with calculated N fixation rates from the $^{15}NO_3^-$ cores, the best estimate of in situ denitrification was determined by adding the calculated N fixation rate to net $^{28}N_2$ fluxes (Figure 26). Mean best estimate rates for each site over the two sampling seasons (MB18 = 89.1 μmol N m^{-2} hr^{-1}; WE2 =

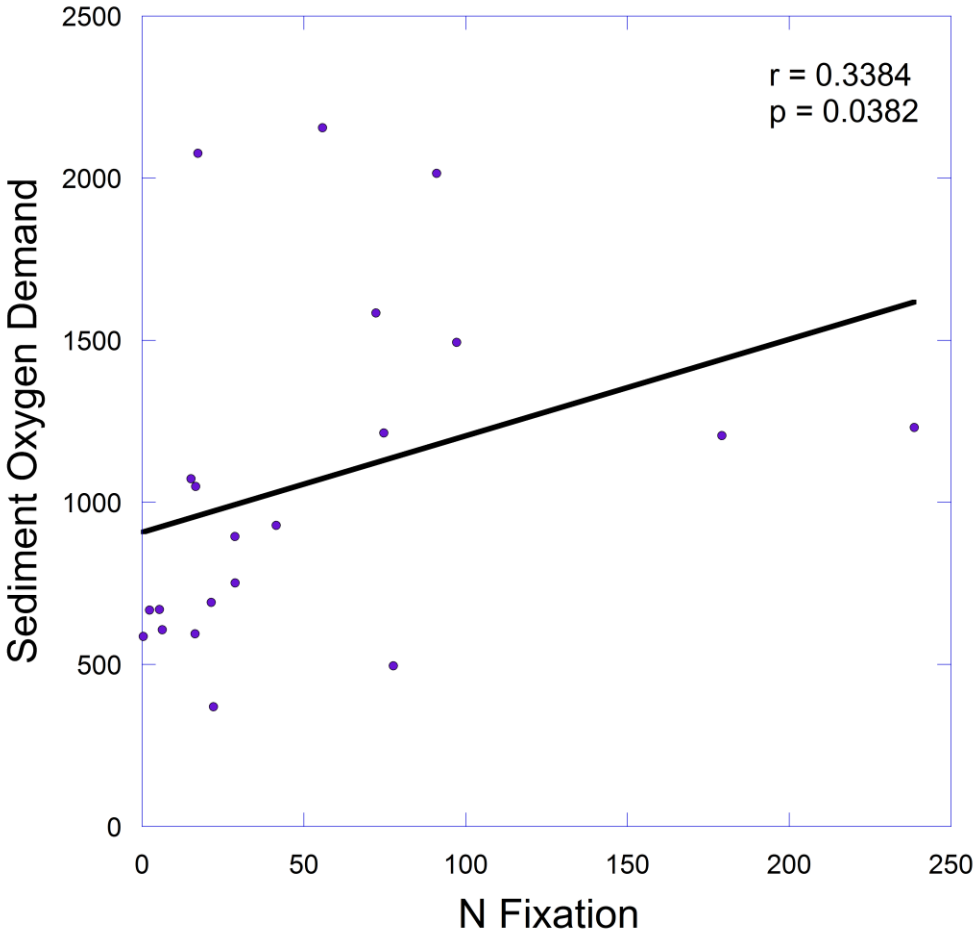

Figure 24: Relationship between calculated N fixation and SOD from all 32 sampling points (4 sites from 8 different sampling events; ρ = 0.37.

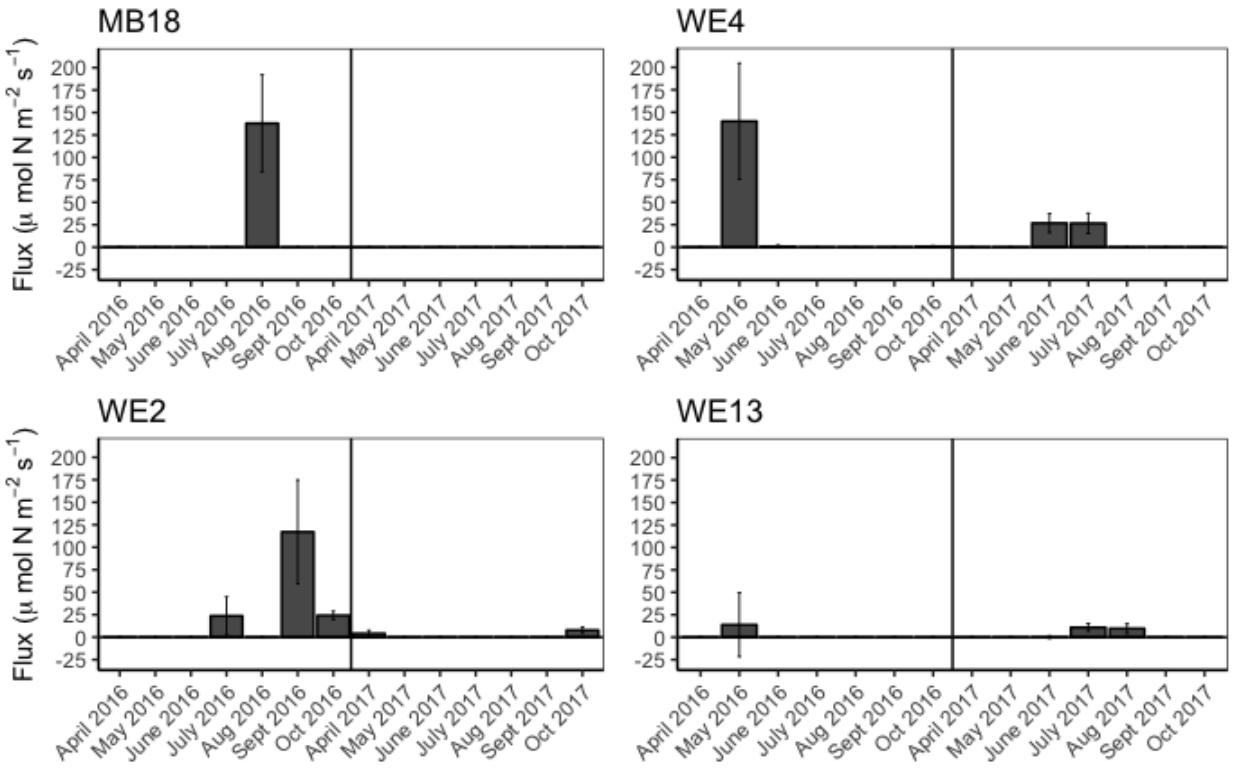

Figure 25: Nitrate induced ammonium flux (NIAF), when detected, measured as the difference between total NH_4^+ flux in unamended and $^{15}NO_3^-$ amended cores. NIAF can be a proxy for DNRA in the absence of $^{15}NH_4^+$ production from $^{15}NO_3^-$ additions.

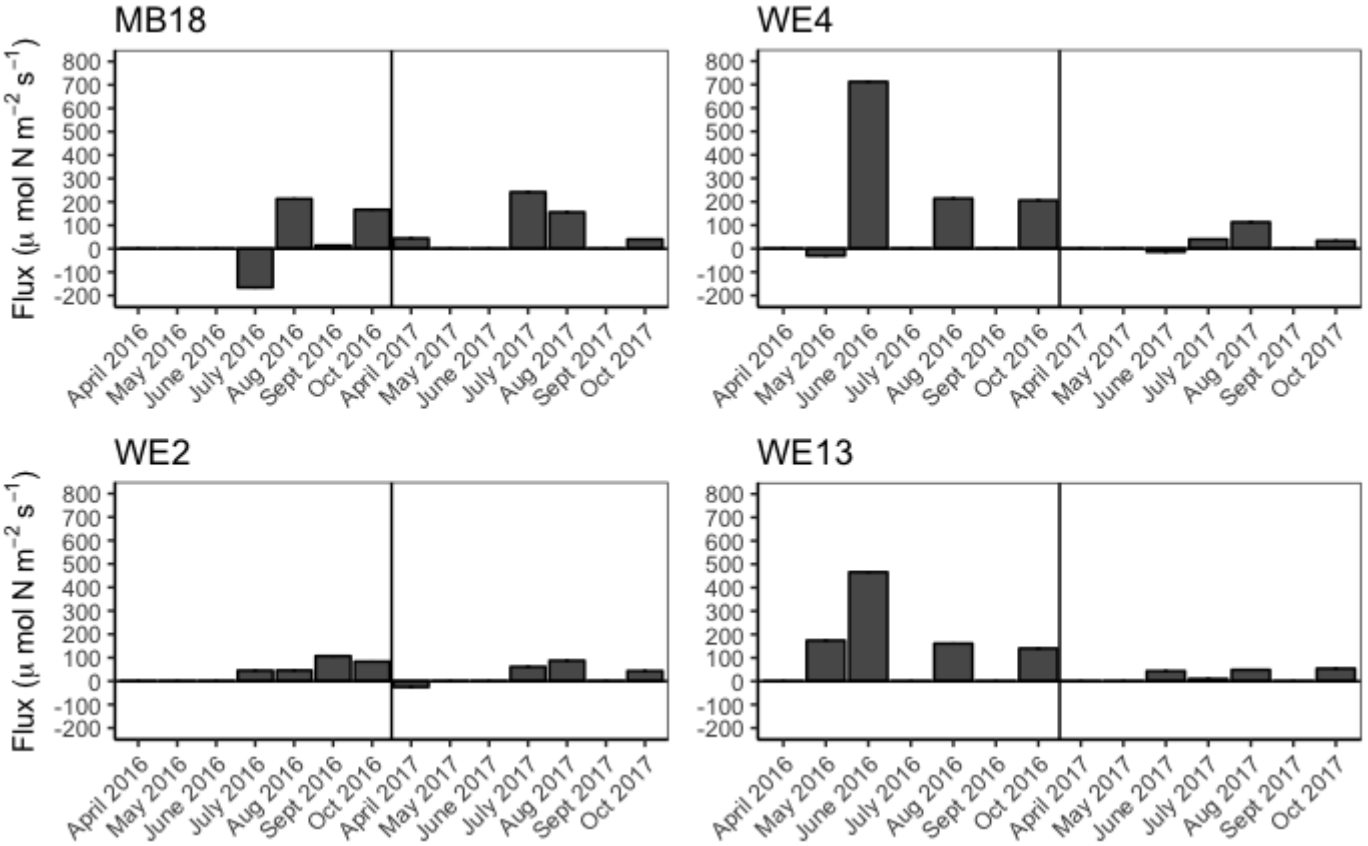

Figure 26: Best estimate of overall N_2 fluxes calculated by adding any determined N fixation (calculated from the $^{15}NO_3^-$ amended cores) to the net $^{28}N_2$ fluxes. Sites MB18/WE2 and WE4/WE13 were sampled together and are stacked for scale.

56.0 μmol N m^{-2} hr^{-1}; WE4 = 159 μmol N m^{-2} hr^{-1}; WE13 = 99.1 μmol N m^{-2} hr^{-1}) were all positive, confirming that western basin sediments acted as a net N sink.

IV. DISCUSSION

This study shows that sediments in the western basin of Lake Erie play a key role in aerobic and anaerobic nutrient cycling, which are important factors driving phytoplankton community structure and biomass (Forsberg 1989). Maumee River nutrient loads drive water column productivity and algal blooms, as well as nutrient cycling within sediments. Precipitation amounts and timing of Maumee River discharges, as well as wind speed, were greater in 2017 than 2016 (Figures 4 and 5), which led to higher suspended sediment and nutrient loads (Figure 27) and lower residence times in 2017. These differences were also reflected in results from the present study in terms of nutrient (N and P), O_2, and N_2 dynamics at the sediment-water interface.

Historically, lakes were considered to ultimately be limited only by P (Schindler et al. 2008; Paterson et al. 2011), relying on the assumption that N fixers could alleviate N-limitation (Schindler 2012). However, studies have shown that N-fixation is too energetically costly to effectively alleviate N-limitation (Scott and McCarthy 2010, 2011). A large body of literature has shown that N and P co-limitation is common, either concurrently or varying spatially and seasonally (Paerl et al. 2014; Pearson et al. 2016). Both the western basin of Lake Erie (Chaffin et al. 2013) and Lake Taihu in China (Xu et al. 2010) exhibit P-limitation in spring and early summer but switch to N-limitation in late summer into fall. This assertion is supported by ratios of ambient nutrient concentrations in this study. Reactive N (NH_4^+ and urea) to reactive P (o- PO_4^{3-}) ratios

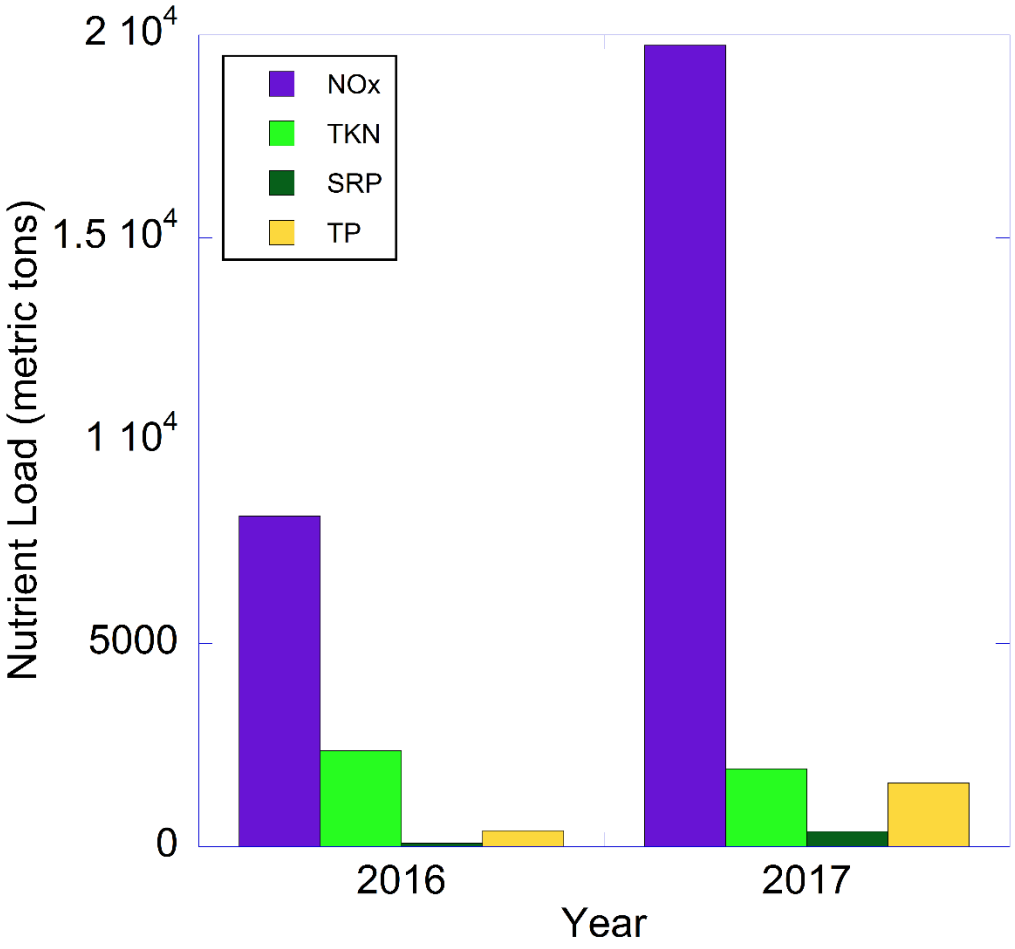

Figure 27: Nutrient loads into the western basin of Lake Erie from the Maumee River in metric tons. NO_x represents NO_2^- + NO_3^-, TKN is Total Kjeldahl Nitrogen (organic N + NH_4^+), SRP is soluble reactive phosphorus, and TP is total phosphorus. Data was downloaded from Heidelberg University's National Center for Water Quality Research (https://ncwqr.org/monitoring/data/).

ranged from 63:1 early in the season to 4:1 in October 2016 and from 61:1 to 8:1 in 2017. Systems have been defined as P limited when N:P is more than 50 and N limited when N:P is less than 20 (Guildford and Hecky 2000). Concentrations of NH_4^+ and NO_3^- in western Lake Erie were high early in the season but decreased later in the year. In fall 2017, ambient bottom water NH_4^+ and NO_3^- concentrations were < 0.04 μM and < 0.03 μM, respectively, which are the detection limits for both methods, while o-PO_4^{3-} maintained a range of 0.087 – 0.365 μM, depending on the site and time sampled.

Sediment Nutrient Fluxes

Unamended cores were used to characterize overall nutrient fluxes from western Lake Erie sediments. Even when sediments were a net sink for N, NH_4^+ and urea were released from sediments into the overlying water, most likely due to organic matter remineralization (Berman et al. 1999), and these internal sources of chemically reduced N may have stimulated or helped maintain phytoplankton growth. NH_4^+ is the most energetically favorable N form for primary producers, including cyanobacteria (Glibert et al. 2016), and only when it is no longer available on a cellular level will they switch to assimilating other N forms (Herrero et al. 2001). Cyanobacteria can also outcompete other phytoplankton for both NH_4^+ and urea (Blomqvist et al. 1994; Small et al. 2013), which makes the efflux of these reduced N forms important for productivity and algal blooms in the western basin and other eutrophic systems (Glibert 2017). In the present study, NH_4^+ effluxes were marginally correlated with chlorophyll-a concentrations in the water column ($\rho = 0.31$; $p = 0.09$), suggesting that sediments played some role in fueling biomass production. High NH_4^+ concentrations are also known to increase the growth and

toxicity of *Microcystis* (Donald et al. 2011; Monchamp et al. 2014; Gobler et al. 2016; Chaffin et al. 2018), which is the main bloom-forming organism in Lake Erie and many other eutrophic systems.

Urea can also be metabolized by cyanobacteria like *Microcystis* and *Dolichospermum* (formerly *Anabaena*, a known N fixer) as a source of N (Belisle et al. 2016). As urea is assimilated, it is hydrolyzed into NH_4^+ by the cell (Mackerras and Smith 1986). Donald et al. (2011) investigated the effect of N additions on algal abundance and reported that both NH_4^+ and urea additions caused increased chlorophyll-a concentrations during the summer. Other studies have evaluated urea and NH_4^+ as drivers for increased bloom toxicity by quantifying microcystin concentrations. Davis et al. (2015) measured the growth and toxicity of *Planktothrix* blooms in response to additions of o-PO_4^{3-} and multiple forms of N and found that additions of o-PO_4^{3-} + NH_4^+ and o-PO_4^{3-} + urea showed higher microcystin concentrations in over 50 percent of the experiments. Another study (Chaffin et al. 2018) found that enrichments of different forms of N along with P showed higher *Microcystis* and *Planktothrix* biomass and microcystin concentrations than P only additions. In the present study, urea fluxes from sediments and chlorophyll-a concentrations were not significantly correlated, but sediments were a continuous source of bioavailable N, as NH_4^+ and urea (49.6 ± 12.9 μmol N m^{-2} hr^{-1} in 2016; 19.2 ± 4.79 μmol N m^{-2} hr^{-1} in 2017), to the water column, which could be used to maintain biomass and toxin production during low discharge months in the summer.

Unlike NH_4^+ and urea, NO_3^- is usually fluxed into sediments rather than released. NO_3^- uptake often occurs in conjunction with a positive net $^{28}N_2$ flux, indicating direct

denitrification of NO_3^- from the overlying water (Mulholland et al. 2008; Nogaro and Burgin 2014). In the present study, net NO_3^- uptake was observed in 62.5 percent of the unamended cores, and net NO_3^- efflux was observed the rest of the time. Nitrification in the oxygenated layer of the sediments could explain net efflux if sediment nitrification rates exceeded the NO_3^- being taken up for denitrification and/or DNRA. Small et al. (2014) found that sediment cores with thicker oxygenated layers (in Lake Superior) had a higher NO_3^- efflux than cores with thinner oxygenated layers (in Lake Erie). The Lake Erie cores in that study mostly showed net NO_3^- uptake but were collected from the central and eastern basins, which often have low bottom water oxygen concentrations, which can inhibit nitrification (Carrick 2004; Brothers et al. 2017). Bottom water DO remained above hypoxia level (2 mg L^{-1}) in the western basin (Table 1), making nitrification and net NO_3^- efflux plausible when there is a lack of organic matter to stimulate denitrification.

Sediment NO_2^- fluxes in unamended cores were also not consistently negative or positive. NO_2^- is an intermediate product of nitrification, denitrification, and DNRA (Lomas and Lipschultz 2006) and can be released or assimilated within all three processes. However, NO_2^- is typically oxidized to NO_3^- or reduced to NO very quickly via nitrification and denitrification, respectively, or to NH_4^+ via DNRA, due in part to its toxicity to many microbes (Glass and Silverstein 1998). In western Lake Erie, NO_2^- fluxes were not significantly different from zero (Wilcoxon Signed Rank Test, $p = 0.19$), suggesting that NO_2^- uptake and efflux rates were generally balanced (mean = -1.67 ± 1.21 μmol N m^{-2} hr^{-1}). Ambient bottom water NO_2^- concentrations were also significantly

lower than ambient NO_3^- concentrations (ANOVA, $p = 0.006$), which implies it is being transformed to other forms of N.

Nitrate-induced ammonium flux (NIAF) was used as a proxy for DNRA rates. NIAF was calculated as the difference between total ($^{15}N+^{14}N$) NH_4^+ fluxes in unamended versus $^{15}NO_3^-$ amended cores (McCarthy et al. 2016). In freshwater sediments, NH_4^+ has a longer residence time due to the absence of other cations (Gardner et al. 1991). When $^{15}NO_3^-$ is transformed into $^{15}NH_4^+$ via DNRA, the heavier $^{15}NH_4^+$ isotope sorbs to sediments and displaces $^{14}NH_4^+$, which is released to the overlying water. Some microbial processes also tend to discriminate against ^{15}N molecules (e.g., isotope fractionation; Townsend-Small et al. 2007). DNRA can also be underestimated by high nitrification rates because it converts NH_4^+ to NO_3^-, which can mask the NH_4^+ released to the overlying water via DNRA. High NIAF values (140 ± 64.6 μmol m^{-2} hr^{-1} at WE4 in spring 2016, 183 ± 54.0 μmol m^{-2} hr^{-1} at MB18 in early summer 2016, and 117 ± 57.8 μmol m^{-2} hr^{-1} at WE2 in late summer 2016) could still indicate significant rates of DNRA; however, NIAF was not significantly correlated with NO_3^- or NH_4^+ fluxes or abundance of the DNRA functional gene (*nrfA*; Niewinski 2018).

Sediments were a consistent source of o-PO_4^{3-} for all but two sampling events, both occurring in 2016 at site WE13. Holdren and Armstrong (1980) reported sediment uptake of o-PO_4^{3-} in winter in Lakes Mendota and Wingra and attributed this pattern to cold temperatures and low biological activity. Lower microbial activity at WE13, both in early summer and fall, is possible since it is farthest from the Maumee River discharge, and the SOD was lower when compared to other sites. Another potential explanation is that o-PO_4^{3-} binds to insoluble metals (i.e., iron) in oxygenated water (Hupfer and

Lewandowski 2008). Many factors can contribute to sediment P release. For example, sediments containing Dreissenid mussels, which include invasive zebra and quagga mussels, release more P than sediments without mussels (Ozersky et al. 2013). However, in this study, all mussels observed in the sediment cores (mostly at site WE4) were removed by hand before incubations. P can also be retained in freshwater sediments by binding with calcium, iron, and aluminum (Fennel et al. 2009), making it susceptible to subsequent release when redox conditions change in the overlying water column and interstitial spaces (i.e., if anoxia is induced; Muenich et al. 2016). In a previous study on western basin sediments, P fluxes measured from anoxic cores were 4-13 times higher than fluxes from aerobic cores from the same locations (Matisoff et al. 2016). The P fluxes measured in their aerobic cores ranged from 0.215 – 3.91 μmol P m^{-2} hr^{-1} (converted from mg P m^{-2} day^{-1}). The western basin of Lake Erie does not normally stratify, so P fluxes reported in the present study were representative of aerobic cores; however, these fluxes spanned over a larger range (-1.01 – 13.0 μmol P m^{-2} hr^{-1}) than those reported from the Matisoff et al. (2016) study.

Sediment Oxygen Dynamics

SOD can be used as a proxy for microbial remineralization of organic-rich detritus (Seiki et al. 1994). In western basin sediments (Figure 14), SOD was significantly higher in 2016 than in 2017 (ANOVA, $p = 0.01$). This increase in SOD could be explained in part by differences in the phytoplankton community composition between years. In 2016, the *Microcystis* bloom was less extensive than in 2017 (HAB Bulletin, NOAA-GLERL), and phytoplankton fluoroprobe data showed that diatoms

comprised 35% of the total phytoplankton biomass in 2016, versus only 14% in 2017 (David Fanslow, NOAA-GLERL, unpublished data). Diatoms are larger than cyanobacteria and rapidly sink to the benthos, where they provide organic matter for remineralization in sediments (Smetacek 1985). In contrast, cyanobacteria, especially colony forming species, are more likely to be remineralized in the water column (e.g., Gardner and Lee 1975). Lower average ambient spring NO_3^- values measured in 2016 (12.9 μM) versus 2017 (89.5 μM) could suggest uptake by the larger diatom population in 2016 (in combination with lower external loading during the drier spring and early summer in 2016 versus 2017), since diatoms are highly competitive for NO_3^- (Glibert et al. 2016).

Another possible explanation for higher SOD in 2016 may involve differences in residence time relative to transport of organic matter from the western to the central basin. Precipitation and discharge volumes were lower in 2016 than 2017 (Figures 4 and 5), resulting in lower residence times in 2017. In April through August, the average daily wind speed was also higher in 2017 (paired t-test, $p = 0.04$), and higher winds prevailing from the west can also facilitate movement from the western to central basin, thus shortening residence times (Safak et al. 2015). Therefore, organic matter may have been transported farther into the western basin in 2017, or even into the central basin. This pattern was observed during the 2011 *Microcystis* bloom, when the bloom itself was transported into the central basin (Michalak et al. 2013). Important factors influencing SOD rates include temperature (Seiki et al. 1994), water depth (Clough et al. 2005), and organic matter availability. Temperature was not a significant driver of SOD in this study ($\rho = 0.09$; $p = 0.62$), perhaps because the western basin does not thermally stratify during

the summer months, maintaining oxic bottom waters. SOD typically decreases with increasing water depth due to less organic matter reaching the sediment-water interface due to water column remineralization (Clough et al. 2005), especially during cyanobacterial blooms (e.g., Gardner and Lee 1975), and this relationship was also observed within the western basin (ρ = -0.51; p = 0.003). Lower SOD at WE13 compared to the other sites could indicate that the most labile organic matter is remineralized before it reaches the middle of the western basin. Therefore, the organic matter accumulating there is more recalcitrant and processed more slowly (Wetzel 1992). This observation is also supported by the negative relationship between SOD and LOI (ρ = -0.495; p = 0.002; Figure 17). In another freshwater system, McCarthy et al. (2016) reported SOD at two sites in Missisquoi Bay, Lake Champlain, of 1700 ± 186 μmol O_2 m^{-2} hr^{-1} near the river input and 1500 ± 142 μmol O_2 m^{-2} hr^{-1} in the middle of the bay. Missisquoi Bay, like the western basin of Lake Erie, is also eutrophic and has high external inputs of nutrients. It also has a mean depth of 2.8 m, like the depth at MB18, where the average SOD (1526 ± 178 μmol O_2 m^{-2} hr^{-1}) was similar to those rates measured in Missisquoi Bay. SOD rates have also been reported in the central and eastern basins of Lake Erie; however, they were much higher than those measured in the western basin, but a different method was used (i.e., sediment slurries; Clevinger et al. 2014), which can cause an overestimation of rates because of destruction of redox gradients and mixing of labile organic matter.

Sediment N_2 Dynamics

Denitrification and anammox are key pathways to naturally reduce N over-enrichment in aquatic systems (Seitzinger 1988), while N fixation provides new,

bioavailable N (Schubert et al. 2006). Denitrification is considered a beneficial ecosystem service because bioavailable N is reduced to N_2, which is then released to the atmosphere. Therefore, higher denitrification rates show that the sediments are providing more of an ecosystem service. All three processes occur simultaneously in sediments and are distinct microbial pathways. The net $^{28}N_2$ fluxes measured from the unamended cores represent the balance between actual denitrification, anammox, and N fixation. However, N fixation can be calculated independently using $^{15}NO_3^-$ additions (An et al. 2001). Potential denitrification was measured as the sum of $^{28,29,30}N_2$ production and calculated N fixation (if any) in $^{15}NO_3^-$ amended cores. However, N_2 production could be due to denitrification and/or anammox (Brin et al. 2014), and isotope additions can help disentangle these pathways in some cases.

Net $^{28}N_2$ Fluxes

Using the MIMS (An et al. 2001), the fluxes calculated using the output of $^{28}N_2$ (Figure 18) indicate whether sediments are net N fixing or net denitrifying. A net $^{28}N_2$ efflux indicates that denitrification and anammox rates exceed N fixation, and net $^{28}N_2$ uptake shows greater N fixation than denitrification and anammox. Since denitrification in freshwater systems typically occurs at greater rates than anammox (e.g., McCarthy et al. 2016), and possible anammox in the present study was low (Figure 29), a positive net $^{28}N_2$ flux will hereafter be referred to as net denitrification.

Net $^{28}N_2$ fluxes differed at each site between 2016 and 2017. In 2016, net N fixation was observed at WE4 in May and MB18 in July, but not at any of the other sites, and in 2017, there was net N fixation at MB18 and WE2 in April and at WE4 in June.

However, variability was high, indicating that one of the duplicate cores was net N fixing, and the other one was net denitrifying. Net N fixation was not observed at WE13 at any time. Denitrification is limited by NO_3^- and organic matter availability (Ward et al. 2009), and a pattern of early net N fixation followed by net denitrification shows early seasonal limitation of either NO_3^- or organic matter to the sediments. MB18 (closest to the river mouth) had the highest net N fixation rates transitioning to WE13 (farthest from the river mouth), which had no net N fixation and the highest rates of net denitrification. With high spring discharge rates and large NO_3^- loads (Figure 27) entering Maumee Bay from the river, it is likely that organic matter was transported offshore and settled at sites farther from the river mouth, leading to net N fixation at sites closer to the Maumee River. However, net $^{28}N_2$ fluxes did not correlate with SOD rates ($p = 0.13$), LOI (both reflecting organic matter content; $p = 0.56$), or ambient bottom water NO_3^- concentrations ($p = 0.87$). Future studies are needed to improve the spatial and temporal resolution and attempt to constrain the factors controlling the distributions of denitrification and N fixation.

Net $^{28}N_2$ fluxes have been measured in other lakes using different methods. Saunders and Kalff (2001) measured denitrification rates using the N_2 flux method (Seitzinger et al. 1980, 1993) on intact sediment cores at 20 sites in Lake Memphremagog, an oligotrophic lake in Quebec (Canada) and Vermont (USA). Denitrification rates ranged from 8-340 μmol N m^{-2} hr^{-1} (mean = 107 ± 20.5 μmol N m^{-2} hr^{-1}), depending on site, temperature, and sediment organic matter content. These rates were more conservative than the range of $^{28}N_2$ fluxes observed in the western basin (-263 ± 93.0 μmol N m^{-2} hr^{-1} to 474 ± 174 μmol N m^{-2} hr^{-1}), but they had a higher overall mean

than the western basin (75.6 ± 25.0 μmol N m^{-2} hr^{-1}). In Lake Okeechobee, a eutrophic lake in Florida, positive net $^{28}N_2$ fluxes lower than those observed in Lake Erie (63.8 ± 2.8 to 68.5 ± 1.8 μmol N m^{-2} hr^{-1}) were observed using the same methods as the present study (James et al. 2011). Compared to Lake Erie, Lake Memphremagog is oligotrophic at a higher latitude with higher mean net denitrification rates and Lake Okeechobee is eutrophic at a lower latitude with lower mean net denitrification rates; thus, trophic status is apparently not the only control on denitrification.

N removal through denitrification and anammox

Potential denitrification was calculated in the $^{15}NO_3^-$-amended cores to measure complete denitrification when NO_3^- is not limiting. It is measured as the total production of N_2 ($^{28, 29, \text{and } 30}N_2$) and corrected for any calculated N fixation. Potential denitrification rates were significantly higher in 2016 than in 2017, both overall and at MB18 and WE4 (Figure 21). Rates also peaked in mid-summer (July – August) at every site except WE4 in 2016, where June showed the highest potential denitrification rates.

Lower ambient NO_3^- concentrations and N_2 effluxes in October of both 2016 and 2017 (when potential denitrification rates exceeded $^{28}N_2$ fluxes) may reflect NO_3^- limitation of denitrification. In addition, WE4 and WE13 in October 2016 and MB18, WE2, and WE13 in October 2017 (WE4 was not measured) had high (>1) ^{15}N:^{14}N ratios for denitrification (Figure 28), which occurs when more $^{15}NO_3^-$ is directly denitrified and stimulates $^{30}N_2$ production relative to coupled nitrification-denitrification. The relative contributions of direct and coupled denitrification was determined by comparing potential denitrification rates with the best estimate of N_2 fluxes to determine if the denitrifiers

were substrate saturated. In October 2016, $^{28}N_2$ fluxes exceeded potential denitrification rates, but in October 2017, they were lower (MB18 = 65.0% of potential denitrification; WE2 = 67.7%; WE4 = not measured; WE13 = 81.1%). This pattern indicates that the sediments were likely NO_3^- or organic matter limited more so in October 2017 than they were in October 2016, or that NO_3^- produced from nitrification was able to sustain denitrification in 2016 but not in 2017.

In July 2017, MB18 had a very high potential denitrification rate (306 ± 21.4 μmol N m^{-2} hr^{-1}) compared to the other three sites (WE2 = 68.4 ± 4.68 μmol N m^{-2} hr^{-1}; WE4 = 84.0 ± 11.3 μmol N m^{-2} hr^{-1}; WE13 = 30.0 ± 2.01 μmol N m^{-2} hr^{-1}) but a low ^{15}N:^{14}N, as the ambient bottom water NO_3^- concentration at MB18 was 482 μM. Even at high ambient NO_3^- concentrations, adding $^{15}NO_3^-$ stimulated potential denitrification by ~30% compared to the net $^{28}N_2$ flux in unamended cores (186 ± 55.7 μmol N m^{-2} hr^{-1}), suggesting high rates of coupled nitrification-denitrification, rather than NO_3^- saturation.

There is a rich literature on denitrification in coastal and freshwater systems, and rates vary widely. Potential denitrification rates measured using continuous-flow core incubations in Old Woman Creek (a coastal Lake Erie wetland) ranged from 150 to 650 μmol N m^{-2} hr^{-1}, which depended mostly on whether the estuary was open to Lake Erie (high flow) or closed by a sand barrier (low flow; McCarthy et al. 2007). In a constructed wetland in central Texas, potential denitrification rates, also measured using continuous-flow sediment core incubations, ranged from 54 to 278 μmol N m^{-2} hr^{-1}, with variability due mostly to location along a NO_3^- gradient and time of year (Scott et al. 2008). In Narragansett Bay, an estuary near Providence, Rhode Island (Fulweiler et al. 2007) reported denitrification rates, measured using core incubations, between zero and 530

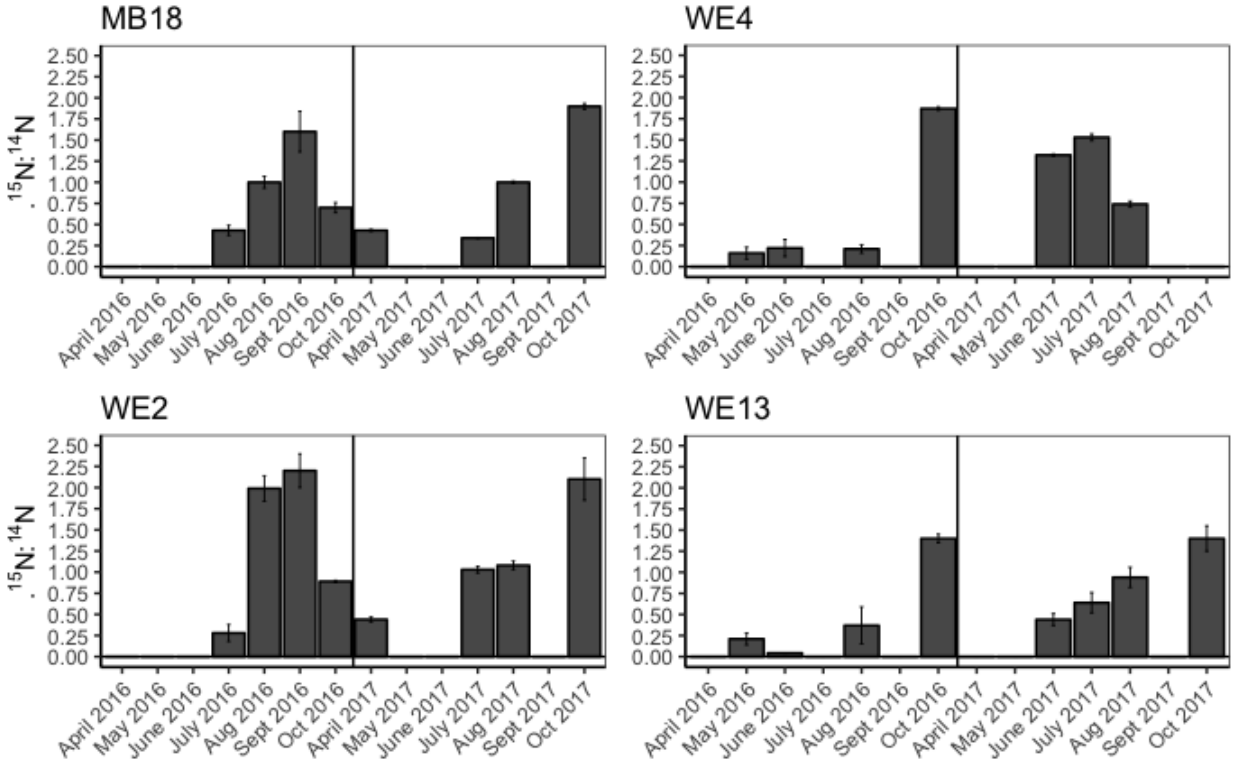

Figure 28: The ratio of $^{15}N:^{14}N$ produced in $^{15}NO_3^-$ cores. Sites MB18/WE2 and WE4/WE13 were sampled together and are stacked for scale.

μmol N m^{-2} hr^{-1}. These studies show ranges in line with the results shown in this study (20.1 ± 2.74 μmol N m^{-2} hr^{-1} to 340 ± 17.6 μmol N m^{-2} hr^{-1}), which indicates that denitrification rates do not necessarily depend on the type of ecosystem or trophic status.

Anammox in freshwater systems, while previously not believed to be a main pathway of N_2 loss, has been quantified in lakes throughout the world (e.g., Schubert et al. 2006; Wenk et al. 2013). In Lake Tanganyika (Africa), Schubert et al. (2006) attributed 13% of total water column N_2 production to anammox, and Wenk et al. (2013) measured low anammox rates in Lake Lugano (Europe) but confirmed the presence of anammox bacteria using genetic methods. While these systems are very different from the western basin of Lake Erie, $^{29}N_2$ produced from $^{15}NH_4^+$ amendments can infer possible anammox rates, while comparing those rates with the total N removal (potential denitrification) indicates the extent to which anammox is a potential N loss mechanism in temperate, eutrophic lakes. In marine sediments, anammox becomes more important farther from organic matter inputs (i.e., river mouths) because heterotrophic denitrifiers are dependent on organic matter supply (Dalsgaard et al. 2005), which may suggest that anammox could be an important process when organic matter is limiting in Lake Erie.

The ratios of possible anammox to potential denitrification ($^{29}N_2$:DNF; Figure 29) were significantly higher in 2017 than in 2016 (ANOVA; $p = 0.001$). In 2017, lower SOD suggests that less organic matter, or less labile organic matter (LOI was higher in 2017), was available in the sediments, potentially favoring anammox. Anammox is performed by autotrophic organisms, giving it a competitive advantage over denitrification when organic matter is limiting (Ward 2013). The sites farthest from the Maumee River mouth (WE4 and WE13) had significantly higher ratios of possible

anammox to total N removal in 2017 (WE4 = 0.145, WE13 = 0.205) than in 2016 (WE4 = 0.048, WE13 = 0.042; ANOVA; $p = 0.003$ for WE4 and $p < 0.001$ for WE13). The highest ratio of possible anammox to potential denitrification occurred in October 2017 at site WE2 (0.47) because of lower potential denitrification when compared to other sites and times. There was also a low best estimate of denitrification to potential denitrification ratio (0.68), suggesting a combination of NO_3^- and organic matter limitation for denitrification. The total N removal was also lower in general when there was higher $^{29}N_2$:DNF, which suggests that the ecosystem services provided by the sediments were impaired.

Adding new N through N fixation

N fixation can be an important process in the sediments when N is limiting, even though sediment N fixation can occur regardless of porewater N concentrations (Newell et al. 2016). N fixation allows primary production to continue even when dissolved inorganic N (DIN; NO_3^-, NO_2^-, and NH_4^+) concentrations are depleted (Howarth et al. 1988); thus, the ability to fix N is an advantage for oligotrophic systems with low external N inputs, but N supply from sediment fixation can exacerbate eutrophication in systems like Lake Erie. In the western basin, N fixation was mostly observed at MB18, and was lowest at WE13, following the trend shown by the net $^{28}N_2$ fluxes. Positive N fixation rates were observed even when high DIN concentrations were present in the water column, supporting observations from other aquatic systems (Gardner et al. 2006; Fulweiler et al. 2007; Knapp 2012; Foster and Fulweiler 2014; Newell et al. 2016) that

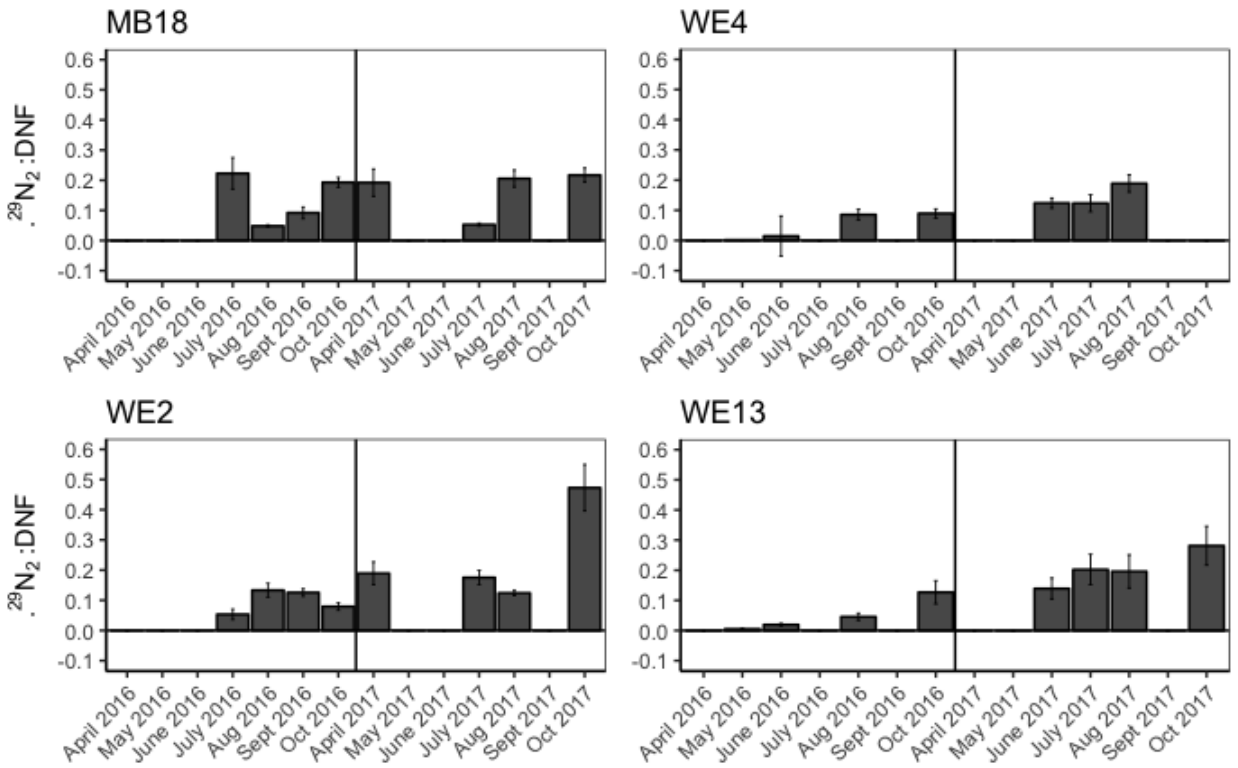

Figure 29: Ratio of possible anammox (as $^{29}N_2$ production from $^{15}NH_4^+$ amended cores) to potential denitrification (measured as the sum of $^{28,29,30}N_2$ from $^{15}NO_3^-$ amended cores). Sites MB18/WE2 and WE4/WE13 were sampled together and are stacked for scale.

sediment N fixation is not sensitive to DIN concentrations. N fixation rates (when greater than zero) were highest earlier in the sampling season but were lower when higher temperatures and organic matter availability stimulated net denitrification. In many cases, net denitrification exceeds net N fixation in freshwater systems due to high inputs of organic carbon and NO_3^-, and the An et al. (2001) calculations allow calculation of N fixation occurring simultaneously, even when denitrification is observed.

In the water column, N fixers use heterocysts to protect the process from oxygen, since N fixation is a strictly anaerobic process (Stewart et al. 1969). In the sediments, however, free living N fixing bacteria exist below the oxic – anoxic boundary, where a reducing environment exists, and the nitrogenase enzyme does not require protection from oxygen. Some diazotrophic bacteria fix N linked to other biogeochemical pathways. Methanotrophs, for example, fix N while consuming methane (Dedysh 2004), and sulfate reducing bacteria use sulfate as their terminal electron acceptor and fix N to incorporate into biomass, while producing hydrogen sulfide as a product (Riederer-Henderson and Wilson 1970).

Best Estimate of Denitrification

The best estimates of denitrification were used from each sampling event to determine whether the sediments were providing an ecosystem service to the lake. An ecosystem service is defined as benefits received from the environment (Fisher et al. 2009), and bioavailable N removal via denitrification and anammox is considered an ecosystem service. When more bioavailable N is removed, it can limit the growth of the cyanobacterial blooms, which benefits both the lake ecosystem and human activities

within the basin. In the western basin sediments, the average best estimate of denitrification was positive at each site over the course of the two years (Figure 26), indicating that the sediments were providing an ecosystem service to the lake by removing N through net denitrification. However, dual-nutrient management (N and P) is still necessary in this system because the sediments cannot completely remove the bioavailable N coming into the lake via external loads from the Maumee and Detroit Rivers, and N-rich toxin production by non-N-fixing *Microcystis* continues in western Lake Erie HABs. In addition, the efficiency of N removal decreases at higher N loading rates (e.g., Mulholland et al. 2008; Gardner and McCarthy 2009), which can enhance N export to downstream systems.

Ability of western basin sediments to remove bioavailable N

Lake Erie is defined by three separate basins, and the western basin is the shallowest, warmest, and most productive of the three (Ludsin et al. 2001). Nutrient loads from the Maumee River (Figure 27) are high in the spring, when precipitation runoff carries nutrients from the agricultural watershed. To scale measured N removal rates for the entire western basin, each sampling site was designated to represent a section of the basin (Figure 30). MB18 represented Maumee Bay, under direct influence of the river, and was the smallest, with a surface area of 78 km^2, followed by WE2, with a surface area of 300 km^2, and then WE4 and WE13 occupied the rest of the western basin with equal surface areas of 1301 km^2 each.

Overall, the sediments were able to significantly impact the nutrient loads coming into the western basin. Total phosphorus (TP) loads into the western basin from both the

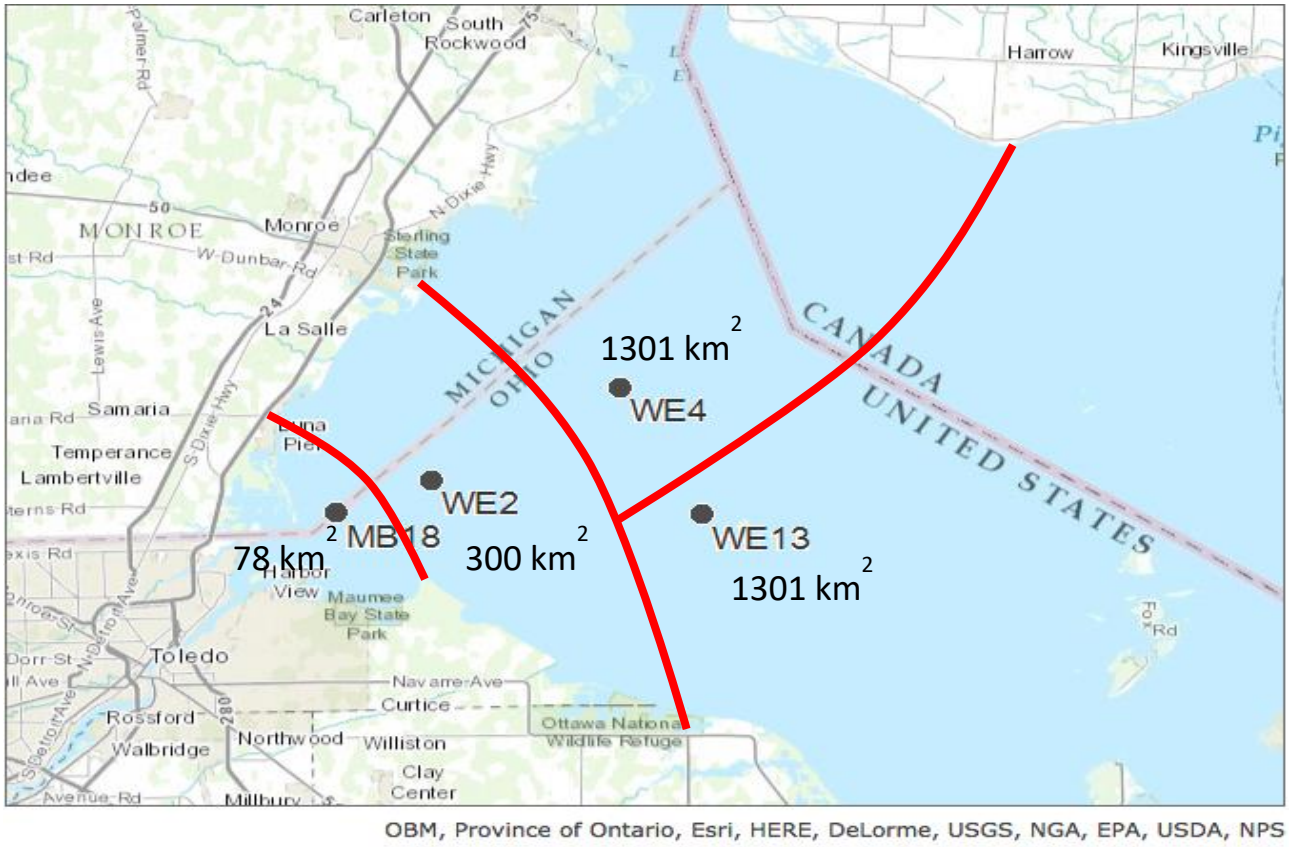

Figure 30: Map showing the sampling sites in the western basin of Lake Erie along with sections showing the area occupied by each site (map created with ArcGIS Online and edited using Microsoft PowerPoint).

Maumee and Detroit Rivers were 4.26×10^6 kg P in 2016 and 5.74×10^6 kg P in 2017. The sediments added o-PO_4^{3-} at an average of 43.5% of the annual TP load in 2016 and 31.5% of the load in 2017. These estimates are similar to those comparing internal P loads in western Lake Erie to target P concentrations (20 – 42%) identified by the IJC for the western basin (Matisoff et al. 2016). The annual amount of total nitrogen (TN) entering the western basin from both rivers was 1.67×10^8 kg N in 2016 and 1.78×10^8 kg N in 2017. The sediments added NH_4^+ and urea to the water column but were a sink for NO_x (NO_3^- + NO_2^-) and had a positive average release of N_2 gas, potentially removing 4.05×10^7 kg of bioavailable N in 2016 and 1.62×10^7 kg in 2017. Using our best estimate of yearly N fluxes, and extrapolating to include estimated winter rates, which in another study, were found to be similar to summer rates in ice-covered Canadian lakes (Cavaliere and Baulch 2018), the sediments removed an average of 34.9% of the TN load in 2016 and 13.4% of the TN load in 2017. These results show that higher N loads and lower residence times reduce the ability of Lake Erie sediments to remove bioavailable N. In lower bloom years (i.e., 2016), when N removal via denitrification/anammox was more efficient, internal recycling mechanisms were more important in providing bioavailable N and P to the water column (Table 6).

Table 6: N budget for the western basin of Lake Erie. Units are in 10^6 kg N yr^{-1}. DNF = denitrification, DIN = dissolved inorganic N, TN = total N, and WB = western basin. These values were scaled to include the entire surface area of the western basin (See Figure 30).

	Yearly Average		Average by site			
	2016	2017	MB18	WE2	WE4	WE13
Best Estimate DNF	-58.3	-22.3	-0.850	-2.06	-25.4	-21.9
DIN-NO_3^- Flux	16.3	3.96	0.633	0.322	4.55	1.20
Urea Flux	1.45	2.17	0.083	0.119	0.622	0.324
Total	-40.5	-16.2	-0.134	-1.62	-20.2	-20.4
TN Load to WB	167	178	3.66	14.1	61.0	61.0
N surplus	126	162	3.53	12.5	40.8	40.6

V. CONCLUSION

This study highlights the critical role that sediments play in nutrient and dissolved gas cycling in the western basin of Lake Erie. Overall, sediments were a source of remineralized NH_4^+, urea, and o-PO_4^{3-} to the water column, while denitrification was the primary N removal mechanism. Anammox may have also been a significant N removal pathway at several sampling events (most notably in October 2017 at WE2); however, molecular work is needed to confirm anammox and distinguish it from coupled nitrification-denitrification. Both pathways (denitrification and anammox) perform an ecosystem service by removing bioavailable N, which fuels HABs. Denitrification was the primary N removal process in both 2016 and 2017, but denitrification rates in 2017 were lower than in 2016. The *Microcystis* bloom was larger in 2017 and, along with differences in phytoplankton community structure and western basin residence time, appears to have suppressed sediment N removal.

Most of the pathways quantified in this study were significantly different between 2016 and 2017. A smaller *Microcystis* bloom occurred in 2016 than in 2017, and 2017 had higher precipitation, wind speed, and river discharge, but lower residence times, which reduces interaction time between NO_3^-, settling organic matter, and the sediments, inhibiting N removal via denitrification (Seitzinger et al. 2002). Average NH_4^+, o-PO_4^{3-}, and net $^{28}N_2$ fluxes, as well as SOD, N fixation, and potential denitrification, were all higher in 2016 than in 2017. These differences between 2016 and 2017 are most likely

due to differences in organic matter delivery to sediments in the western basin. In 2016, diatoms were more pronounced with respect to the proportion of total biomass, and those cells likely sank to the sediment-water interface and provided more labile organic matter for remineralization and subsequent nitrification and denitrification (Smetacek 1985; Glibert et al. 2016). In 2017, a combination of higher cyanobacteria biomass (less prone to sinking) with respect to total biomass and shorter residence times in the western basin led to organic matter transport farther into the basin (Michalak et al. 2013; Safak et al. 2015). Therefore, when there are smaller diatom blooms and larger *Microcystis* blooms, sediments do not denitrify as efficiently because less organic matter reaches the sediments, allowing possible anammox to account for a higher proportion of total N removal.

We quantified nutrient removal and recycling rates in the sediments at four sites in the western basin of Lake Erie. The sediments removed a large amount of the total N load (34.9% in 2016; 13.4% in 2017), mostly through denitrification, with a smaller contribution possibly attributed to anammox. Net N fixation was a source of bioavailable N from sediments in the spring, and N fixation occurred concurrently with denitrification throughout the study. As hypothesized, sediments were a source of NH_4^+ and o-PO_4^{3-}, which can contribute to sustaining toxin-producing, non-N-fixing HABs and eutrophication. These results support recent calls to initiate dual nutrient (N and P) management efforts to mitigate HABs in the western basin of Lake Erie and other eutrophic systems, with emphasis on best management practices to reduce non-point, agricultural sources of both N and P. High nutrient loads lead to larger HABs, both of

which inhibit the efficiency of sediments in removing bioavailable N via denitrification and performing a valuable ecosystem service.

VI. REFERENCES

An, S., and W. Gardner. 2002. Dissimilatory nitrate reduction to ammonium (DNRA) as a nitrogen link, versus denitrification as a sink in a shallow estuary (Laguna Madre/Baffin Bay, Texas). Marine Ecology Progress Series **237**: 41–50. doi:10.3354/meps237041

An, S., W. S. Gardner, and T. Kana. 2001. Simultaneous Measurement of Denitrification and Nitrogen Fixation Using Isotope Pairing with Membrane Inlet Mass Spectrometry Analysis. Applied and Environmental Microbiology **67**: 1171–1178. doi:10.1128/AEM.67.3.1171-1178.2001

An, S., and S. B. Joye. 2001. Enhancement of coupled nitrification-denitrification by benthic photosynthesis in shallow estuarine sediments. Limnology and Oceanography **46**: 62–74. doi:10.4319/lo.2001.46.1.0062

Babbin, A. R., R. G. Keil, A. H. Devol, and B. B. Ward. 2014. Organic Matter Stoichiometry, Flux, and Oxygen Control Nitrogen Loss in the Ocean. Science **344**: 406–408. doi:10.1126/science.1248364

Baker, D. B., R. Confesor, D. E. Ewing, L. T. Johnson, J. W. Kramer, and B. J. Merryfield. 2014. Phosphorus loading to Lake Erie from the Maumee, Sandusky and Cuyahoga rivers: The importance of bioavailability. Journal of Great Lakes Research **40**: 502–517. doi:10.1016/j.jglr.2014.05.001

Beaulieu, J. J., J. L. Tank, S. K. Hamilton, and others. 2011. Nitrous oxide emission from denitrification in stream and river networks. Proceedings of the National Academy of Sciences **108**: 214–219. doi:10.1073/pnas.1011464108

Belisle, B. S., M. M. Steffen, H. L. Pound, S. B. Watson, J. M. DeBruyn, R. A. Bourbonniere, G. L. Boyer, and S. W. Wilhelm. 2016. Urea in Lake Erie: Organic nutrient sources as potentially important drivers of phytoplankton biomass. Journal of Great Lakes Research **42**: 599–607. doi:10.1016/j.jglr.2016.03.002

Berman, T., C. Béchemin, and S. Maestrini. 1999. Release of ammonium and urea from dissolved organic nitrogen in aquatic ecosystems. Aquatic Microbial Ecology **16**: 295–302. doi:10.3354/ame016295

Bernard, R. J., B. Mortazavi, and A. A. Kleinhuizen. 2015. Dissimilatory nitrate reduction to ammonium (DNRA) seasonally dominates NO3 − reduction pathways in an anthropogenically impacted sub-tropical coastal lagoon. Biogeochemistry **125**: 47–64. doi:10.1007/s10533-015-0111-6

Blomqvist, P., A. Pettersson, and P. Hyenstrand. 1994. Ammonium-nitrogen: A key regulatory factor causing dominance of non-nitrogen-fixing cyanobacteria in aquatic systems. Archiv Für Hydrobiologie **132**: 141–164.

Bridgeman, T. B., J. D. Chaffin, and J. E. Filbrun. 2013. A novel method for tracking western Lake Erie Microcystis blooms, 2002–2011. Journal of Great Lakes Research **39**: 83–89. doi:10.1016/j.jglr.2012.11.004

Brin, L. D., A. E. Giblin, and J. J. Rich. 2014. Environmental controls of anammox and denitrification in southern New England estuarine and shelf sediments. Limnology and Oceanography **59**: 851–860. doi:10.4319/lo.2014.59.3.0851

Brothers, S., Y. Vadeboncoeur, and P. Sibley. 2017. A decline in benthic algal production may explain recent hypoxic events in Lake Erie's central basin. Journal of Great Lakes Research **43**: 73–78. doi:10.1016/j.jglr.2017.03.016

Burgin, A. J., and S. K. Hamilton. 2007. Have we overemphasized the role of denitrification in aquatic ecosystems? A review of nitrate removal pathways. Frontiers in Ecology and the Environment **5**: 89–96. doi:10.1890/1540-9295(2007)5[89:HWOTRO]2.0.CO;2

Canfield, D. E., A. N. Glazer, and P. G. Falkowski. 2010. The Evolution and Future of Earth's Nitrogen Cycle. Science **330**: 192–196. doi:10.1126/science.1186120

Carmichael, W. W., and G. L. Boyer. 2016. Health impacts from cyanobacteria harmful algae blooms: Implications for the North American Great Lakes. Harmful Algae **54**: 194–212. doi:10.1016/j.hal.2016.02.002

Carrick, H. J. 2004. Algal Distribution Patterns in Lake Erie: Implications for Oxygen Balances in the Eastern Basin. Journal of Great Lakes Research **30**: 133–147. doi:10.1016/S0380-1330(04)70336-6

Cavaliere, E., and H. M. Baulch. 2018. Denitrification under lake ice. Biogeochemistry **137**: 285–295. doi:10.1007/s10533-018-0419-0

Chaffin, J. D., T. B. Bridgeman, and D. L. Bade. 2013. Nitrogen Constrains the Growth of Late Summer Cyanobacterial Blooms in Lake Erie. Advances in Microbiology **03**: 16–26. doi:10.4236/aim.2013.36A003

Chaffin, J. D., T. B. Bridgeman, D. L. Bade, and C. N. Mobilian. 2014. Summer phytoplankton nutrient limitation in Maumee Bay of Lake Erie during high-flow and low-flow years. Journal of Great Lakes Research **40**: 524–531. doi:10.1016/j.jglr.2014.04.009

Chaffin, J. D., T. W. Davis, D. J. Smith, M. M. Baer, and G. J. Dick. 2018. Interactions between nitrogen form, loading rate, and light intensity on Microcystis and Planktothrix growth and microcystin production. Harmful Algae **73**: 84–97. doi:10.1016/j.hal.2018.02.001

Clevinger, C. C., R. T. Heath, and D. L. Bade. 2014. Oxygen use by nitrification in the hypolimnion and sediments of Lake Erie. Journal of Great Lakes Research **40**: 202–207. doi:10.1016/j.jglr.2013.09.015

Clough, L. M., P. E. Renaud, and W. G. Ambrose Jr. 2005. Impacts of water depth, sediment pigment concentration, and benthic macrofaunal biomass on sediment oxygen demand in the western Arctic Ocean. Canadian Journal of Fisheries and Aquatic Sciences **62**: 1756–1765. doi:10.1139/f05-102

Dalsgaard, T., B. Thamdrup, and D. E. Canfield. 2005. Anaerobic ammonium oxidation (anammox) in the marine environment. Research in Microbiology **156**: 457–464. doi:10.1016/j.resmic.2005.01.011

Davis, T. W., G. S. Bullerjahn, T. Tuttle, R. M. McKay, and S. B. Watson. 2015. Effects of Increasing Nitrogen and Phosphorus Concentrations on Phytoplankton Community Growth and Toxicity During *Planktothrix* Blooms in Sandusky Bay, Lake Erie. Environmental Science & Technology **49**: 7197–7207. doi:10.1021/acs.est.5b00799

Dean, W. E. 1974. Determination of Carbonate and Organic Matter in Calcareous Sediments and Sedimentary Rocks by Loss on Ignition: Comparison With Other Methods. SEPM Journal of Sedimentary Research **Vol. 44**: 242–248. doi:10.1306/74D729D2-2B21-11D7-8648000102C1865D

Dedysh, S. N. 2004. NifH and NifD phylogenies: an evolutionary basis for understanding nitrogen fixation capabilities of methanotrophic bacteria. Microbiology **150**: 1301–1313. doi:10.1099/mic.0.26585-0

Donald, D. B., M. J. Bogard, K. Finlay, and P. R. Leavitt. 2011. Comparative effects of urea, ammonium, and nitrate on phytoplankton abundance, community composition, and toxicity in hypereutrophic freshwaters. Limnology and Oceanography **56**: 2161–2175. doi:10.4319/lo.2011.56.6.2161

Elser, J. J., M. E. S. Bracken, E. E. Cleland, and others. 2007. Global analysis of nitrogen and phosphorus limitation of primary producers in freshwater, marine and terrestrial ecosystems. Ecology Letters **10**: 1135–1142. doi:10.1111/j.1461-0248.2007.01113.x

Fennel, K., D. Brady, D. DiToro, and others. 2009. Modeling denitrification in aquatic sediments. Biogeochemistry **93**: 159–178. doi:10.1007/s10533-008-9270-z

Fisher, B., R. K. Turner, and P. Morling. 2009. Defining and classifying ecosystem services for decision making. Ecological Economics **68**: 643–653. doi:10.1016/j.ecolecon.2008.09.014

Forsberg, C. 1989. Importance of sediments in understanding nutrient cyclings in lakes. Hydrobiologia **176**: 263–277.

Foster, S. Q., and R. W. Fulweiler. 2014. Spatial and historic variability of benthic nitrogen cycling in an anthropogenically impacted estuary. Frontiers in Marine Science **1**. doi:10.3389/fmars.2014.00056

Fraser, A. S. 1987. Tributary and Point Source Total Phosphorus Loading to Lake Erie. Journal of Great Lakes Research **13**: 659–666. doi:10.1016/S0380-1330(87)71680-3

Fulweiler, R. W., S. W. Nixon, B. A. Buckley, and S. L. Granger. 2007. Reversal of the net dinitrogen gas flux in coastal marine sediments. Nature **448**: 180–182. doi:10.1038/nature05963

Fulweiller, R., and E. Heiss. 2014. (Nearly) A Decade of Directly Measured Sediment N2 Fluxes: What Can Narragansett Bay Tell Us About the Global Ocean Nitrogen Budget? Oceanography **27**: 184–195. doi:10.5670/oceanog.2014.22

Gardner, W. S., and G. F. Lee. 1975. The role of amino acids in the nitrogen cycle of Lake Mendota1: Amino acids in Lake Mendota. Limnology and Oceanography **20**: 379–388. doi:10.4319/lo.1975.20.3.0379

Gardner, W. S., M. J. McCarthy, S. An, D. Sobolev, K. S. Sell, and D. Brock. 2006. Nitrogen fixation and dissimilatory nitrate reduction to ammonium (DNRA)

support nitrogen dynamics in Texas estuaries. Limnology and Oceanography **51**: 558–568. doi:10.4319/lo.2006.51.1_part_2.0558

Gardner, W. S., M. J. McCarthy, S. A. Carini, A. C. Souza, H. Lijun, K. S. McNeal, M. K. Puckett, and J. Pennington. 2009. Collection of intact sediment cores with overlying water to study nitrogen- and oxygen-dynamics in regions with seasonal hypoxia. Continental Shelf Research **29**: 2207–2213. doi:10.1016/j.csr.2009.08.012

Gardner, W. S., S. P. Seitzinger, and J. M. Malczyk. 1991. The Effects of Sea Salts on the Forms of Nitrogen Released from Estuarine and Freshwater Sediments: Does Ion Pairing Affect Ammonium Flux? Estuaries **14**: 157. doi:10.2307/1351689

Glass, C., and J. Silverstein. 1998. Denitrification kinetics of high nitrate concentration water: pH effect on inhibition and nitrite accumulation. Water Research **32**: 831–839. doi:10.1016/S0043-1354(97)00260-1

Glibert, P. M. 2017. Eutrophication, harmful algae and biodiversity — Challenging paradigms in a world of complex nutrient changes. Marine Pollution Bulletin **124**: 591–606. doi:10.1016/j.marpolbul.2017.04.027

Glibert, P. M., J. Harrison, C. Heil, and S. Seitzinger. 2006. Escalating Worldwide use of Urea – A Global Change Contributing to Coastal Eutrophication. Biogeochemistry **77**: 441–463. doi:10.1007/s10533-005-3070-5

Glibert, P. M., D. C. Hinkle, B. Sturgis, and R. V. Jesien. 2014a. Eutrophication of a Maryland/Virginia Coastal Lagoon: a Tipping Point, Ecosystem Changes, and Potential Causes. Estuaries and Coasts **37**: 128–146. doi:10.1007/s12237-013-9630-3

Glibert, P. M., R. Maranger, D. J. Sobota, and L. Bouwman. 2014b. The Haber Bosch–harmful algal bloom (HB–HAB) link. Environmental Research Letters **9**: 105001. doi:10.1088/1748-9326/9/10/105001

Glibert, P. M., F. P. Wilkerson, R. C. Dugdale, and others. 2016. Pluses and minuses of ammonium and nitrate uptake and assimilation by phytoplankton and implications for productivity and community composition, with emphasis on nitrogen-enriched conditions: Pluses and minuses of NH4+ *and* NO3−. Limnology and Oceanography **61**: 165–197. doi:10.1002/lno.10203

Gobler, C. J., J. M. Burkholder, T. W. Davis, M. J. Harke, T. Johengen, C. A. Stow, and D. B. Van de Waal. 2016. The dual role of nitrogen supply in controlling the growth and toxicity of cyanobacterial blooms. Harmful Algae **54**: 87–97. doi:10.1016/j.hal.2016.01.010

Guildford, S. J., and R. E. Hecky. 2000. Total nitrogen, total phosphorus, and nutrient limitation in lakes and oceans: Is there a common relationship? Limnology and Oceanography **45**: 1213–1223. doi:10.4319/lo.2000.45.6.1213

Han, H., J. D. Allan, and N. S. Bosch. 2012. Historical pattern of phosphorus loading to Lake Erie watersheds. Journal of Great Lakes Research **38**: 289–298. doi:10.1016/j.jglr.2012.03.004

Heathwaite, A. L., and P. J. Johnes. 1996. Contribution of nitrogen species and phosphorus fractions to stream water quality in agricultural catchments. Hydrological Processes **10**: 971–983.

Heiri, O., A. F. Lotter, and G. Lemcke. 2001. Loss on ignition as a method for estimating organic and carbonate content in sediments: reproducibility and comparability of results. Journal of Paleolimnology **25**: 101–110.

Heisler, J., P. M. Glibert, J. M. Burkholder, and others. 2008. Eutrophication and harmful algal blooms: A scientific consensus. Harmful Algae **8**: 3–13. doi:10.1016/j.hal.2008.08.006

Herdendorf, C. E. 1990. Great Lakes Estuaries. Estuaries **13**: 493. doi:10.2307/1351795

Herrero, A., A. M. Muro-Pastor, and E. Flores. 2001. Nitrogen Control in Cyanobacteria. Journal of Bacteriology **183**: 411–425. doi:10.1128/JB.183.2.411-425.2001

Herrman, K. S., and J. R. White. 2008. Denitrification in intact sediment cores from a constructed wetland: Examining the isotope pairing technique. Applied Geochemistry **23**: 2105–2112. doi:10.1016/j.apgeochem.2008.04.024

Holdren, G. C., and D. E. Armstrong. 1980. Factors affecting phosphorus release from intact lake sediment cores. Environmental Science & Technology **14**: 79–87. doi:10.1021/es60161a014

Holmes, R. M., A. Aminot, R. Kérouel, B. A. Hooker, and B. J. Peterson. 1999. A simple and precise method for measuring ammonium in marine and freshwater ecosystems. **56**: 8.

Howarth, R. W., R. Marino, J. Lane, and J. Cole J. 1988. Nitrogen fixation in freshwater, estuarine, and marine ecosystems. 1. Rates and importance. Limnology and Oceanography **33**: 669–687.

Hupfer, M., and J. Lewandowski. 2008. Oxygen Controls the Phosphorus Release from Lake Sediments - a Long-Lasting Paradigm in Limnology. International Review of Hydrobiology **93**: 415–432. doi:10.1002/iroh.200711054

James, R. T., W. S. Gardner, M. J. McCarthy, and S. A. Carini. 2011. Nitrogen dynamics in Lake Okeechobee: forms, functions, and changes. Hydrobiologia **669**: 199–212. doi:10.1007/s10750-011-0683-7

Joosse, P. J., and D. B. Baker. 2011. Context for re-evaluating agricultural source phosphorus loadings to the Great Lakes. Canadian Journal of Soil Science **91**: 317–327. doi:10.4141/cjss10005

Kana, T. M., C. Darkangelo, M. D. Hunt, J. B. Oldham, G. E. Bennett, and J. C. Cornwell. 1994. Membrane lnlet Mass Spectrometer for Rapid High-Precision Determination of N2, 0 2 , and Ar in Environmental Water Samples. Analytical Chemistry **66**: 4166–4170.

Kane, D. D., J. D. Conroy, R. Peter Richards, D. B. Baker, and D. A. Culver. 2014. Re-eutrophication of Lake Erie: Correlations between tributary nutrient loads and phytoplankton biomass. Journal of Great Lakes Research **40**: 496–501. doi:10.1016/j.jglr.2014.04.004

Kelso, B. H. L., R. V. Smith, R. J. Laughlin, and S. D. Lennox. 1997. Dissimilatory Nitrate Reduction in Anaerobic Sediments Leading to River Nitrite Accumulation. APPL. ENVIRON. MICROBIOL. **63**: 7.

de Klein, J. J. M., C. C. Overbeek, C. Juncher Jørgensen, and A. J. Veraart. 2017. Effect of Temperature on Oxygen Profiles and Denitrification Rates in Freshwater Sediments. Wetlands **37**: 975–983. doi:10.1007/s13157-017-0933-1

Knapp, A. N. 2012. The sensitivity of marine N2 fixation to dissolved inorganic nitrogen. Frontiers in Microbiology **3**: 1–14. doi:10.3389/fmicb.2012.00374

Laursen, A. E., and S. P. Seitzinger. 2002. Measurement of denitrification in rivers: an integrated, whole reach approach. Hydrobiologia **485**: 67–81.

Lavrentyev, P., W. Gardner, and L. Yang. 2000. Effects of the zebra mussel on nitrogen dynamics and the microbial community at the sediment-water interface. Aquatic Microbial Ecology **21**: 187–194. doi:10.3354/ame021187

Lewis, W. M., and W. A. Wurtsbaugh. 2008. Control of Lacustrine Phytoplankton by Nutrients: Erosion of the Phosphorus Paradigm. International Review of Hydrobiology **93**: 446–465. doi:10.1002/iroh.200811065

Lomas, M. W., and F. Lipschultz. 2006. Forming the primary nitrite maximum: Nitrifiers or phytoplankton? Limnology and Oceanography **51**: 2453–2467. doi:10.4319/lo.2006.51.5.2453

Ludsin, S. A., M. W. Kershner, K. A. Blocksom, R. L. Knight, and R. A. Stein. 2001. Life after death in Lake Erie: Nutrient controls drive fish species richness, rehabilitation. Ecological Applications **11**: 731–746. doi:10.1890/1051-0761(2001)011[0731:LADILE]2.0.CO;2

Maccoux, M. J., A. Dove, S. M. Backus, and D. M. Dolan. 2016. Total and soluble reactive phosphorus loadings to Lake Erie. Journal of Great Lakes Research **42**: 1151–1165. doi:10.1016/j.jglr.2016.08.005

Mackerras, A. H., and G. D. Smith. 1986. Urease activity of the cyanobacterium Anabaena cylindrica. Journal of General Microbiology **132**: 2749–2752.

Matisoff, G., E. M. Kaltenberg, R. L. Steely, and others. 2016. Internal loading of phosphorus in western Lake Erie. Journal of Great Lakes Research **42**: 775–788. doi:10.1016/j.jglr.2016.04.004

McCarthy, M. J., W. S. Gardner, P. J. Lavrentyev, K. M. Moats, F. J. Jochem, and D. M. Klarer. 2007. Effects of Hydrological Flow Regime on Sediment-water Interface and Water Column Nitrogen Dynamics in a Great Lakes Coastal Wetland (Old Woman Creek, Lake Erie). Journal of Great Lakes Research **33**: 219–231. doi:10.3394/0380-1330(2007)33[219:EOHFRO]2.0.CO;2

McCarthy, M. J., W. S. Gardner, M. F. Lehmann, A. Guindon, and D. F. Bird. 2016. Benthic nitrogen regeneration, fixation, and denitrification in a temperate, eutrophic lake: Effects on the nitrogen budget and cyanobacteria blooms: Sediment N cycling in Missisquoi Bay. Limnology and Oceanography **61**: 1406–1423. doi:10.1002/lno.10306

McCarthy, M. J., R. T. James, Y. Chen, T. L. East, and W. S. Gardner. 2009. Nutrient ratios and phytoplankton community structure in the large, shallow, eutrophic, subtropical Lakes Okeechobee (Florida, USA) and Taihu (China). Limnology **10**: 215–227. doi:10.1007/s10201-009-0277-5

McCarthy, M. J., S. E. Newell, S. A. Carini, and W. S. Gardner. 2015. Denitrification Dominates Sediment Nitrogen Removal and Is Enhanced by Bottom-Water Hypoxia in the Northern Gulf of Mexico. Estuaries and Coasts **38**: 2279–2294. doi:10.1007/s12237-015-9964-0

McTigue, N. D., W. S. Gardner, K. H. Dunton, and A. K. Hardison. 2016. Biotic and abiotic controls on co-occurring nitrogen cycling processes in shallow Arctic shelf sediments. Nature Communications **7**: 13145. doi:10.1038/ncomms13145

Michalak, A. M., E. J. Anderson, D. Beletsky, and others. 2013. Record-setting algal bloom in Lake Erie caused by agricultural and meteorological trends consistent with expected future conditions. Proceedings of the National Academy of Sciences **110**: 6448–6452. doi:10.1073/pnas.1216006110

Mitsch, W. J. 1992. Landscape design and the role of created, restored, and natural riparian wetlands in controlling nonpoint source pollution. Ecological Engineering **1**: 27–47. doi:10.1016/0925-8574(92)90024-V

Monchamp, M.-E., F. R. Pick, B. E. Beisner, and R. Maranger. 2014. Nitrogen Forms Influence Microcystin Concentration and Composition via Changes in Cyanobacterial Community Structure B. Neilan [ed.]. PLoS ONE **9**: e85573. doi:10.1371/journal.pone.0085573

Moog, D. B., and P. J. Whiting. 2002. Climatic and Agricultural Factors in Nutrient Exports from Two Watersheds in Ohio. J. ENVIRON. QUAL. **31**: 12.

Mørkved, P. T., A. K. Søvik, B. Kløve, and L. R. Bakken. 2005. Removal of nitrogen in different wetland filter materials: use of stable nitrogen isotopes to determine factors controlling denitrification and DNRA. Water Science and Technology **51**: 63–71. doi:10.2166/wst.2005.0289

Muenich, R. L., M. Kalcic, and D. Scavia. 2016. Evaluating the Impact of Legacy P and Agricultural Conservation Practices on Nutrient Loads from the Maumee River Watershed. Environmental Science & Technology **50**: 8146–8154. doi:10.1021/acs.est.6b01421

Mulholland, P. J., A. M. Helton, G. C. Poole, and others. 2008. Stream denitrification across biomes and its response to anthropogenic nitrate loading. Nature **452**: 202–205. doi:10.1038/nature06686

Murphy, T., K. Irvine, J. Guo, J. Davies, H. Murkin, M. Charlton, and S. Watson. 2003. New Microcystin Concerns in the Lower Great Lakes. Water Quality Research Journal **38**: 127–140. doi:10.2166/wqrj.2003.008

Newell, S. E., M. J. McCarthy, W. S. Gardner, and R. W. Fulweiler. 2016. Sediment Nitrogen Fixation: a Call for Re-evaluating Coastal N Budgets. Estuaries and Coasts **39**: 1626–1638. doi:10.1007/s12237-016-0116-y

Nogaro, G., and A. J. Burgin. 2014. Influence of bioturbation on denitrification and dissimilatory nitrate reduction to ammonium (DNRA) in freshwater sediments. Biogeochemistry **120**: 279–294. doi:10.1007/s10533-014-9995-9

Ozersky, T., D. R. Barton, R. E. Hecky, and S. J. Guildford. 2013. Dreissenid mussels enhance nutrient efflux, periphyton quantity and production in the shallow littoral zone of a large lake. Biological Invasions **15**: 2799–2810. doi:10.1007/s10530-013-0494-z

Paerl, H. W., W. S. Gardner, M. J. McCarthy, B. L. Peierls, and S. W. Wilhelm. 2014. Algal blooms: Noteworthy nitrogen. Science **346**: 175–175. doi:10.1126/science.346.6206.175-a

Paerl, H. W., J. T. Scott, M. J. McCarthy, and others. 2016. It Takes Two to Tango: When and Where Dual Nutrient (N & P) Reductions Are Needed to Protect Lakes and Downstream Ecosystems. Environmental Science & Technology **50**: 10805–10813. doi:10.1021/acs.est.6b02575

Paterson, M. J., D. W. Schindler, R. E. Hecky, D. L. Findlay, and K. J. Rondeau. 2011. Comment: Lake 227 shows clearly that controlling inputs of nitrogen will not reduce or prevent eutrophication of lakes. Limnology and Oceanography **56**: 1545–1547. doi:10.4319/lo.2011.56.4.1545

Paytan, A., K. Roberts, S. Watson, S. Peek, P.-C. Chuang, D. Defforey, and C. Kendall. 2017. Internal loading of phosphate in Lake Erie Central Basin. Science of The Total Environment **579**: 1356–1365. doi:10.1016/j.scitotenv.2016.11.133

Pearson, L. A., E. Dittmann, R. Mazmouz, S. E. Ongley, P. M. D'Agostino, and B. A. Neilan. 2016. The genetics, biosynthesis and regulation of toxic specialized

metabolites of cyanobacteria. Harmful Algae **54**: 98–111. doi:10.1016/j.hal.2015.11.002

Peterson, B. J., M. Bahr, and G. W. Kling. 1997. A tracer investigation of nitrogen cycling in a pristine tundra river. Canadian Journal of Fisheries and Aquatic Sciences **54**: 2361–2367.

Rich, J. J., O. R. Dale, B. Song, and B. B. Ward. 2008. Anaerobic Ammonium Oxidation (Anammox) in Chesapeake Bay Sediments. Microbial Ecology **55**: 311–320. doi:10.1007/s00248-007-9277-3

Richards, R. P., and D. B. Baker. 2002. Trends in Water Quality in LEASEQ Rivers and Streams (Northwestern Ohio), 1975–1995. J. ENVIRON. QUAL. **31**: 7.

Riederer-Henderson, M.-A., and P. W. Wilson. 1970. Nitrogen Fixation by Sulphate-reducing Bacteria. Journal of General Microbiology **61**: 27–31. doi:10.1099/00221287-61-1-27

Safak, I., P. L. Wiberg, D. L. Richardson, and M. O. Kurum. 2015. Controls on residence time and exchange in a system of shallow coastal bays. Continental Shelf Research **97**: 7–20. doi:10.1016/j.csr.2015.01.009

Salk, K. R., G. S. Bullerjahn, R. M. L. McKay, J. D. Chaffin, and N. E. Ostrom. 2018. Nitrogen cycling in Sandusky Bay, Lake Erie: oscillations between strong and weak export and implications for harmful algal blooms. Biogeosciences **15**: 2891–2907. doi:10.5194/bg-15-2891-2018

Saunders, D. ., and J. Kalff. 2001. Denitrification rates in the sediments of Lake Memphremagog, Canada–USA. Water Research **35**: 1897–1904. doi:10.1016/S0043-1354(00)00479-6

Schindler, D. W. 2012. The dilemma of controlling cultural eutrophication of lakes. Proceedings of the Royal Society B: Biological Sciences **279**: 4322–4333. doi:10.1098/rspb.2012.1032

Schindler, D. W., R. E. Hecky, D. L. Findlay, and others. 2008. Eutrophication of lakes cannot be controlled by reducing nitrogen input: Results of a 37-year whole-ecosystem experiment. Proceedings of the National Academy of Sciences **105**: 11254–11258. doi:10.1073/pnas.0805108105

Schubert, C. J., E. Durisch-Kaiser, B. Wehrli, B. Thamdrup, P. Lam, and M. M. M. Kuypers. 2006. Anaerobic ammonium oxidation in a tropical freshwater system (Lake Tanganyika). Environmental Microbiology **8**: 1857–1863. doi:10.1111/j.1462-2920.2006.01074.x

Scott, J. T., and M. J. McCarthy. 2010. Nitrogen fixation may not balance the nitrogen pool in lakes over timescales relevant to eutrophication management. Limnology and Oceanography **55**: 1265–1270. doi:10.4319/lo.2010.55.3.1265

Scott, J. T., and M. J. McCarthy. 2011. Response to Comment: Nitrogen fixation has not offset declines in the Lake 227 nitrogen pool and shows that nitrogen control deserves consideration in aquatic ecosystems. Limnology and Oceanography **56**: 1548–1550. doi:10.4319/lo.2011.56.4.1548

Scott, J. T., M. J. McCarthy, W. S. Gardner, and R. D. Doyle. 2008. Denitrification, dissimilatory nitrate reduction to ammonium, and nitrogen fixation along a nitrate concentration gradient in a created freshwater wetland. Biogeochemistry **87**: 99–111. doi:10.1007/s10533-007-9171-6

Seiki, T., H. Izawa, E. Date, and H. Sunahara. 1994. Sediment oxygen demand in Hiroshima Bay. Water Research **28**: 385–393. doi:10.1016/0043-1354(94)90276-3

Seitzinger, S. P. 1988. Denitrification in freshwater and coastal marine ecosystems: Ecological and geochemical significance: Denitrification. Limnology and Oceanography **33**: 702–724. doi:10.4319/lo.1988.33.4part2.0702

Seitzinger, S. P., L. P. Nielsen, J. Caffrey, and P. B. Christensen. 1993. Denitrification measurements in aquatic sediments: A comparison of three methods. Biogeochemistry **23**: 147–167. doi:10.1007/BF00023750

Seitzinger, S. P., R. V. Styles, E. W. Boyer, R. B. Alexander, G. Billen, R. W. Howarth, B. Mayer, and N. Van Breemen. 2002. Nitrogen retention in rivers: model development and application to watersheds in the northeastern U.S.A., p. 199–237. *In* E.W. Boyer and R.W. Howarth [eds.], The Nitrogen Cycle at Regional to Global Scales. Springer Netherlands.

Small, G. E., G. S. Bullerjahn, R. W. Sterner, B. F. N. Beall, S. Brovold, J. C. Finlay, R. M. L. McKay, and M. Mukherjee. 2013. Rates and controls of nitrification in a large oligotrophic lake. Limnology and Oceanography **58**: 276–286. doi:10.4319/lo.2013.58.1.0276

Small, G. E., J. B. Cotner, J. C. Finlay, R. A. Stark, and R. W. Sterner. 2014. Nitrogen transformations at the sediment–water interface across redox gradients in the Laurentian Great Lakes. Hydrobiologia **731**: 95–108. doi:10.1007/s10750-013-1569-7

Smetacek, V. S. 1985. Role of sinking in diatom life-history cycles: ecological, evolutionary and geological significance. Marine Biology **84**: 239–251. doi:10.1007/BF00392493

Smith, R. A., G. E. Schwarz, and R. B. Alexander. 1997. Regional interpretation of water-quality monitoring data. Water Resources Research **33**: 2781–2798. doi:10.1029/97WR02171

Stewart, W. D. P., A. Haystead, and H. W. Pearson. 1969. Nitrogenase Activity in Heterocysts of Blue-Green Algae. Nature **224**: 226–228.

Stow, C. A., Y. Cha, L. T. Johnson, R. Confesor, and R. P. Richards. 2015. Long-Term and Seasonal Trend Decomposition of Maumee River Nutrient Inputs to Western Lake Erie. Environmental Science & Technology **49**: 3392–3400. doi:10.1021/es5062648

Stumpf, R. P., T. T. Wynne, D. B. Baker, and G. L. Fahnenstiel. 2012. Interannual Variability of Cyanobacterial Blooms in Lake Erie I. Álvarez [ed.]. PLoS ONE **7**: e42444. doi:10.1371/journal.pone.0042444

Townsend-Small, A., M. J. McCarthy, J. A. Brandes, L. Yang, L. Zhang, and W. S. Gardner. 2007. Stable isotopic composition of nitrate in Lake Taihu, China, and major inflow rivers. Hydrobiologia **581**: 135–140. doi:10.1007/s10750-006-0505-5

Verhamme, E. M., T. M. Redder, D. A. Schlea, J. Grush, J. F. Bratton, and J. V. DePinto. 2016. Development of the Western Lake Erie Ecosystem Model (WLEEM): Application to connect phosphorus loads to cyanobacteria biomass. Journal of Great Lakes Research **42**: 1193–1205. doi:10.1016/j.jglr.2016.09.006

Vitousek, P. M., J. D. Aber, R. W. Howarth, G. E. Likens, P. A. Matson, D. W. Schindler, W. H. Schlesinger, and D. G. Tilman. 1997. Human alteration of the global nitrogen cycle: Sources and consequences. Ecological Applications **7**: 737–750. doi:10.1890/1051-0761(1997)007[0737:HAOTGN]2.0.CO;2

Vitousek, P. M., D. N. L. Menge, S. C. Reed, and C. C. Cleveland. 2013. Biological nitrogen fixation: rates, patterns and ecological controls in terrestrial ecosystems. Philosophical Transactions of the Royal Society B: Biological Sciences **368**: 20130119–20130119. doi:10.1098/rstb.2013.0119

Vymazal, J. 2007. Removal of nutrients in various types of constructed wetlands. Science of The Total Environment **380**: 48–65. doi:10.1016/j.scitotenv.2006.09.014

Ward, B. B., A. H. Devol, J. J. Rich, B. X. Chang, S. E. Bulow, H. Naik, A. Pratihary, and A. Jayakumar. 2009. Denitrification as the dominant nitrogen loss process in the Arabian Sea. Nature **461**: 78–81. doi:10.1038/nature08276

Welsh, D. T. 2000. Nitrogen fixation in seagrass meadows: Regulation, plant-bacteria interactions and significance to primary productivity. Ecology Letters **3**: 58–71. doi:10.1046/j.1461-0248.2000.00111.x

Wenk, C. B., J. Blees, J. Zopfi, M. Veronesi, A. Bourbonnais, C. J. Schubert, H. Niemann, and M. F. Lehmann. 2013. Anaerobic ammonium oxidation (anammox) bacteria and sulfide-dependent denitrifiers coexist in the water column of a meromictic south-alpine lake. Limnology and Oceanography **58**: 1–12. doi:10.4319/lo.2013.58.1.0001

Wetzel, R. G. 1992. Gradient-dominated ecosystems: sources and regulatory functions of dissolved organic matter in freshwater ecosystems. Hydrobiologia **229**: 181–198.

Wilson, T., and V. DePaul. 2017. *In Situ* Benthic Nutrient Flux and Sediment Oxygen Demand in Barnegat Bay, New Jersey. Journal of Coastal Research **78**: 46–59. doi:10.2112/SI78-005.1

Xu, H., H. W. Paerl, B. Qin, G. Zhu, and G. Gaoa. 2010. Nitrogen and phosphorus inputs control phytoplankton growth in eutrophic Lake Taihu, China. Limnology and Oceanography **55**: 420–432. doi:10.4319/lo.2010.55.1.0420

Yin, G., L. Hou, M. Liu, Z. Liu, and W. S. Gardner. 2014. A Novel Membrane Inlet Mass Spectrometer Method to Measure $^{15}NH_4^+$ for Isotope-Enrichment Experiments in Aquatic Ecosystems. Environmental Science & Technology **48**: 9555–9562. doi:10.1021/es501261s

Zhou, Y., D. R. Obenour, D. Scavia, T. H. Johengen, and A. M. Michalak. 2013. Spatial and Temporal Trends in Lake Erie Hypoxia, 1987–2007. Environmental Science & Technology **47**: 899–905. doi:10.1021/es303401b